REPUBLIC OF TÜRKİYE
YILDIZ TECHNICAL UNIVERSITY
GRADUATE SCHOOL OF SCIENCE AND ENGINEERING

PREDICTION OF SYNGAS AND EXERGY DATA FROM GASIFICATION OF LIGNITE COAL AND BIOMASS BLENDS WITH MACHINE LEARNING ALGORITHMS

Mislina ÇAKAR

MASTER OF SCIENCE THESIS

Department of Chemical Engineering

Program of Chemical Engineering

Supervisor

Prof. Dr. Hasan SADIKOĞLU

Co-Supervisor

Asst. Prof. Dr. Özgün YÜCEL

February, 2025

REPUBLIC OF TÜRKİYE

YILDIZ TECHNICAL UNIVERSITY

GRADUATE SCHOOL OF SCIENCE AND ENGINEERING

PREDICTION OF SYNGAS AND EXERGY DATA FROM GASIFICATION OF LIGNITE COAL AND BIOMASS BLENDS WITH MACHINE LEARNING ALGORITHMS

A thesis submitted by Mislina ÇAKAR in partial fulfillment of the requirements for the degree of **MASTER OF SCIENCE** is approved by the committee on 03.02.2025 in Department of Chemical Engineering, Program of Chemical Engineering.

Prof. Dr. Hasan SADIKOĞLU Yildiz Technical University Supervisor	Asst. Prof. Dr. Özgün YÜCEL Gebze Technical University Co- supervisor

Approved By the Examining Committee

Prof. Dr. Hasan SADIKOĞLU, Supervisor
Yildiz Technical University _____

Prof. Dr. Nil ACARALI, Member
Yildiz Technical University _____

Assoc. Prof. Dr. Fatih TARLAK, Member
Gebze Technical University _____

I hereby declare that I have obtained the required legal permissions during data collection and exploitation procedures, that I have made the in-text citations and cited the references properly, that I haven't falsified and/or fabricated research data and results of the study and that I have abided by the principles of the scientific research and ethics during my Thesis Study under the title of "PREDICTION OF SYNGAS AND EXERGY DATA FROM GASIFICATION OF LIGNITE COAL AND BIOMASS BLENDS WITH MACHINE LEARNING ALGORITHMS" supervised by my supervisor, Prof. Dr. Hasan SADIKOĞLU and Asst. Prof. Dr. Özgün YÜCEL. In the case of a discovery of false statement, I am to acknowledge any legal consequence.

Mislina ÇAKAR

The research was funded by TÜBİTAK with the project number 123M784 and Yildiz Technical University's Scientific Research Projects Council, with the project identified as FBA_2023_5648.

Dedicated to those who have supported and inspired me throughout this journey, my mentors and loved ones, whose encouragement and guidance have been invaluable.

ACKNOWLEDGEMENTS

I would like to extend my deepest gratitude and sincere appreciation to my esteemed supervisor, **Prof. Dr. Hasan SADIKOĞLU**, for his invaluable guidance, unwavering support, and profound expertise throughout this research. His insightful advice, encouragement, and dedication have been instrumental in shaping this study, and I am truly honored to have had the opportunity to work under his supervision. I am also profoundly grateful to my co-supervisor, **Asst. Prof. Dr. Özgün YÜCEL**, for his invaluable contributions, constructive feedback, and continuous support. His expertise and thoughtful suggestions have greatly enriched the quality of this research, and I deeply appreciate his guidance throughout this journey. Furthermore, I would like to express my heartfelt appreciation to **Res. Asst. Mert Akın İNSEL** for his generous assistance, valuable discussions, and unwavering support. His contributions have been of great significance in the successful completion of this study.

Their mentorship, patience, and encouragement have played an essential role in this research, and I am truly indebted to them for their time, effort, and dedication.

Mislina ÇAKAR

TABLE OF CONTENTS

LIST OF SYMBOLS ix
LIST OF ABBREVIATIONS x
LIST OF FIGURES xi
LIST OF TABLES xiii
LIST OF MAPS xv
ABSTRACT xvi
ÖZET xviii
1 INTRODUCTION 1
1.1 The Quest for Sustainable Energy 1
1.2 Aim of Thesis 2
2 BACKGROUND OF HYDROGEN ENERGY 4
2.1 Climate Actions Worldwide 4
2.2 Climate Actions in Türkiye 5
2.3 Hydrogen 7
2.3.1 Hydrogen in the World 7
2.3.2 Hydrogen in Türkiye 9
2.4 Hydrogen Technologies 13
2.4.1 Electrolytic Processes 13
2.4.2 Direct Solar Water Splitting Processes 14
2.4.3 Biological Processes 15
2.4.4 Thermochemical Processes 16
2.5 Biomass Gasification 16
2.5.1 Biomass and Lignite 20
2.6 Physical and Chemical Exergy 22
2.7 Machine Learning for Hydrogen Energy Applications 23
2.7.1 Decision Tree Regression 24
2.7.2 Support Vector Machines 24
2.7.3 Gaussian Process Regression 25

2.7.4 Random Forest (RF) 25
2.8 Performance Metrix 26
2.8.1 Coefficient of determination (R^2) 26
2.8.2 Adjusted coefficient of determination (Adj R^2) 26
2.8.3 Root Means Square Error (RMSE), ... 27
3 LITERATURE REVIEW 28
4 METHODOLOGY 37
4.1 Method 37
4.2 Biomass Characterization 39
4.3 Modelling in Aspen Plus® 40
5 SIMULATION 41
5.1 Modeling 41
5.1.1 Modeling of downdraft fixed-bed gasifier in Aspen Plus® 42
5.1.2 Modeling of fluidized-bed gasifier in Aspen Plus® 44
5.2 Process Development 47
5.3 Calculations 48
5.3.1 Yield Calculations 48
5.3.2 Air Mass Flow Calculations 51
5.4 Fixed-Bed Process Development 54
5.5 Fluidized-Bed Process Development 56
5.6 Machine Learning 57
6 RESULTS AND DISCUSSION 59
6.1 Fixed-Bed Sensitivity Analysis 59
6.1.1 Validation Results for Fixed-Bed Gasifier 59
6.1.2 Model Results for Fixed-Bed Gasifier 61
6.2 Fluidized-Bed Sensitivity Analysis 67
6.2.1 Validation Results of Fluidized-Bed Gasifer 67
6.2.2 Model Results of Fluidized-Bed Gasifier 68
6.3 Results of Machine Learning Applications 78
6.3.1 Model Results of CO 79
6.3.2 Model Results of CO_2 81
6.3.3 Model Results of CH_4 82
6.3.4 Model Results of H_2 84
6.3.5 Model Results for the Exergy of Syngas 86
6.4 Cross Validation 87

6.4.2 10-Fold Cross Validation for Hydrogen 89
7 CONCLUSION **91**
7.1 Recommendation 94
REFERENCES **96**
PUBLICATIONS FROM THE THESIS **106**

LIST OF SYMBOLS

^{O}C	Celcius
$\widetilde{Ex}_{chem}$	Chemical Exergy [kJ/mol]
Ex_{phys}	Physical Exergy
$\tilde{f}_{form}$	Specific Chemical Exergy of Formation [kJ/mol]
h	Specific Enthalpy [kJ kg^{-1}]
h_0	Specific Enthalpy at T_0, P_0 [kJ kg^{-1}]
S	Specific Entropy [kJ kg^{-1} K^{-1}]
S_0	Specific Entropy at T_0, P_0 [kJ kg^{-1} K^{-1}]
P_0	Stable Reference State Pressure [1 atm]
T_0	Stable Reference State Temperature [298.15 K]

LIST OF ABBREVIATIONS

BTL	Biomass to lignite ratio
CO_2	Carbon dioxide
C	Carbon graphite
CO	Carbon monoxide
Cl_2	Chlorine
DT	Decision Tree
ER	Equivalence ratio
H_2	Hydrogen
HCl	Hydrogen-Chloride
GPR	Gaussian Process Regression
CH_4	Methane
N_2	Nitrogen
NO_2	Nitrogen dioxide
O_2	Oxygen
P&D	Production and Development
R&D	Research and Development
SBR	Steam to biomass ratio
S	Sulfur
SO_2	Sulfur dioxide
SO_3	Sulfur trioxide
SVM	Support Vector Machines
T	Temperature
H_2O	Water

LIST OF FIGURES

Figure 2.1 Turkey's electricity generation trends by source [16].....**6**

Figure 2.2 Hydrogen use by region [17].....**8**

Figure 2.3 A chart illustrating the disclosed low-emission hydrogen production initiatives [17] **9**

Figure 2.4 Sources of primary clean energy for Türkiye's H2 energy evolution [18] **12**

Figure 5.1 Main flowsheet of biomass gasification in a downdraft fixed-bed gasifier.....**44**

Figure 5.2 Main flowsheet of biomass gasification in a downdraft fluidized-bed gasifier.....**46**

Figure 5.3 Flowsheet of decomposition unit.....**49**

Figure 6.1 Comparison of gas compositions.....**60**

Figure 6.2 Comparison of gas compositions.....**61**

Figure 6.3 Effect of biomass-to-lignite ratio on gas compositions **62**

Figure 6.4 Effect of biomass-to-lignite ratio on on exergy of syngas gas compositions **63**

Figure 6.5 Effect of temperature on gas compositions **64**

Figure 6.6 Effect of temperature on exergy of syngas gas compositions **64**

Figure 6.7 Effect of ER on gas compositions **66**

Figure 6.8 Effect of ER on exergy of syngas gas compositions **66**

Figure 6.9 T and ER effect on hydrogen, when SBR:0 .....**67**

Figure 6.10 Comparison of gas compositions at ER: 0.163.....**68**

Figure 6.11 Effect of biomass-to-lignite ratio on gas compositions **70**

Figure 6.12 Effect of biomass-to-lignite ratio on on exergy of syngas gas compositions **71**

Figure 6.13 Effect of temperature on gas compositions **72**

Figure 6.14 Effect of temperature on exergy of syngas gas compositions **72**

Figure 6.15 Effect of ER on gas compositions **73**

Figure 6.16 Effect of ER on exergy of syngas gas compositions **74**

Figure 6.17 Effect of SBR on gas compositions **75**
Figure 6.18 Effect of SBR on exergy of syngas gas compositions **75**
Figure 6.19 Effect of T and ER on hydrogen with 0.1 SBR **76**
Figure 6.20 Effect of T and ER on hydrogen with 0.2 SBR **76**
Figure 6.21 Effect of T and ER on hydrogen with 0.3 SBR **77**
Figure 6.22 Effect of T and ER on hydrogen with 0.4 SBR **77**
Figure 6.23 Effect of T and ER on hydrogen with 0.4 SBR **78**
Figure 6.24 The R^2 results of the models using overall data for CO **80**
Figure 6.25 The R^2 results of the models learned using only the test data for CO **80**
Figure 6.26 The R^2 results of the models using overall data for CO_2 ..... **82**
Figure 6.27 The R^2 results of the models learned using only the test data for CO_2 ..... **82**
Figure 6.28 The R^2 results of the models using overall data for CH_4 ..... **83**
Figure 6.29 The R^2 results of the models learned using only the test data for CH_4 ..... **84**
Figure 6.30 The R^2 results of the models using overall data for H_2 ..... **85**
Figure 6.31 The R^2 results of the models learned using only the test data for H_2 **85**
Figure 6.32 The R^2 results of the models using overall data for exergy **86**
Figure 6.33 The R^2 results of the models learned using only the test data for exergy **87**

LIST OF TABLES

Table 2.1 Types of gasifiers [32]**.....20**

Table 4.1 Results of ultimate and proximate analyses for biomass samples (wt%, dry basis)**.....38**

Table 4.2 Reactions in the process of biomass gasification [38] **.....39**

Table 5.1 Physical and chemical characterization of the rubber wood and redwood **.....42**

Table 5.2 The experimental parameters for waste tire gasification in a bubbling fluidized bed gasifier**.....44**

Table 5.3 Gasification parameters**.....47**

Table 5.4 Biomass to lignite ratio values **.....48**

Table 5.5 Yield calculation of hazelnut shell for 0.3 kg/hour feed mass flow**.....49**

Table 5.6 Yield calculation of lignite coal for 0.7 kg/hour feed mass flow**.....50**

Table 5.7 Yield calculation of biomass and lignite coal mixtures for 0.3/0.7 ratio **.....50**

Table 5.8 Air mass flow calculations for hazelnut shell **.....52**

Table 5.9 Air mass flow for different ER**.....53**

Table 5.10 Results of air mass flow for ER: 0.12 **.....53**

Table 5.11 Block units, identity and functions of fixed-bed gasifier in Aspen Plus® **.....55**

Table 5.12 Block units, identity and functions of fluidized-bed gasifier in Aspen Plus®**.....56**

Table 6.1 Comparison of syngas composition among the model and experimental works **.....59**

Table 6.2 Results of ultimate and proximate analyses for hazelnut shell and lignite coal (wt%, dry basis)**.....61**

Table 6.3 Results of sensitivity analysis for biomass-to-lignite ratio variables**....62**

Table 6.4 Results of sensitivity analysis for temperature variables **.....63**

Table 6.5 Results of sensitivity analysis for ER variables **.....65**

Table 6.6 Validation results of fluidized-bed model**.....68**

Table 6.7 Results of ultimate and proximate analyses for hazelnut shell and lignite coal (wt%, dry basis)**.....69**

Table 6.8 Results of sensitivity analysis **.....69**

Table 6.9 The sensitivity analysis results based on temperature**.....71**

Table 6.10 The sensitivity analysis results based on ER**.....73**

Table 6.11 The sensitivity analysis results based on SBR **.....74**

Table 6.12 A comparison of the models' R^2 values based on the size of the training data for CO**.....79**

Table 6.13 A comparison of the models' R^2 values based on the size of the training data for CO_2**.....81**

Table 6.14 A comparison of the models' R^2 values based on the size of the training data for CH_4**.....82**

Table 6.15 A comparison of the models' R^2 values based on the size of the training data for H_2 **.....84**

Table 6.16 A comparison of the models' R^2 values based on the size of the training data for exergy**.....86**

Table 6.17 10-Fold cross-validation results for exergy**.....88**

Table 6.18 10- Fold cross validation results for H_2**.....89**

LIST OF MAPS

Map 1.1 Lignite map [8]**.....2**

ABSTRACT

Prediction of Syngas and Exergy Data from Gasification of Lignite Coal And Biomass Blends with Machine Learning Algorithms

Mislina ÇAKAR

Department of Chemical Engineering

Program of Chemical Engineering

Master of Science Thesis

Supervisor: Prof. Dr. Hasan SADIKOĞLU

Co- supervisor: Asst. Prof. Dr. Özgün YÜCEL

The Earth is currently facing severe environmental challenges, including climate change, air pollution, and habitat degradation, all of which disrupt ecological balance. To mitigate these impacts, processes contributing to greenhouse gas emissions must be eliminated. In this context, syngas production through biomass gasification plays a crucial role in achieving clean hydrogen as a sustainable energy carrier. Biomass gasification is a thermochemical process that converts carbon-based materials into CH_4, H_2, CO_2, H_2O, CO, tar, and heavy hydrocarbons, enabling high carbon conversion efficiency with lower greenhouse gas emissions.

This study investigates the gasification of nine different biomass samples blended with lignite using two models: fluidized-bed gasifiers and fixed-bed gasifiers. Simulations are conducted in ASPEN Plus® under various conditions, including biomass-to-lignite ratio, steam-to-biomass ratio (SBR), equivalence ratio (ER), and temperature, to assess their effects on syngas composition and system efficiency.

Additionally, the chemical exergy values of syngas and product gas compositions are predicted using four machine learning algorithms— Gaussian Process Regression (GPR), Random Forest (RF), Support Vector Machine (SVM), and Decision Tree (DT). These models, implemented in MATLAB, aim to analyze the complex relationships between process parameters and gasification performance, providing a data-driven approach for optimization.

By integrating process simulations with machine learning techniques, this study seeks to enhance syngas yield and quality while minimizing environmental impacts. The findings will contribute to the advancement of biomass gasification technology, supporting the transition to cleaner hydrogen production.

Key Words: Biomass gasification, hydrogen, exergy, simulation, machine learning

ÖZET

Linyit Kömürü ve Biyokütle Karışımlarının Gazlaştırılmasından Elde Edilen Sentez Gaz ve Ekserji Verilerinin Makine Öğrenmesi Algoritmaları ile Tahmini

Mislina ÇAKAR

Kimya Mühendisliği Anabilim Dalı
Kimya Mühendisliği Programı
Yüksek Lisans Tezi

Danışman: Prof. Dr. Hasan SADIKOĞLU

Eş-Danışman: Dr. Öğr. Üyesi Özgün YÜCEL

Dünya, iklim değişikliği, hava kirliliği ve habitat bozulması gibi ekolojik dengeyi tehdit eden ciddi çevresel sorunlarla karşı karşıyadır. Bu etkileri azaltmak için sera gazı emisyonlarına neden olan süreçlerin ortadan kaldırılması gerekmektedir. Bu bağlamda, biyokütle gazlaştırma yoluyla sentez gazı (syngas) üretimi, temiz hidrojenin sürdürülebilir bir enerji taşıyıcısı olarak elde edilmesinde önemli bir rol oynamaktadır. Biyokütle gazlaştırma, karbon bazlı malzemeleri CH_4, H_2, CO_2, H_2O, CO, katran ve ağır hidrokarbonlara dönüştüren termo-kimyasal bir süreç olup, yüksek karbon dönüşüm verimi sağlarken sera gazı emisyonlarını da azaltmaktadır.

Bu çalışmada, dokuz farklı biyokütle numunesinin linyit kömürü ile karıştırılarak gazlaştırılması, sabit yataklı (fixed-bed) ve akışkan yataklı (fluidized-bed) gazlaştırıcılar olmak üzere iki model kullanılarak incelenmiştir. ASPEN Plus® yazılımında gerçekleştirilen simülasyonlar kapsamında biyokütle-linyit oranı, denklik oranı (ER), buhar-biyokütle oranı (SBR) ve sıcaklık gibi işlem

parametreleri değerlendirilerek sentez gazı bileşimi ve sistem verimliliği üzerindeki etkileri analiz edilmiştir.

Ayrıca, sentez gazının kimyasal ekserji değerleri ve ürün gazı bileşimleri, dört farklı makine öğrenmesi algoritması—Destek Vektör Makinesi (SVM), Rastgele Orman (RF), Gauss Süreç Regresyonu (GPR) ve Karar Ağacı (DT)—kullanılarak tahmin edilmiştir. MATLAB ortamında uygulanan bu modeller, süreç parametreleri ile gazlaştırma performansı arasındaki karmaşık ilişkileri analiz ederek veri odaklı bir optimizasyon yaklaşımı sunmayı amaçlamaktadır.

Bu çalışma, süreç simülasyonları ile makine öğrenmesi tekniklerini entegre ederek sentez gazı verimi ve kalitesini artırmayı, çevresel etkileri en aza indirmeyi hedeflemektedir. Elde edilen bulgular, biyokütle gazlaştırma teknolojisinin geliştirilmesine katkı sağlayarak temiz hidrojen üretimine yönelik sürdürülebilir çözümleri destekleyecektir.

Anahtar Kelimeler: Biyokütle gazlaştırma, hidrojen, ekserji, simülasyon, makine öğrenmesi

1
INTRODUCTION

1.1 The Quest for Sustainable Energy

The energy business is a critical component of society as it is inextricably linked to global economic growth and living standards [1]. Population growth, commercial needs, economic considerations, and new technical outputs all contribute to an increase in energy demand [2], [3]. Crude oil and natural gas comprise petroleum, the main source of energy for over a century. It has served as the major energy transporter for oil and natural gas. Oil products make up roughly 154 Exajoules (almost 40%) of total world final consumption, surpassing natural gas (18%) and electricity (23%). The transportation and industrial sectors together account for 58% of worldwide energy consumption and 43% of carbon dioxide emissions. The combustion of petroleum has resulted in environmental challenges and climate change, forcing the search for other, sustainable energy sources [4]. Researchers have developed energy-linked networking and can predict future patterns, representing energy issues. According to the World Energy Council, renewable energy will be the major energy source by 2060 [5]. Wind, solar, and hydropower are examples of renewable energy sources that are leading the energy transformation. These sources are critical for reducing our reliance on fossil fuels and reducing carbon emissions [6].

As to the International Energy Agency (IEA) estimates that current policies will increase global energy demand by roughly 25% by 2040. This rise is especially noticeable in developing economies, where industrialization and living standards are quickly improving. The United Nations predicts that the global population will reach 9.7 billion by 2050, rising energy consumption. People moving from rural areas to cities boost energy demand since urban living requires more energy. Cities are economic centers that require energy for transportation, manufacturing, and

services. Economic progress is closely linked to rising energy consumption. As countries advance from low- to middle-income status, energy demand grows rapidly, driven by the expansion of energy-intensive sectors like manufacturing, transportation, and construction. Industrialization and urbanization further amplify this demand, reflecting the strong connection between economic growth and energy use [7].

1.2 Aim of Thesis

Turkey aims to reduce its dependence on imported energy resources, particularly natural gas, and to utilize domestic resources, particularly lignite coal. Lignite resources will be utilized to contribute to this goal.

Turkey has rich lignite deposits. Low caloric lignite coal (with high moisture and ash content) will be properly utilized for hydrogen economy. An example of lignite beds are given in Map 1.1 [8].



Map 1.1 Lignite map [8]

The study contributes to the sustainable development goals of Affordable and Clean Energy (SDG-7), Industry, Innovation and Infrastructure (SDG-9) and Climate Action (SDG-13).

A wide range of waste will be utilized. It is aimed to simulate various and unique biomasses from sewage sludge to plastic waste and electronic waste in the gasification process.

It is aimed to serve the needs specified in the Turkish Hydrogen Technologies Strategy and Roadmap published by the Turkish Ministry of Energy and Natural Resources.

Based on the following items in the Turkish Hydrogen Technologies Strategy and Roadmap published by the Ministry of Energy and Natural Resources of the Republic of Turkey,

"Carrying out hydrogen production studies from domestic sources (natural gas, lignite and organic wastes)", 'Establishing a sector to produce hydrogen from renewable energy sources' and 'Improving existing infrastructures (laboratories, test systems, etc.) related to hydrogen technologies in universities, public and private sector research centers, ensuring cooperation and coordination".

While using Aspen Plus, biomass gasification processes will be simulated

Exergy analysis of different biomass gasification processes after validation of the simulation study

Modeling of simulated data with various machine learning methods

Determining the optimal model for each method through hyperparameter optimization

To examine the application of machine learning methods in the energy sector by comparing their performance within themselves and with the values obtained in the literature.

The project aims to reduce foreign dependency, use local fuel, produce clean fuel (hydrogen), develop processes used in industry, examine the applicability and performance of machine learning methods in the energy sector, and shed light on related studies by publishing articles.

2
BACKGROUND OF HYDROGEN ENERGY

2.1 Climate Actions Worldwide

Several organizations worldwide are actively engaged in acting on climate actions. These organizations work at multiple levels global, regional, national, and local and address various aspects of climate change, such as policy lobbying, scientific research, mitigation, adaptation, and public awareness. Established in 1992, the United Nations Framework Convention on Climate Change (UNFCCC) is the principal international body overseeing global initiatives to address climate change. As the parent treaty of the 2015 Paris Agreement, it plays a crucial role in efforts to limit global warming. The UNFCCC holds annual Conferences of the Parties (COPs) during which countries negotiate climate accords, establish global climate policy, and track progress using systems such as Nationally Determined Contributions (NDCs) [9]. An intergovernmental organization, the International Renewable Energy Agency (IRENA) is focused on aiding countries in their transition to sustainable energy systems. It promotes the extensive and sustainable utilization of renewable energy resources. IRENA collects data, provides policy advice, and develops financing solutions for renewable energy deployment, as well as tracking worldwide renewable energy progress [10]. In this regard, the United Nations has issued a universal call to action by 2030 known as the Goals for Achieving Sustainable Development. The Sustainable Development Goals (SDGs) of the United Nations constitute an inclusive framework designed to address global challenges, such as poverty, inequality, environmental degradation, and the advancement of peace.

Established in 2015 as a component of the 2030 Agenda for Sustainable Development, the SDGs consist of 17 goals and 169 targets designed to secure a sustainable future for humanity [11]. An additional milestone in addressing climate

change occurred on December 12, 2015, when 196 nations convened at the 21st Conference of the Parties (COP21) under the UNFCCC in Paris, France, to negotiate and formally adopt the Paris Agreement. The primary objective of this accord is to restrict the rise in global mean temperature to well below 2°C above pre-industrial levels, with an aspirational target of limiting the increase to 1.5°C. Central to the Paris Agreement is the concept of a carbon budget, which plays a pivotal role in guiding its implementation. It refers to the maximum quantity of CO2 that can be emitted while still having a good chance of keeping global warming under a given temperature target. The remaining carbon budget for the 1.5°C objective was expected to be around 420 gigatons of CO2 in 2020, emphasizing the importance of swift and deep emissions cutbacks [12].

2.2 Climate Actions in Türkiye

Turkey has signed the Paris Agreement in 2016 which is approved by TBMM in 2021, 7th of October. Turkey aims to reduce the fossil fuel usage and apply using renewable sources and sustainable processes to produce required energy due to the affection of climate change. The area of Akdeniz is highly damaged, the source of water decreases and desertization are the outcomes of climate change foreseen so far in Turkey [13]. Turkey also, has been a participant member of the UNFCCC since 2004 when it was recognized as a developing country. Since then, Turkey has been involved in the UNFCCC process, attending Conferences of the Parties (COPs) and other international climate negotiations. Turkey periodically provides National Communications and Biennial Update Reports (BURs) to the UNFCCC, which outline its emissions, climate initiatives, and achievement of its commitments. Turkey's newest (7th) National Communication, submitted in 2018, outlines its climate mitigation and adaptation policies, strategies, and projections [14]. In addition, Turkey has made major investments in renewable energy, hoping to diversify its energy sources and minimize its reliance on fossil fuels. The Renewable Energy Resources Support Mechanism (YEKDEM) offers subsidies for renewable energy projects. YEKDEM and YEKA (Renewable Energy Resource Areas) are two organizations to encourage the use of renewable sources in renewable energy sector. They both have different approaches to achieving their

objectives. While YEKDEM focusses on improving the overall financial situation when using renewable resources, YEKA focusses on establishing large-scale Renewable Energy Designated Areas ("REDAs") on either public / treasury or privately owned property in order to make the most of renewable energy sources. In this regard, completing investment projects quickly by assigning these regions to investors, as well as allowing high-tech equipment used in generation facilities to be built or supplied locally, will help with technology transfer [15]. The Turkish ministry has declared hydrogen as a priority area due to its role in a sustainable energy future. The goal is to establish a carbon zero economy model based on H_2 that is consistent with our economic development goals and net zero carbon emission targets for 2053. To attain this purpose, the "Turkey Hydrogen Technologies Strategy and Roadmap" has been developed [16]. Consequently, strategic visions and policy recommendations have been formulated for Turkey. Key proposals outlined in the roadmap include the following: According to the Hydrogen Technologies Strategy and Roadmap released in April 2023, the installed capacity of electrolysis systems is projected to reach 5 GW by 2035 and expand further to 70 GW by 2053.

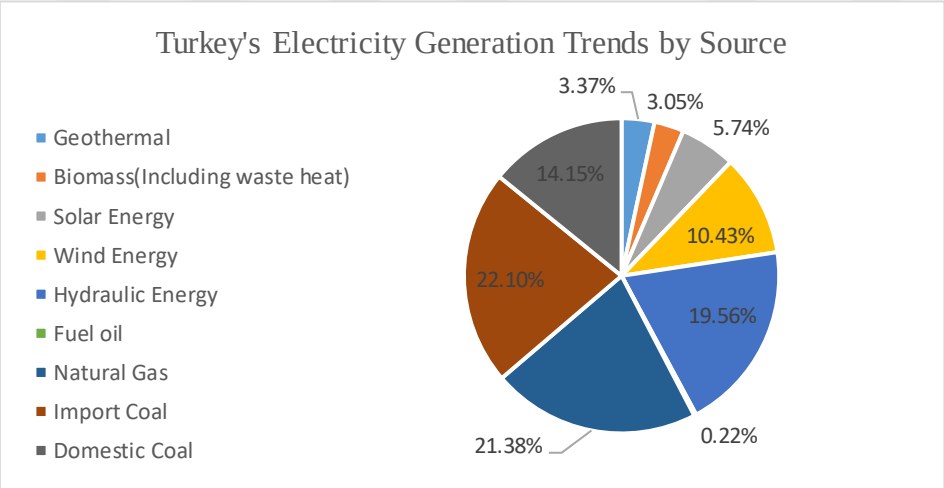


Figure 2.1 Turkey's electricity generation trends by source [16]

Sources used in electricity generation in Turkey is presented in Figure 2.1. Additionally, it is projected that the expense of generating green hydrogen will reduce from USD 2.4 per kilogram in 2035 to half that amount by 2053. As part of Turkey's 2030 National Energy Plan, a targeted electrolysis capacity of 1.9 GW has been established [16].

When looked Turkey's total energy generation in 2023 is 326.3 TWh, with Renewable Energy Sources accounting for only 42.15% [15].

Renewable energy sources are expected to account for 54.8% of total electricity output by 2035, up from 42.15% in 2023. Renewable energy sources are expected to account for 64.7% of installed capacity by 2035, up from 55.53% in 2023 [15].

2.3 Hydrogen

2.3.1 Hydrogen in the World

Hydrogen, with its high volumetric energy density (120 MJ/kg) and minimal environmental impact, represents a crucial alternative energy carrier to conventional fossil fuels. It is currently widely employed in various sectors, including the steel industry (as a reducing agent), the chemical industry (as a feedstock), petroleum refining, and specialized applications across other industries. In 2022, the H_2 utilization in refining exceeded 41 million tons. North America and the Middle East saw the highest year-on-year demand growth, accounting for over 1 Mt, or over 75% of worldwide growth in 2022. In 2022, the manufacturing of hydrogen for refining emitted 240-380 Mt of CO_2 into the environment. The projection for the Net Zero Emissions (NZE) scenario indicates that by 2030, over 4 million tonnes of low-emission hydrogen will be produced and utilized in refineries. Approximately two-thirds of this hydrogen will be generated through electrolysis powered by low-emission electricity, while the remaining one-third will be sourced from fossil fuels in combination with Carbon Capture, Utilization, and Storage (CCUS) technologies. As of 2022, hydrogen consumption in the industrial sector amounted to 53 million tonnes. Within the iron and steel industry, approximately 60% of this hydrogen was allocated for ammonia production, 30% for methanol synthesis, and 10% for Direct Reduced Iron (DRI) processes [17].

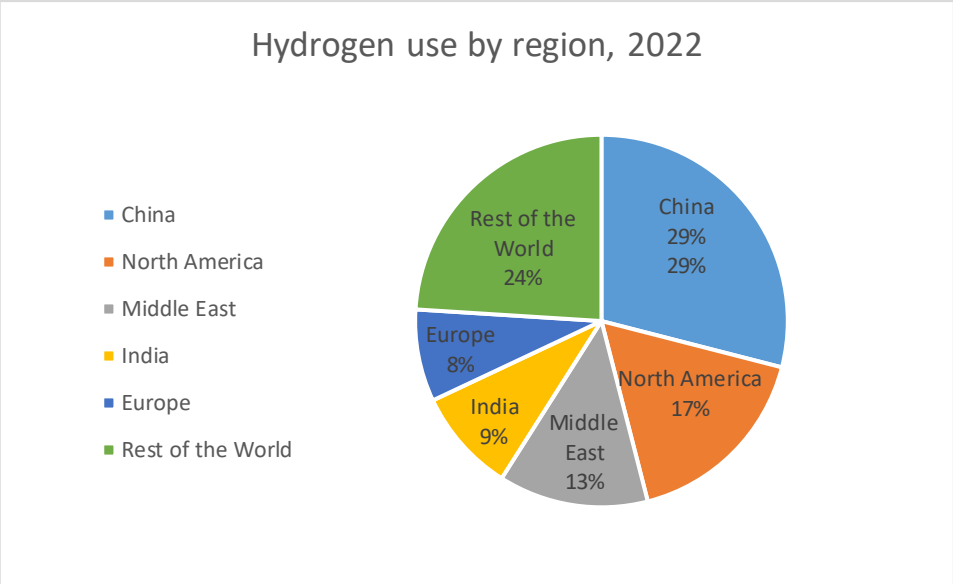


Figure 2.2 Hydrogen use by region [17]

Figure 2.2 illustrates hydrogen use worldwide. In 2022, global hydrogen demand in industrial applications increased by 2% compared to 2021, with the primary drivers being a 0.4% rise in ammonia demand, a 5% increase in methanol demand, and a 4% increase in DRI consumption. However, these growth rates were notably lower than the averages observed in previous years. China is the largest consumer of hydrogen in industrial applications, accounting for 35% of global demand, followed by the Middle East at 14%, North America at 10%, and India at 9%. In 2022, the energy crisis triggered by Russia's invasion of Ukraine resulted in a decline in industrial hydrogen consumption in Europe, which remains the only major consumer region affected. Under the Net Zero Emissions (NZE) scenario, hydrogen demand in the industrial sector is expected to rise to 70 million tonnes by 2030 [17]. A chart given in Figure 2.3 illustrates the disclosed low-emission hydrogen production initiatives [17].

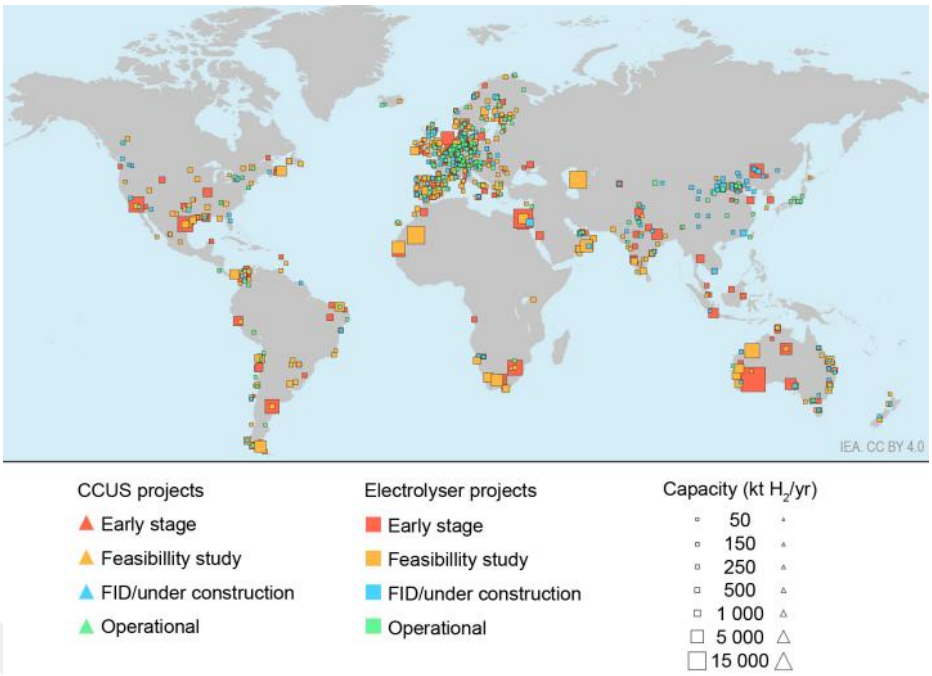


Figure 2.3 A chart illustrating the disclosed low-emission hydrogen production initiatives [17]

2.3.2 Hydrogen in Türkiye

The "Medium Term Program (2023-2025)," published in the Official Gazette on September 4, 2022 (No. 31943), outlines the steps to be taken across all sectors to achieve Turkey's 2053 net zero emissions target. This will be done within the framework of resource-efficient, competitive green transformation policies, aligned with ongoing EU initiatives, which is Turkey's primary export market. However, in Turkey:

Research and development projects focused on green technologies, especially within the industrial, agricultural, transportation, and energy sectors, will continue to receive support to establish a robust infrastructure for green transformation. Additionally, the investment ecosystem for technologies that facilitate emissions reductions, such as green hydrogen and energy storage, will be further developed.

A medium-term low-carbon growth strategy will be presented on the path to the net-zero emissions goal, the quantity of extra funds that businesses require for a green revolution will be determined, and various support mechanisms will be designed to safeguard their ability to compete,

Access to environmental financing will be increased by addressing the demands of the private market, with a focus on transformative, high-value-added projects that raise productivity, decrease emissions of greenhouse gases, and develop environmentally friendly abilities.

To achieve the 2053 net zero emissions target, the Ministry of Energy and Natural Resources released the "National Energy Plan of Turkey," outlining plans to explore the blending of natural gas with hydrogen and synthetic methane, aiming for a 3.5% hydrogen share in the gas mixture [16].

The actions which are applied for hydrogen technology and its usage are mentioned above. In addition to it, knowing the struggles of this technology helps to provide the requirements. In this regard, Türkiye's Hydrogen Technology Needs and Technological/Supportive Solutions are listed below. Deficiencies in our country's the manufacturing of locally produced and nationally developed electrolyzers will be determined, and special project calls will be issued to ensure electrolysis innovation. In this manner, the nation's requirements for electrolysis technologies, essential for the production of green hydrogen, will be met domestically, eliminating the dependence on foreign suppliers.

For mass manufacture of domestic and national electrolysis, including cell and module design.

The manufacture of catalyst, electrode, membrane, and membrane electrode units.

Development of system control hardware and software.

Collaboration between universities and industry will result in the establishment of a test infrastructure. Technology transfer to multinational firms with a high Technology Readiness Level (TRL) in the production of electrolyzes and subcomponents would be facilitated.

Organizations, scholars, research institutions, and innovators focusing on fuel cell technology will come together to identify requirements and form cooperation. The level of localization will be established, along with the strengths and limitations. R&D and P&D calls will be issued to raise the level of technology readiness and popularize fuel cells, as well as to establish mass manufacture and use of fuel cells

in Turkey. Fuel cell technology, to improve technological readiness for mass production:

New cell and module designs,

Development and manufacturing of catalysts, bipolar plates, electrodes, membranes,

Advancement of control system hardware, software solutions, and power regulation systems,

Our services include prototype and mass production support, infrastructure and testing, and project and production support, critical technology transfer partnerships will be formed.

It is vital to evaluate our country's stocks of raw materials in the unique element class that are essential in fuel cell manufacture, and to construct a supply chain based on the amount of requirement by preparing ahead of time in order to avoid disrupting future production. Similarly, if our country's reserves surpass the national demand, the precious metals will be treated and exported.

Our country's hydrogen combustion technology studies will be conducted after determining the current situation, inventorying domestic and national mass production of components, and analyzing strengths and weaknesses, opportunities, and threats.

The integration of hydrogen production facilities with renewable energy plants will yield considerable benefits in terms of efficiency, storage, transmission, and cost. To produce green hydrogen at a low cost, locations with high wind, solar, and hydroelectric energy potential should be identified as hydrogen production zones. A large-scale hydrogen pilot zone will be established, encompassing the refinery, cement, and natural gas distribution industries [16]. In addition, a pilot "pumped storage Hydroelectric Power Plant (HPP)" hydrogen production application will be implemented, allowing surplus electricity to be stored as hydrogen.

In some instances, power plants must restrict or halt electricity generation while balancing supply and demand. This prevents Wind Power Plants (WPP) and Solar Power Plants (SPP) from operating at full capacity, extending the return on

investment period. Hydrogen generation can be achieved by allocating a portion of WPP and SPP production to hydrogen production. Domestic and national electrolysers can be developed and produced by prioritizing domestic enterprises for hydrogen production [16].

In the following some of the possibilities are mentioned for green sustainable H_2 manufacturing on the grand scale which is presented in Figure 2.4.

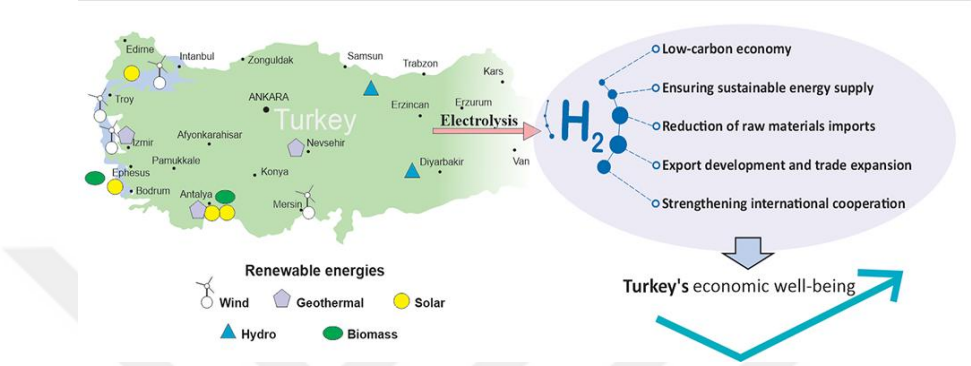


Figure 2.4 Sources of primary clean energy for Türkiye's H2 energy evolution [18]

Türkiye possesses a significant amount of solar energy. To produce hydrogen, photovoltaic systems which are used in water electrolysis have a great opportunity around the country to be built, especially in Antalya, Türkiye.

The winds flow from many directions throughout Türkiye's coast line, offering ideal conditions for wind energy. Wind farms at Aydin and Mugla can power hydrogen production.

Türkiye possesses one among world's greatest geothermal energy reservoirs. Energy from geothermal sources can be used for electrolysis and hydrogen generation in locations like Cappadocia and Pamukkale, which have subsurface thermal pools.

The abundance of H_2O supplies (including lakes, seas, and rivers) holds an opportunity to create hydroelectricity, which could then be utilized to make hydrogen.

The use of biomass and organic waste for hydrogen processes is critical in Türkiye farming and the sawmilling process [18].

2.4 Hydrogen Technologies

H_2 is a safer option than other gases due to its light-weight nature. In its natural condition, H_2 acts as an energy transporter rather than being freely available. H_2's high energy density allows for the storage of large amounts of energy in tiny volumes. H_2 can be created from several energy sources, providing flexibility and cost-effective extraction processes. Using H_2 is economically beneficial as it has applications in manufacturing, energy and transportation [18].

2.4.1 Electrolytic Processes

2.4.1.1 Electrolysis

In hydrogen production, the electrolysis process employs electrical energy to decompose the components of a hydrogen-bearing substance, which functions as the feedstock for electrolysis. The type of feedstock utilized in electrolysis determines the production of hydrogen within separate electrode compartments of an electrolytic system, referred to as an electrolyzer, along with byproduct gases such as oxygen, nitrogen, and carbon dioxide. Typically, hydrogen is generated at the negatively charged cathode, whereas other gases are formed at the positively charged anode, all occurring within the electrolyzer. Electrolysis' ability to separate hydrogen from other gases allows for the creation of high-purity H_2 [19].

Water electrolysis, the electrolysis of water necessitates a fundamental thermodynamic voltage of 1.23 V and an energy input of 285.8 kJ/mol under standard ambient temperature and pressure (SATP) conditions of 1 atm and 25°C. A water-driven electrolyzer employs either a solid or liquid electrolyte to facilitate ion transport and enable electrical conductivity. In a liquid-based electrolyte water electrolyser, a permeable separator infused with an electrolyte solution is utilized to enhance ion transport while preventing the intermixing of gases. In contrast, A liquid-based electrolyzer incorporating the need for a separator is eliminated by a solid-state electrolyte, as the solid-state electrolyte simultaneously functions as an ion conductor and a barrier between gases. Business-wise accessible water

electrolysers operate at temperatures below 100◦C, categorizing them as low temperature.

The alkaline water electrolyser (AWE) operates at ranges of 65-100◦C with an alkaline liquid electrolyte (20-30 wt% sodium hydroxide or potassium solution). Several types of water electrolysers exist, including the proton-conducting membrane electrolyser (PCME), which employs an acidic solid polymer electrolyte membrane, and the anion-conducting membrane electrolyser (ACME), which utilizes an alkaline solid polymer electrolyte membrane and operates at temperatures between 40 and 80°C. The solid oxide water electrolyser (SOWE) is an advanced high-temperature water electrolyser currently in development. This system functions under highly elevated temperatures ranging from 650 to 1000°C and utilizes a solid oxide electrolyte membrane capable of facilitating the transport of oxide ions [19].

In other variants of electrolysis, water electrolysis is a popular method for producing H_2, however the slow kinetics of multiple electron transfer at the anode considerably reduces the conversion of energy yield. Furthermore, this water frequently requires further purification stages to obtain ultra-pure purity before being used in current water electrolysers to preserve its durability, resulting in additional costs, operational complications, and engineering limits. Thus, discovering new electrolysis raw materials such as organic and inorganic carry a great importance. These materials are naturally available and abundant. These possibilities range from commonly found supplies in the environment such as saltwater and various forms of wastewater (which include those organic and inorganic), to raw biomass including rice chaff and switchgrass, as well as its components like cellulose and lignin, and derivatives like glucose etc. [19].

2.4.2 Direct Solar Water Splitting Processes

2.4.2.1 Photoelectrochemical (PEC)

Solar power is gaining popularity as an alternative clean energy supply since although the solar system merely distributes 2.2 billionths of its entire radiant energy into the atmosphere of the earth, the sun nevertheless emits a staggering 173,000 TW [20].

Among the most crucial approaches to harnessing solar energy is solar-induced water decomposition, which converts sunlight into hydrogen (H_2), a readily storable energy carrier. Photocatalysis, Photovoltaic-supported electrolysis, and photoelectrochemical cells are methods of solar water-splitting systems [21].

Nonetheless, the low conversion efficiency of solar-to-hydrogen (STH) remains a source of ongoing research [20].

2.4.3 Biological Processes

2.4.3.1 Microbial Biomass Coversion

The microbial conversion of biomass can be utilized in the production of bio-derived polymers, highlighting the significance of bio-monomers obtained through the fermentation of renewable feedstocks as essential building blocks in the polymer synthesis process. Bio-based polymers are regarded as promising alternatives to petroleum-derived polymers and can be categorized into two types: those fully produced from renewable resources and those derived from a blend of bio-based and petroleum-based monomers. Recent studies have explored a range of fermentation-derived products as potential bio-monomers to produce bio-based plastics [22].

2.4.3.2 Photobiological

Hydrogen gas can be produced by converting solar energy into chemical energy through the photosynthetic mechanisms of both oxygenic and anoxygenic microorganisms. Photosynthetic microorganisms can convert light energy into hydrogen (H_2) as chemical energy. Oxygen-producing microorganisms employ water as an electron donor, releasing molecular oxygen (O_2), whereas non-oxygenic microbes obtain electrons from various organic or inorganic sources. It is conventionally accepted that unbound hydrogen ions present in aqueous solutions combine with electrons provided to generate hydrogen (H_2). However, in practice, protons can also be derived in conjunction with electrons supplied by organic or inorganic substrates. Furthermore, hydrogen can be generated in the absence of light through the activity of fermentative microorganisms [23].

2.4.4 Thermochemical Processes

2.4.4.1 Natural Gas Reforming (SMR, Steam Methane Reforming)

Biomass, recognized as a sustainable carbon resource, presents substantial opportunities for the generation of fuels with low emissions [24]. Steam methane reforming is an established production method that utilizes high-temperature steam (ranging from 700°C to 1,000°C) to generate hydrogen from methane sources, including natural gas. During methane steam reforming, methane interacts with steam under pressures between 3 and 25 bar (1 bar = 14.5 psi) in the presence of a catalyst, generating carbon monoxide, hydrogen, and minor quantities of carbon dioxide. As an endothermic process, it necessitates heat input for the reaction to occur [25].

2.4.4.2 Biomass Gasification

Gasification is a technique that transforms carbon-containing substances into synthesis gas (syngas) at high temperatures, utilizing an oxidizing agent to promote the reaction. The production of hydrogen is highly influenced by the operating parameters of gasification process, including the thermal condition of the steam stream, as well as the kind of feedstock used, that presents a significant challenge [26]. Biomass gasification will be explained in section 2.5.

2.5 Biomass Gasification

There are various ways to use biomass as feedstock to produce energy thus burning of biomass for heat or converting biomass into fuels that are renewable [27]. Thermochemical conversion of biomass via gasification recently gained much interest. Storage and transportation of raw biomass is inefficient economically by comparison to traditional fuels. Besides, the energy density of biomass forms is lower than petroleum-based fuels. Biomass gasification transforms organic solids or liquids into both gaseous and solid phases. The gas phase, known as "syngas," is rich in energy and can be utilized for power generation or the creation of biofuels. The solid phase, termed "char," consists of unreacted organic material and inert components from the biomass. This method involves the partial oxidation of carbon

within the feedstock and is typically performed in the presence of a gasifying agent like oxygen, steam, carbon dioxide or air [28].

The main reactions in gasification are endothermic, with the energy needed for these reactions generally provided by the oxidation of part of the biomass, either through an allo-thermal or autothermal method. In the autothermal method, the gasifier is heated internally by partial combustion, while in the allo-thermal method, the energy for gasification is supplied externally. The gasification process encompasses several essential stages [28]:

Oxidation is an exothermic phase.

Drying represents an endothermic phase.

Pyrolysis occurs as an endothermic phase.

Reduction takes place as an endothermic phase.

Drying consists of eliminating moisture from the feedstock via evaporation. The thermal energy needed for this process is directly related to the feedstock's initial moisture level [28]. The moisture content of biomass feedstock generally varies between 5% and 35% and is reduced to below 5% in the drying stage [29]. The drying process is considered finished when the biomass reaches a temperature of 150 °C [28]. During the pyrolysis phase, the thermochemical decomposition of carbon-based materials occurs, specifically involving the cleavage of chemical bonds to generate molecules with reduced molecular weights. Through pyrolysis, several fractions can be produced: A solid component, a liquid/condensate component, and a gas phase component [28]. In this phase, biomass is heated to temperatures ranging from 200°C to 700°C in an environment with restricted air or oxygen. Under these circumstances, the volatile substances in the biomass are transformed into vapor. This volatile gas is composed of a blend of carbon monoxide, hydrogen, methane, carbon dioxide, water vapor, and heavier hydrocarbons (such as tar) [29].

$$Biomass \leftrightarrow H2 + CO + CO2 + CH4 + H2O(g) + Tar + Char\ (Endothermic)\ [28] \quad (2.1)$$

The solid components consists of the non-reactive substances present in the biomass, which are converted into ash, along with a carbon-rich fraction known as "char". The liquid fraction, commonly referred to as "tars," and the gaseous fraction, which typically constitutes 70–90 wt% of the input material, are both products of pyrolysis. The gaseous phase, referred to as "pyrolysis gas," is predominantly composed of carbon dioxide, carbon monoxide, hydrogen, and light hydrocarbons like methane, in addition to another hydrocarbons containing two and three carbon atoms. It also contains smaller amounts of acid or inert gases. The gases are non-condensable at ambient temperature [28]. Partial oxidation of biomass plays a vital role in generating the heat energy required to drive endothermic reactions and maintain the necessary operating temperature. This oxidation process takes place under oxygen-limited conditions, where the oxygen present is insufficient to completely oxidize the fuel. The partial oxidation process affects all carbon-rich components, including tars; however, for the sake of simplicity, it is commonly assumed that only the char and hydrogen present in the syngas participate in the oxidation reactions. The main reactions taking place during the oxidation phase are outlined below:

$$C + O_2 \rightarrow CO_2 \qquad \Delta H = -394\text{kJ/mol Char combustion} \qquad (2.2)$$

$$C + \tfrac{1}{2} O_2 \rightarrow CO \qquad \Delta H = -111\text{kJ/mol Partial oxidation} \qquad (2.3)$$

$$H_2 + \tfrac{1}{2} O_2 \rightarrow H_2O \qquad \Delta H = -242\text{kJ/mol Hydrogen combustion} \qquad (2.4)$$

Endothermic reduction reactions (2.5-2.6) take place within the gasifier, with the energy required for these processes being supplied by the combustion of char and volatile compounds. Through a series of chemical transformations, these reactions convert the biomass into combustible gases, including hydrogen, carbon monoxide, and methane [29].

$$C + H_2O \leftrightarrow H_2 + CO_2 \quad \Delta H = -41\text{kJ/mole Water gas shift reaction [28]} \qquad (2.5)$$

$$C + 2H_2 \leftrightarrow CH_4 \qquad \Delta H = -75\text{kJ/mole Methanation [28]} \qquad (2.6)$$

$$C + CO_2 \leftrightarrow 2CO \qquad \Delta H = 172\text{kJ/mole Boudouard reaction [28]} \qquad (2.7)$$

$$C + H_2O \leftrightarrow CO + H_2 \qquad \Delta H = 131\text{kJ/mole Reforming of the char [28]} \qquad (2.8)$$

Reactions (2.7) and (2.8) are characterized as endothermic, whereas Reactions (2.5) and (2.6) are exothermic. Despite this distinction, the overall reduction step remains endothermic due to the energy requirements of both the Boudouard reaction (2.7) and char reforming (2.8). As a result, the entire reduction phase demands energy, which is provided by oxidation reactions. Reactions (2.5 to 2.8) are governed by the principles of chemical equilibrium, indicating that the reactants and products exist in fixed proportions, determined by thermodynamic equilibrium. In general, endothermic reactions (2.7 and 2.8) are more favorable at elevated temperatures, causing the equilibrium to shift toward the formation of products, whereas reactions (2.5 and 2.6) are more favorable at lower temperatures. The composition of the syngas, which directly impacts its properties like the lower heating value and tar formation, is primarily determined by the temperature at which the reduction process occurs. The syngas composition is influenced by temperature reduction, which plays a pivotal role in determining both the solid residue properties and the final gas mixture [28], [29]. Biomass gasification as a conversion of biomass solids into desired liquid or gaseous fuels is a way to improve the properties to prevent these problems. Serious chemical reactions, pressure changes, heat and mass transfer phases occur during biomass gasification which make the process complicated [30]. It is therefore essential to assess how operational parameters impact the gasification process. Also, obtaining the applicability of the process is highly matter. Simulation of the gasification process can help optimization of the parameters and generate better conditions for commercial area. Thus, as well as provides cost-efficient and timesaving [31].

Table 2.1 presents the various types of gasifiers that can be employed in the gasification process [32]:

Table 2.1 Types of gasifiers [32]

Type of the gasifier	The positive aspects	The negative aspects
Down-draft	The ability to adjust gas production according to load variations, with minimal sensitivity to the presence of charcoal dust and tar in the fuel.	The design is generally vertical and not suitable for fuels with very small particle sizes.
Cross-draft	A compact design height, rapid load response time, and adaptable gas production.	Extremely high sensitivity to slag formation and significant pressure drops.
Up-draft	Low pressure drops, high thermal efficiency, and minimal propensity for slag formation.	High sensitivity to tar and moisture content in the fuel. A relatively extended duration is needed for the start-up of the internal combustion engine.

2.5.1 Biomass and Lignite

Nowadays, biomass is commonly used form of renewable source of energy. Additionally, its utilization is growing steadily as concerns about the harmful effects of fossil fuel consumption—such as global warming, adverse health impacts, and climate change —continue to rise. Biomass refers to organic matter that stores energy from sunlight in the form of chemical bonds. It is produced by green plants, which convert sunlight into plant material through the process of photosynthesis. It is important to highlight that biomass is a fully renewable energy source, as the CO_2 emitted during its combustion and use does not contribute to a net increase in atmospheric carbon dioxide, since it originates from biological

sources. In other words, plants absorb CO_2 from the atmosphere during their growth and metabolic processes, which is later released through the decomposition of other plants. As a result, utilizing biomass simply accelerates the transfer of CO_2 into the atmosphere, where it can subsequently be absorbed by plants to produce new biomass [33], [34].

Turkey's advantageous geographic location positions it as a key bridge between the energy-rich regions of the Middle East and Central Asia. In light of the nation's ongoing social and economic development, there has been a significant surge in the demand for energy, with a particular emphasis on electricity consumption. Energy has become one of Turkey's key priorities for development. The swift rise in domestic energy consumption has led Turkey to rely more heavily on foreign energy sources. Turkey's primary domestic energy resources include lignite, hydroelectric power, and biomass. The majority of electricity in the country is generated by thermal power plants, which utilize coal, lignite, natural gas, fuel oil, and geothermal energy, as well as by hydropower plants [34].

Lignite is the primary domestic energy source in Turkey and has been the main contributor to electricity generation for many years. Lignite, a coal variety in the early stages of coalification, exhibits properties that are intermediate between bituminous coal and peat. It is characterized by high moisture content and relatively low energy value. Currently, it is considered one of the most cost-effective energy sources. Lignite is a crucial resource for electricity generation in Turkey due to the country's vast lignite reserves. By the end of 2015, Turkey's proven lignite reserves totaled approximately 15.6 billion tons, representing about 7.1% of the global lignite reserves (Turkish Coal Enterprises). The electricity generation sector is the primary consumer of lignite, accounting for 88% of its total use, while industrial sectors and residential/office use make up 6.3% and 4.7%, respectively (Turkish Coal Enterprises, 2015) [35]. Additionally, According to the Turkish Statistical Institute, lignite production was 7 million 259 thousand 375 tons in December 2022 [36].

Understanding the combustion behavior of coal and biomass fuels, both individually and in combination, is crucial, as interactions between the two may influence the overall process efficiency. Factors like flue gas emissions and the

tendency for fouling often do not vary in a linear manner with the fuel mixture. It is important to thoroughly assess the compatibility of alternative fuels with combustion performance to ensure the effective design and operation of thermochemical conversion systems [37]. Since lignite coal is a big amount of energy source in Turkey, many biomass samples and lignite coal mixture is a promising potential for clean energy goal. Additionally, reducing external dependence carries quite importance when local energy sources are used.

2.6 Physical and Chemical Exergy

There are four types of exergies to be described thus physical, chemical, potential, and kinetic. Kinetic and potential exergies can be neglected. Physical exergy is the maximum quantity of work gained from the available system with the changes in temperature and pressure. The changes happen with temperature and pressure of the reference system. Chemical exergy shows the maximum quantity of work of the system with temperature and pressure that changes in composition, besides temperature and pressure of the reference system. Reference-area situation and dead-state are the conditions represented respectively. Since chemical reactions are present in a system, it is important to determine the chemical exergy of the system. Chemical exergy is a major factor in electricity production loops which use combustion unit, fuel cells, biomass gasification systems, distillation unit and petrochemical production facilities [38].

Exergy analysis of complex energy systems involves extensive computations, making it challenging to quickly analyze systems when environmental parameters change. Recently, researchers have integrated the process simulator Aspen Plus with exergy analysis, enabling exergy evaluations of complex energy systems through its tools. Compared to other methods, exergy analysis using Aspen Plus offers a simpler calculation process and facilitates easier analysis of the relationships between variables [39].

Aspen Plus is capable of simultaneously calculating the exergy values for all streams within the flowsheet. In Aspen Plus, exergy is determined solely based on enthalpy and entropy, meaning that factors such as heat, pressure, and work generated or consumed during interactions are accounted for only to the extent that

they can be represented by the stream's enthalpy and entropy [40]. Exergy calculations for material streams can be broken down into several components, some of which are excluded in the analysis: potential exergy and kinetic exergy. However, these terms can be included in the calculated exergy values if needed. Currently, only internal exergy has been considered, which is determined as the sum of chemical and physical exergy [41]. Stream exergy is determined by calculating the differences in enthalpy and entropy between the process state and the reference environmental state [40]. Physical exergy is determined using Equation (2.9), which relies on data obtained from the Aspen Plus simulation [41].

$$Exphys = h - h0 - T0(S - S0) \quad (2.9)$$

Chemical exergy can be calculated using equation (2.10) below and after calculating the chemical exergy of each element, the chemical exergy of each stream is determined. However, this calculation is performed only once for each unique stream composition since the specific chemical exergy (kJ/kg) remains consistent across all streams with the same composition [41].

$$\widetilde{Ex}_{\text{chem}}(X) = \sum_i n_i \widetilde{Ex}_{chem,i}(elementals) + \tilde{f}_{form}(X) \quad (2.10)$$

Exergy analysis is conducted on the modeled system using data derived from simulations and exergy equations. Furthermore, Aspen Plus's sensitivity analysis function is employed to examine the factors contributing to exergy loss, enabling the evaluation of how these factors influence the system's exergy efficiency. The findings from the exergy analysis identify the distribution of energy losses within the thermal power plant, offering objectives and strategies for improving energy efficiency and reducing environmental impacts [39].

2.7 Machine Learning for Hydrogen Energy Applications

A class of algorithms known as Machine Learning (ML) allows software systems to autonomously improve their predictive accuracy, eliminating the need for direct programming. At its core, ML involves developing algorithms that process input data, employ statistical methods to predict outcomes, and refine these predictions as new data is introduced. Machine Learning is widely applied in areas like image

processing, cybersecurity, forensics, forecasting, and more. Extensive research has been conducted on biomass gasification, with a significant focus on the application of machine learning techniques to develop regression models, as highlighted in existing studies [42].

Machine learning offers a dependable alternative to traditional models for analyzing and understanding the complexities of waste biomass gasification. Recently, machine learning (ML) has been applied to investigate the reaction mechanisms of various biomass conversion processes. In this work, four machine learning algorithms are applied to study syngas gas compositions that are H_2, CH_4, CO, CO_2, and exergy value of the gasification process: Decision Tree Regression, Support Vector Machines, Random Forest, and Gaussian Process Regression [42], [43].

2.7.1 Decision Tree Regression

Decision Trees (DT) are a commonly employed and easy-to-understand machine learning technique used to construct predictive models through simple logical conditions. Decision Trees (DT) generate a sequence of queries, such as "is equal to" or "is greater than," based on the feature set. Depending on the "yes" or "no" response, another question follows. This process continues until no further queries are required, at which point the final outcome is determined. The tree is constructed by iteratively splitting the dataset into two parts. Each possible split for all features is evaluated using a measure of randomness, like entropy [44]. When constructing a decision tree, the algorithm divides the feature space into multiple regions. For each region, a specific split point is identified, and the splitting process is applied to the resulting sub-regions. This initially produces a large tree structure, which often leads to overfitting. To address this issue, a technique called pruning is used, which eliminates unnecessary branches to simplify the model [45].

2.7.2 Support Vector Machines

Support Vector Machines (SVMs) are a class of algorithms primarily designed for binary classification tasks, but their approach is also highly effective for handling other classification and regression challenges [45]. Support Vector Machine (SVM) is a supervised learning method that utilizes labeled data for its operations. It is one of the most commonly applied techniques for addressing classification and

regression problems. In SVM modeling, the objective is to position data points as close to the hyperplane as possible. Hinge loss is employed to maximize the margin between data points and the hyperplane. Additionally, the regularization parameter in SVM plays a crucial role in balancing margin maximization with loss minimization [46].

2.7.3 Gaussian Process Regression

Gaussian Process Regression (GPR) is a machine learning method that is kernel-based, nonparametric, and grounded in probabilistic principles. As a fully probabilistic approach, GPR provides flexible and straightforward regression modeling, making it widely applicable across diverse fields. Its versatility and ease of implementation contribute to its extensive use in various domains [47]. The objective, given a specific training dataset, is to derive a function capable of mapping the input feature vector (X) to its associated output value (y), as represented in the equation:

$$y = (X) + \mathcal{E} \tag{2.11}$$

$$\log (y| X, \theta) = ½y^T K^{-1} y - ½\log | Ky | - \log 2л \tag{2.12}$$

$$Y \sim N (0, . K (X, X) + \sigma^2 I) \tag{2.13}$$

This equation can be expressed using a Gaussian distribution, as illustrated in equation (2.13). In the provided equation, K(X, X) signifies the kernel function, while ε represents Gaussian noise characterized by a mean of zero and a variance of σ^2. The significance of θ lies in its role in regulating the model's complexity and ensuring effective generalization. Proper adjustment of θ is crucial to avoid both overfitting and underfitting, thereby enhancing the model's robustness when applied to unseen data [48].

2.7.4 Random Forest (RF)

Random forest (RF) is an ensemble learning algorithm, which was first proposed by Breiman [46]. Random Forest as an advanced machine learning approach that combines multiple decision trees into a unified model [47]. The Random Forest algorithm constructs multiple individual decision trees and aggregates their outputs to enhance prediction accuracy. It employs a random sampling approach, using

subsets of the training data to develop the final model. Each tree is trained using a bootstrap sampling method applied to the training dataset. Ultimately, the RF algorithm determines the class by selecting the one with the majority vote among the trees [49]. The Random Forest algorithm addresses variance by employing the bootstrap aggregating (bootstrapping) technique introduced by Breiman. In this approach, for "a" data samples and "b" features, "a" random subsamples are created for each tree. These subsamples are split into in-bag and out-of-bag datasets, typically in a 0.67/0.33 ratio. The in-bag dataset is used to train the regression model, while the out-of-bag dataset provides fresh training instances during repeated iterations of the decision tree, allowing the trees to grow fully without pruning. The optimal tree splits are determined by selecting "b" random features during training, where "b" is a parameter set to be less than the total number of decision trees. These inherent validation capabilities enhance the Random Forest's ability to generalize when tested with independent datasets [50].

2.8 Performance Metrix

In the conducted studies, various performance metrics are employed to assess the reliability and precision of the proposed models. These metrics serve as tools to evaluate the models' applicability and facilitate comparisons with alternative modeling methodologies [51].

2.8.1 Coefficient of determination (R^2)

A statistical measure that quantifies the extent to which the variance in the dependent variable is accounted for by the independent variable. Higher values, approaching 1, signify superior model performance [52].

$$R^2 = 1 - \left[\frac{\sum_{i=1}^{m}(y-\hat{y}_i)^2}{\sum_{i=1}^{m}(y-\bar{y}_i)^2}\right] \quad (2.14)$$

2.8.2 Adjusted coefficient of determination (Adj R^2)

The R^2 value evaluates a model's fit by measuring the degree of variability in one parameter explained by another. A value near 1 signifies stronger model performance [52].

R^2 =1 - (sums of squares error/sums of squares total) (2.15)

2.8.3 Root Means Square Error (RMSE),

This metric is particularly advantageous for models with substantial errors that could significantly impact their effectiveness. Since it does not rely on the absolute value of the error, it serves as a highly practical parameter. A lower value signifies improved model performance [52].

$$\text{RMSE} = \sqrt{\frac{\sum_{i=1}^{m}(y_i - \hat{y}_i)^2}{m}} \quad (2.16)$$

3
LITERATURE REVIEW

The effectiveness of machine learning models will be assessed using data derived from the gasification processes of biomass and lignite. As a subfield of artificial intelligence, machine learning has demonstrated its efficacy in predicting gasifier performance, as evidenced by numerous studies in literature. In this context, a study conducted by Kim et al. 2023, utilized Random Forest (RF), Artificial Neural Network (ANN), and Support Vector Machine (SVM) algorithms to predict syngas compositions and lower heating values (LHV) under a broad range of operating conditions in a fluidized bed gasifier, using various lignocellulosic biomass feedstocks [53]. Similarly, research by Elmaslar Ozbas et al. 2019 investigated syngas production using a laboratory-scale fixed-bed updraft gasifier with pure oxygen (O_2) and dry air as gasifying agents. The gas compositions were analyzed in real-time using an online gas analyzer, and the prediction of hydrogen (H_2) concentration was performed using Linear Regression (LR), K-Nearest Neighbors (KNN), Support Vector Machine (SVM), and Decision Tree (DT) algorithms. These predictions were based on process parameters such as time, temperature, CO, CO_2, CH_4, O_2 compositions, and heating values [54]. Kartal and Özveren, 2022 underscored the importance of calculating the chemical exergy of roasted biomass as a critical factor in assessing and optimizing the efficiency of biochar-based power plants. They calculated the exergy of roasted material based on the parameters of heat treatment conditions prior to the roasting process. Subsequently, an Artificial Neural Network (ANN) model was created to directly predict the chemical exergy of roasted biomass based on the proximate analysis results of raw biomass samples [55]. Similarly, in the study conducted by Sezer et al. 2021, the chemical exergy value of syngas was estimated using ANN, a machine learning approach, in a downdraft gasifier with 22 different biomass samples. Among these,

hazelnut shell was specifically selected for further analysis, and the effects of gasifier operating parameters on chemical exergy value, syngas composition, and lower heating value were examined. The parameter study in the downdraft gasifier revealed that temperature and the steam-to-biomass ratio significantly influenced both the composition and exergy value of syngas. It was determined that an increase in temperature led to higher concentrations of H_2 (hydrogen) and CO (carbon monoxide) while reducing CH_4 (methane) content in the syngas composition. Additionally, the chemical exergy of syngas increased with rising temperatures. The predictive performance of the ANN model using hazelnut shell as biomass feedstock was validated, demonstrating its high accuracy. The ANN model proved to be a highly effective tool for accurately estimating the chemical exergy value of syngas in downdraft gasifiers, eliminating the need for complex calculations and costly experimental studies [2]. S. Sezer et al. 2021, investigated syngas production using the Aspen Plus simulation program with a bubbling fluidized bed gasifier and 16 different biomass samples. Gasification temperature, steam as an oxidizing agent, and fuel flow rate were selected as input parameters. Based on the defined system and operational parameters, the exergy estimation of the syngas was modeled using the Levenberg-Marquardt algorithm, which was employed to train the Artificial Neural Network (ANN) model. The hydrogen mole fraction in syngas was further analyzed under varying steam-to-fuel ratios and gasification temperatures. It was found that when the hydrogen content in syngas peaks, the corresponding exergy value demonstrates a minimal relative error [56]. Similarly, Ascher et al. 2022, analyzed the machine learning techniques frequently applied in modeling gasification and pyrolysis processes, discussing their applications, advantages, and limitations. Artificial Neural Networks (ANNs) were identified as one of the most widely utilized machine learning techniques for these thermochemical processes, which are inherently complex and require advanced modeling approaches. The ability of ANNs to model complex, non-linear relationships between input and output variables makes them particularly advantageous in various applications. However, alternative methods, including regression techniques, tree-based models, and support vector machines, may also be suitable depending on factors such as specific application requirements, data

availability, and computational efficiency. Their findings indicate that machine learning has considerable potential for developing models with improved accuracy in gasification and pyrolysis studies [57]. Ascher and colleagues utilized seven distinct machine learning techniques to model biomass and waste gasification under diverse operating conditions. This study developed and systematically compared various machine learning (ML) approaches for modeling biomass and waste gasification. Unlike many previous studies that focused on a limited range of feedstocks and operating conditions, Ascher et al., 2022b, this research utilized an extensive dataset encompassing diverse feedstock types and gasifier configurations. The performance of the model was improved by optimizing the preprocessing stages for each machine learning technique and refining hyperparameters through a search algorithm. The variables selected for model development encompassed feedstock composition (such as carbon, hydrogen, sulfur, ash, and moisture content), particle size, gasifier temperature, operating mode (batch or continuous), scale of the gasifier, equivalence ratio (ER), catalyst use, type of gasifying agent, reactor configuration, and bed material. Gradient boosting regression demonstrated superior performance compared to other model types, achieving an average coefficient of determination (R^2) of 0.90 across ten critical gasification outputs. The models analyzed showed the greatest sensitivity to the particle size of the feedstock and the type of gasifying agent used. The integration of global and local interpretability techniques has enhanced the comprehension of black-box models [58]. Yang and co-researchers sought to develop a comprehensive machine learning (ML) model for predicting and analyzing the municipal solid waste (MSW) gasification process. This approach facilitates the safe disposal of MSW while enabling its sustainable conversion into bioenergy, contributing to regional planning initiatives. The goal is to create a unified and standardized database that encompasses municipal solid waste (MSW) sources under varying gasification conditions, followed by statistical analysis of the collected data. To predict the distribution of syngas, char, and tar, as well as the quality of syngas during municipal solid waste (MSW) gasification, three machine learning techniques—support vector machine (SVM), random forest regression (RFR), and gradient boosting regressor (GBR)—are employed, utilizing feedstock characteristics and

gasification parameters as input. Utilizing a gradient boost regressor for modeling achieves the highest prediction accuracy, with R^2 exceeding 0.926, RMSE below 6.318, and RRMSE under 0.304. Additionally, SHapley Additive exPlanations (SHAP) analysis is effectively applied to interpret the importance and impact of descriptors on the target variables in the modeling process [59]. Olca and Yucel, explored the impact of incorporating operating time as a predictor on the performance of developed models. Including this parameter introduced phase-specific information, enabling the integration of sequential experimental datasets. In contrast to most prior studies that favor the holdout method, this research adopted nested cross-validation for model evaluation, emphasizing its impartiality. Various modeling techniques, including least squares, Gaussian kernels, generalized additive models, random forests, and artificial neural networks (ANN), were employed to predict the syngas composition and higher heating value (HHV) of the process. The analysis of feature importance revealed that operating time plays a pivotal role in the gasification process, with temperature emerging as a key determinant in influencing both hydrogen production and the calorific value of the produced products [60]. The performance of Decision Tree (DT) and Multilayer Perceptron (MLP) models was assessed using k-fold cross-validation, achieving an R^2 score exceeding 0.9. The dataset comprises 5,237 samples, with Principal Component Analysis (PCA) applied for feature selection to identify key independent variables. In machine learning, combining multiple methods is a common strategy to enhance model accuracy. For instance, Kardani and collaborators developed an algorithm for constructing ensemble models, leveraging Particle Swarm Optimization (PSO) to fine-tune and optimize these models [61]. Ayub and collaborators employed artificial intelligence (AI) algorithms to forecast the production of high-quality syngas, characterized by enhanced mole fractions of hydrogen and methane, through the process of hydrothermal gasification (HTG). A comparative assessment of various AI-based methodologies, including Convolutional Neural Networks (CNN), Artificial Neural Networks (ANN), Gradient Boost Regressor (GBR), Extreme Gradient Boost Regressor (XGB), and Random Forest Regressor (RFR), was conducted by the researchers to determine the most effective model. Inputs for these predictive models included the ultimate

analysis of biomass, along with process parameters such as temperature, pressure, biomass solid content percentage, and residence time. The results indicate that XGB outperformed the other algorithms, achieving a coefficient of determination (R^2) between 0.85 and 0.95 and mean squared errors in the range of 0.008 to 0.01. Additionally, the analysis revealed that process temperature and residence time are key factors influencing the mole fractions of hydrogen and methane, with higher hydrogen and oxygen content in biomass playing a significant role in producing high-quality syngas [62]. Pan and colleagues focused on the development of a machine learning (ML) model designed to optimize the co-gasification process of biomass and coal. Additionally, they incorporated an evolutionary algorithm for multi-objective optimization, with the goal of maximizing hydrogen (H_2) production and improving the efficiency of the Fischer-Tropsch process. To underpin their analysis, a comprehensive dataset was assembled from reliable literature sources, covering a range of biomass-to-coal blending ratios and varied process conditions. This dataset underwent thorough statistical evaluation, and mechanistic insights were offered to elucidate the influence of each parameter on the overall process. Among the four machine learning models evaluated, gradient boosting regression yielded the most favorable results, attaining an R^2 value exceeding 0.92, with mean absolute error (MAE) and root mean square error (RMSE) recorded below 2.92 and 3.39, respectively. The study pinpointed optimal conditions for hydrogen (H_2) production at steam yields and temperatures near 1480°C, while the Fischer-Tropsch process exhibited its peak performance under air conditions and temperatures approaching 1570°C. A biomass-to-coal blending ratio between 50% and 70% was found to be effective across nearly all gasifying agents under both optimization criteria.

Additionally, a techno-economic assessment based on the identified optimal conditions revealed that steam outperforms other gasifying agents in terms of economic feasibility and process efficiency [63]. A machine learning algorithm-based Tunable Decision Support System (TDSS) and Tunable Recommendation System (TRS) were developed by Gopirajan and colleagues to optimize process parameters and enhance product yield in biomass hydrothermal gasification (HTG). The research incorporated over 500 datasets, derived from a range of studies and

laboratory experiments, to inform the model. The datasets were initially subjected to analysis to identify correlations, with coefficients calculated using the Pearson matrix. Through statistical assessments, weighted rank aggregates were formed, trends were recognized, and the results were stored in a cloud-based repository. Subsequently, test datasets were evaluated against these identified trends, undergoing iterative refinements until the desired outcomes were achieved. A comparison between the predicted and actual results revealed an accuracy of over 94% in forecasting the HTG process conditions for specific biomass input characteristics. The correlation analysis highlighted that variables such as hydrogen, carbon, volatile matter, moisture, and oxygen content in biomass significantly influence the quality and yield of product gases by affecting key HTG parameters, including temperature (°C), pressure (MPa), catalyst loading (wt.%), solvent-to-biomass ratio (S/B), and reaction time (minutes). As part of the optimization process, the system also modeled the production of pollutant gases like CO and CO2, collectively contributing to the pollution index. The TRS functionality within the framework provides alternative recommendations when input conditions are unsuitable for achieving the desired response. This system demonstrates efficiency in optimizing complex, parameter-driven processes such as HTG [64]. Lian and collaborators employed artificial neural networks (ANNs), a supervised machine learning technique, to assess operational parameters extracted from 52 scholarly sources. These parameters were utilized to evaluate performance in both qualitative and quantitative terms, with a particular focus on metrics such as hydrogen yield (HY), hydrogen content (HC), and carbon conversion efficiency (CCE). A comprehensive analysis was conducted on seven pivotal operational factors: steam-to-biomass ratio (SBR), equivalence ratio (ER), temperature, feedstock particle size, residence time, lower heating value (LHV), and carbon content (CC). Statistical analysis using analysis of variance (ANOVA) identified six binary parameters as having significant effects on the performance metrics (HY, HC, and CCE). Machine learning results were used to recommend optimal operating conditions tailored to desired outcomes. This study provides valuable insights for researchers aiming to optimize operational parameters to enhance hydrogen production in fluidized bed reactors for biomass gasification [65]. Singh

and Kumar conducted a comparative study between circulating fluidized bed (CFB) gasification and traditional coal combustion, identifying CFB gasification as the superior technology due to its adaptability to various feedstocks, proven technological reliability, and cost-efficiency. Their comprehensive financial evaluation revealed favorable results for a 65 MWth circulating fluidized bed (CFB) gasifier, showcasing a net present value (NPV) of ₹20,150 million, an internal rate of return (IRR) of 9.54%, and a payback period of 8.3 years. Sensitivity analysis revealed that factors such as syngas yield, initial investment, and selling prices significantly impact the financial feasibility of the system. Additionally, the environmental advantages of CFB gasification, such as lower emissions and effective waste management, emphasize its potential for sustainable energy generation. The study aligns with governmental efforts like the National Coal Gasification Mission, encouraging further exploration into co-gasification technologies and comprehensive techno-economic evaluations for similar initiatives [66]. Rahimi and Salaudeen utilized machine learning (ML) techniques to optimize and predict the production of hydrogen-rich syngas while minimizing CO_2 emissions. Their study focused on hydrogen concentration enhancement using a calcium oxide-based adsorbent in the gasification process. Four ML models were employed to analyze biomass composition, adsorbent characteristics, the steam-to-biomass ratio, and operating temperature, enabling accurate predictions of hydrogen and CO_2 concentrations. The machine learning (ML) models demonstrated robust performance, achieving an R-squared (R^2) value of 0.92 and root-mean-square errors (RMSE) ranging between 6.77 and 7.44 vol%. Support vector machines (SVMs) were fine-tuned by modifying the training dataset size and employing a radial basis function (RBF) kernel. Additionally, single and multi-objective genetic algorithms were employed to maximize hydrogen concentration, achieving approximately 84vol% and 88vol%, respectively. Through sensitivity analysis, critical parameters such as the fixed carbon-to-volatile matter ratio, oxygen content, adsorbent-to-biomass ratio, and gasification temperature were identified as influential factors. The hydrogen content prediction exhibited a mean absolute percentage error (MAPE) ranging from 7–20 vol%. By optimizing the input configurations for the machine learning models, hydrogen concentration

predictions were improved to within 5 vol%, thereby demonstrating the effectiveness of machine learning methods in precise modeling and optimization of the gasification process [67]. Sakheta and collaborators proposed a hybrid approach that integrates Aspen Plus simulations with machine learning (ML) algorithms to improve the accuracy of gasification output predictions. The study utilized a baseline gasification process flowsheet simulated in Aspen Plus under thermodynamic equilibrium assumptions, which often result in inaccuracies. To overcome these limitations, six ML algorithms were employed to analyze experimental data, focusing on their precision and efficiency. The research explored the significance of feature selection, enhancements in prediction accuracy, and the impact of incorporating ML-derived predictions into the gasification model on the overall process flowsheet. This work highlights the importance of developing more accurate predictive models and demonstrates the significant potential of ML techniques in achieving reliable gasification process predictions [68]. Santhappan and colleagues assessed the performance and accuracy of 27 supervised machine learning (ML) models, each with multiple inputs and a single output, to predict the composition of CO, H_2, CH_4, and CO_2, as well as the higher heating value (HHV) of producer gas (PG) produced through the co-gasification of peanut shell (PS) and spent tea residue (STR). The experiments utilized a 90 m^3/h gas-yield open-core, downdraft gasifier, employing air as the gasification agent while varying equivalence ratios (ERs) and mixing ratios (MRs). After evaluating several performance metrics, 18 models were selected, with their accuracy confirmed across 12 sample runs involving different combinations of ER and MR. The study identified 16 reliable ML models from categories such as linear, neural network, support vector machine, Gaussian process, tree-based, and ensemble methods. These models achieved R^2 values exceeding 0.931, 0.937, 0.962, 0.806, and 0.971 for CO, H_2, CH_4, CO_2, and HHVPG, respectively, except for the tree ensemble (TRE) model. Furthermore, these models exhibited over 95% prediction accuracy for all examined parameters, demonstrating strong reliability in the co-gasification of PS and STR compared to random experimental runs [69]. Azadvar and Tavakoli, 2024 combined machine learning models—namely Decision Tree, Ensemble Learning Tree, Support Vector Machine, and Gradient Boost Regression—with

Differential Evolution Optimization (DEO) to predict and optimize hydrogen production from Supercritical Water Gasification (SCWG). This approach incorporated 24 biomass characteristics and process parameters. The Ensemble Learning Tree enhanced by DEO (ELA-DEO) outperformed the other models, yielding an R^2 of 0.95 and an RMSE of 0.091 for predicting hydrogen yield, while the Support Vector Machine exhibited a relatively lower performance, with an R^2 of 0.73. SHAP analysis revealed that temperature, catalyst type and quantity, and the concentrations of hydrogen and oxygen were the critical factors influencing the process. Further optimization with DEO significantly boosted hydrogen production, which was validated through experiments. For instance, Dunaliella salina generated 12 mmol of hydrogen with 35% selectivity, while black liquor containing 3% wood produced 17.21 mmol, and crude glycerol with $RuCl_3$ yielded 18.7 mmol. Additionally, Dunaliella salina achieved a gas output mole fraction of 64%, which was in agreement with the model's predictions [70].

Kundu and colleagues evaluated Gaussian Process Regression (GPR) for predicting syngas yield (Ysyn) and carbon conversion efficiency with high accuracy ($R^2 > 0.9$), outperforming other ML models. Experimental data were collected under reaction conditions of 550–1000 °C, air flow rates of 0.02–0.04 L/min, and a 2-hour reaction time in a two-stage fixed-bed reactor. Bayesian optimization was applied within a weighted multi-objective framework to maximize both yield and conversion, with results validated experimentally to confirm the optimization's reliability [71]. Bai and co-researchers examined the effects of reaction temperature, residence time, and feedstock concentration on producing hydrogen-rich gases via SCWG of straw in a quartz tube reactor. Higher temperatures, longer residence times, and lower feedstock concentrations enhanced gas production. The gas achieved a maximum LHV of 21 MJ/Nm^3 with CO_2 and 38 MJ/Nm^3 after CO_2 removal. A machine learning model was developed to predict gas yield and LHV, showing strong generalization and potential for broad application in SCWG process optimization [72].

4
METHODOLOGY

4.1 Method

Biomass gasification is one of the most effective methods for converting biomass into a valuable energy source. To achieve higher efficiency in the biomass gasification process, optimization of operating conditions is necessary. Exergy analysis, based on the second law of thermodynamics, allows for the enhancement of process conditions and improved efficiency. Exergy represents the maximum potential useful work that can be extracted from a system. To improve an existing system or process, or to design a new one, exergy analysis is used to identify and quantify exergy losses [73].

The study consists of two stages: simulation of the biomass gasification process in ASPEN PLUS program and modeling with Machine Learning methods. In the first stage, the biomass gasification process using several biomasses will be simulated in ASPEN PLUS program [74]. Biomass gasification encompasses drying, pyrolysis, combustion, and gasification processes. Each kilogram of moisture in the biomass requires a minimum of 2260 kJ of additional energy to evaporate the water within the gasifier, and this energy is not recoverable. As a result, high moisture content in the feedstock presents a challenge, particularly in energy-related applications. [75]. In the biomass gasification process, the first step involves removing moisture from the raw material in the drying unit. The next stage is pyrolysis, where thermal decomposition of larger hydrocarbon molecules in the biomass occurs, breaking them down into smaller gas molecules, some of which may condense, without undergoing chemical reactions with air, gases, or any gasification agents. During gasification, a medium such as air, oxygen, steam, or

supercritical water is required to facilitate the reaction. In this process, oxygen is removed from the fuel to increase its energy density. Both gasification and pyrolysis processes are inherently endothermic, necessitating the input of heat for their progression. In thermal gasification systems, reaction temperatures typically range from 800 to 1000 °C, thereby requiring significant energy to convert biomass or other feedstocks into fuel gases. This heat is usually supplied by burning a portion of the hydrocarbons or carbon present in the raw material within the gasifier, but this results in some energy loss. The final stage, combustion, involves the high-temperature conversion of excess biomass into carbon dioxide and steam in the presence of air [76], [77]. Results of ultimate and proximate analyses for biomass samples used in this study are presented in Table 4.1 [78].

Table 4.1 Results of ultimate and proximate analyses for biomass samples (wt%, dry basis)

		Ultimate Analysis					Proximate Analysis				
	Sample	C	H	O	N	S	MC	Ash	VM	FC	Ref.
1	Hazelnut Shell	41.07	4.83	39.87	0.09	0.75	12.8	0.59	63.7	22.8	[78]
2	Lignite	21.32	1.25	16.12	0.57	0.45	48	14.0	23.4	14.5	[78]
3	Cattle Manure	39.09	4.61	26.68	0.83	0.25	13.8	13.6	60.5	11.9	[78]
4	Electronic Scrap	67.4	6.84	7.66	2.94	0.11	0	10.6	0	0	[78]
5	Sewage Sludge	30.63	4.41	18.03	4.23	1.17	9.9	31.5	48.2	10.3	[78]
6	Agricultural Waste	17.21	2.03	18.39	1.37	1.81	37.8	26.9	29.6	5.56	[78]
7	Microalgae	49.98	6.84	27.34	7.59	0.46	5.22	2.39	77.5	14.8	[78]
8	Macroalgae (Ulva Lacutca)	29.53	5.25	0	2	6.62	0	33.1	0	0	[78]
9	Treated Wood (Recycled wood)	37.1	4.58	0	0.41	0.02	24.9	1.2	0	0	[78]

Table 4.1 Results of ultimate and proximate analyses for biomass samples (wt%, dry basis, continued)

10	Plastic (PVC)	40.02	5.09	0.6	0	0	0.2	0	92.3	7.5	[78]

The following reactions in Table 4.2 occur during the biomass gasification process:

Table 4.2 Reactions in the process of biomass gasification [38]

Oxidation	Drying	Pyrolysis	Reduction
$C+ O_2 \rightarrow CO_2$ $H+1/2O_2 \rightarrow H_2O$ $H+1/2O_2 \rightarrow H_2O$	WET BIOMASS $\rightarrow$ BIOMASS + H_2O (g)	BIOMASS $\leftrightarrow H_2$ + CO + CO_2 + CH_4 + $H_2O_{(g)}$ + Tar + Ash	$C + CO_2 \leftrightarrow 2CO$ $C + H_2O \leftrightarrow CO + H_2$ $CO + H_2O \leftrightarrow CO2 + H_2$ $C + 2\ H_2 \leftrightarrow CH_4$

This study presents the gasification of 9 biomass samples and lignite blends in Aspen Plus. The ratio of biomass to lignite was changed from 0.3 to 0.7 in 0.1 intervals. Fixed bed and fluidized bed gasifiers are used. There are two types of models that can be applied to the system: the Kinetic model and Equilibrium model. Since biomass gasification contains many reactions, it is hard to control kinetics. Therefore, an equilibrium model based on the minimization of Gibbs free energy was employed. Biomass and ash were defined based on ultimate and proximate analyses, and non-conventional components were specified and modeled. The Peng-Robinson equation of state was used to calculate the physical properties of the conventional components in the simulation [38].

4.2 Biomass Characterization

Characterizing biomass is essential for enhancing gasification efficiency and improving the quality of syngas. The properties of biomass are evaluated through proximate analysis, which quantifies volatile matter (VM), moisture content (MC), fixed carbon (FC), and ash content, as well as elemental analysis to determine the levels of hydrogen (H), carbon (C), oxygen (O), sulfur (S), and nitrogen (N). Nine biomass samples, mixed with lignite, were selected from Phyllis [74] to serve as

feedstock for the gasification process. The results of the proximate and ultimate analyses for these samples are shown in Table 4.1.

4.3 Modelling in Aspen Plus®

Simulation programs are valuable tools for modeling and optimizing physical, chemical, and biological systems. Aspen Plus® is a process simulation software that aids in optimizing process parameters, thereby reducing operational time and costs. Based on energy and mass balance principles, the Aspen Plus® simulator enables analysis of how various operating parameters influence the model.

5
SIMULATION

5.1 Modeling

Utilized widely to evaluate the impact of various parameters on gasifier performance and generate essential data for the gasification process, Aspen Plus® is a process simulation tool that combines energy and mass balance calculations with a detailed thermodynamic database. Known for its rapid computational efficiency, the software predicts process outputs such as composition, exergy, and lower heating value under defined conditions. Through predefined blocks and modular structures, it constructs precise simulation models for accurate process representation.

Operational conditions, along with the proximate and ultimate analysis of the selected biomass, govern the mechanisms of chemical reactions in the gasification process, which are modeled based on chemical equilibrium. However, due to inherent kinetic constraints, the process may not achieve equilibrium under practical conditions. As a result, the simulation model must be adjusted for improved accuracy, either by incorporating the equilibrium constant (stoichiometric approach) or minimizing Gibbs free energy (non-stoichiometric approach). The non-stoichiometric modeling approach, which minimizes Gibbs free energy, was chosen for its simplicity in applying to complex processes like gasification. At constant pressure and temperature, the Gibbs free energy reaches its minimum under thermodynamic equilibrium conditions for multicomponent systems. Some assumptions is made and listed below:

The model is based on steady-state conditions.

Ash is considered inert and does not participate in the reactions.

All gases are treated as ideal gases in the model.

Heat losses and pressure reductions are assumed to be negligible.

Sufficient residence time is assumed to allow for chemical reactions to reach equilibrium.

The composition of syngas includes H_2, H_2O, CH_4, CO_2, and CO.

Chlorine and sulfur are represented as HCl and H_2S, respectively.

Char is composed solely of carbon and ash.

5.1.1 Modeling of downdraft fixed-bed gasifier in Aspen Plus®

Rubberwood, Redwood waste pellet and wood pellet were chosen as biomass samples for this simulation to be converted into syngas to produce hydrogen. Since biomass samples are complex feedstock, it's stated as non-conventional in the simulation system. Non-conventional material is required to be merged into conventional to react with an agent to complete its transformation into syngas. Therefore, biomass properties were introduced to the system which were obtained from ultimate and proximate analyses [2], [79]. Proximate and ultimate analyses are shown in Table 5.1:

Table 5.1 Physical and chemical characterization of the rubber wood and redwood

Ultimate analysis (wt.%)	Rubber Wood	Redwood Waste Pellet
C	50.6	47.1
H	6.5	5.5
O	42	45
N	0.2	0.5
S	0	0.1

Table 5.1 Physical and chemical characterization of the rubber wood and redwood (continued)

Proximate analysis (wt.%)		
Moisture	18.5	9.3
Volatile Matter	81.1	87.9
Fixed Carbon	19.2	1.4
Ash	0.7	1.4

While ultimate analyses show the effects on the characteristics of syngas that are produced from biomass gasification; The quantity of Fixed Carbon, Moisture, Volatile Matter and Ash contents are determined by proximate analyses.

The system utilized air as an oxidizing agent and various biomass feedstocks, including rubber wood and redwood waste pellets. Biomass was initially fed into the DECOMP unit to undergo elementary decomposition. A RYIELD reactor was then employed to distribute components based on input parameters obtained from the proximate and ultimate analysis of the biomass samples. Following decomposition, elemental components such as solid carbon (C), H_2O, H_2, N_2, O_2, and non-conventional char and tar were directed to SEP1, which separated gaseous components and carbon from non-conventional materials, as these materials negatively impact hydrogen conversion efficiency.

The resulting feed stream entered the "FUELSPLT" block, where it was divided into three sub-streams ("Z1-F," "Z2-F," and "Z3-F"). These streams were then directed to the "ZONE1," "ZONE2," and "ZONE3" units, which function as Gibbs reactors to minimize Gibbs free energy and simulate gasification and combustion processes."ZONE1" (673.15 K) represented pyrolysis, "ZONE2" (1073.15 K) simulated gasification, and "ZONE3" (1273.15 K) modeled combustion. The "STM-SPL" block controlled the oxidant ratios within the reactors. Additionally, the "SEP1" block removed 5% of the solid carbon, representing unconverted carbon, while "SEP2" and "SEP3" were responsible for isolating specific

components to prevent their entry into the Gibbs reactors. The gaseous products from all reactors were combined in the "MIX" block, and the "SEP4" block extracted undesirable components, such as water, from the syngas.

Figure 5.1 illustrates the flowsheet of fixed bed model designed via Aspen Plus.

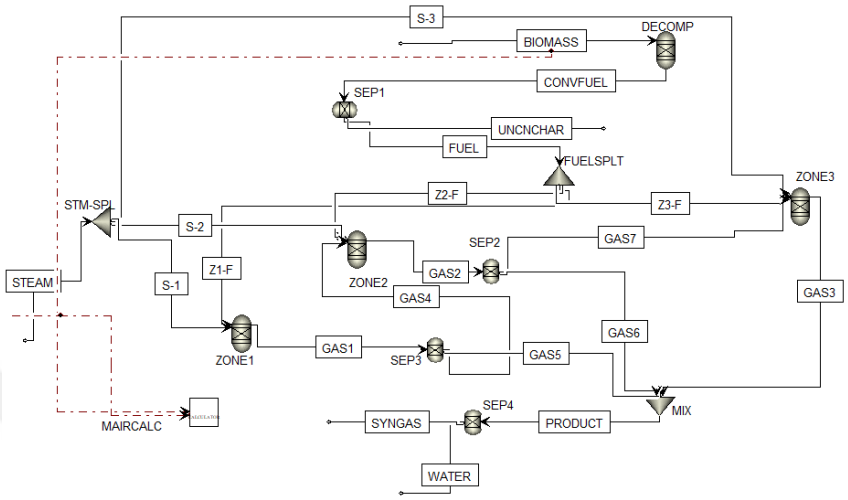


Figure 5.1 Main flowsheet of biomass gasification in a downdraft fixed-bed gasifier

5.1.2 Modeling of fluidized-bed gasifier in Aspen Plus®

Waste tire was chosen as a biomass sample for gasification simulation in a fluidized bed gasifier to be converted into syngas to produce hydrogen. SBR, ER, T and B/L are the input parameters to be further studied.

Experimental conditions were mentioned in Table 5.2 [80].

Table 5.2 The experimental parameters for waste tire gasification in a bubbling fluidized bed gasifier

Temperature (K)	1
Pressure (bar)	973
Gasification agent	Steam and air
Steam / Air	0.20 – 0.27

Table 5.2 The experimental parameters for waste tire gasification in a bubbling fluidized bed gasifier (continued)

Feed amount (biomass, kg/h)	0.825
Pressure (bar)	1
Temperature (K)	983-1028
Equivalence ratio (ER)	0.15-0.45

Given the complexity of waste tire gasification in a bubbling fluidized bed gasifier, the following assumptions were made:

The gasification process was assumed to operate under steady-state, isothermal conditions at atmospheric pressure.

The devolatilization products were primarily H_2O, CO_2, CO, CH_4, and H_2, while tar, heavy hydrocarbons, and compounds containing sulfur or nitrogen were excluded from the syngas composition.

The char was considered to consist solely of carbon and was assumed to be free of ash.

Devolatilization was treated as an instantaneous process.

Heat losses from the gasifier to the surroundings were disregarded.

The Aspen flow diagram for the waste tire gasification process, conducted in a bubbling fluidized bed, was structured into seven distinct units, as shown in Fig. 5.2. Since waste tires do not constitute a standard component in Aspen, direct simulation was unfeasible. As a result, the waste tire was first decomposed into its constituent elements—carbon (char), hydrogen, oxygen, nitrogen, sulfur, ash, and moisture—based on both ultimate and proximate analysis, utilizing the RYIELD reactor. Subsequently, these components were separated into volatile and solid fractions within the SEPARATION unit.

The volatile components were converted into CO, H_2, CH_4 and CO_2 in the RGIBBS reactor, assuming chemical reactions achieved Gibbs equilibrium. The solid

fraction (char), gasification agents carbon dioxide, and water, and the product gas from the RGIBBS-I reactor were combined in the MIXER unit.

The char underwent further gasification in the CSTR reactor under the assumption that chemical reactions reached thermodynamic equilibrium. In the SEP-II-unit, the amount of CO and N_2 separated from the syngas. Furthermore, present syngas gases were fed to RGIBBS-II to complete the combustion reactions and conversion of syngas. Finally, at the final SEP-III ash was removed from the final syngas products. Figure 5.2 illustrates the flowsheet of fluidized bed model designed via Aspen Plus.

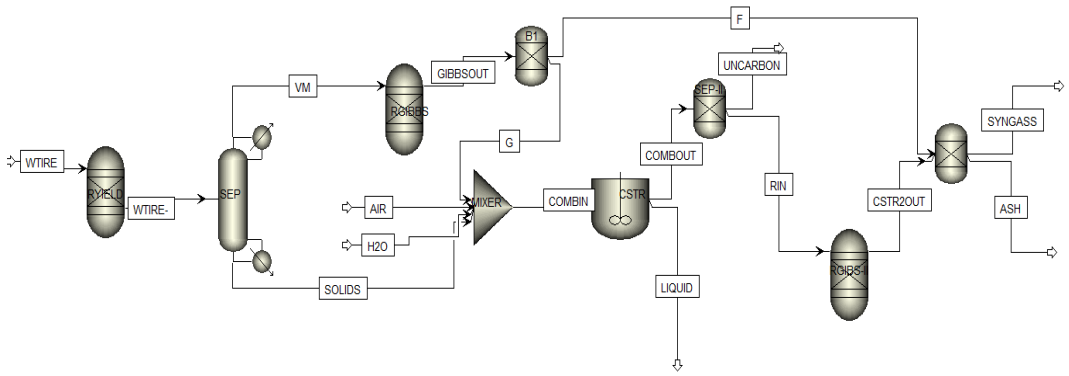


Figure 5.2 Main flowsheet of biomass gasification in a downdraft fluidized-bed gasifier

The reactions presumed to take place in the downdraft fixed bed and fluidized bed gasifiers models are summarized as follows:

$$\text{Hydrogasification: } C+2H_2 \leftrightarrow CH_4 \quad 74.8\text{kJ/mol} \tag{5.1}$$

$$\text{Water-gas reaction: } C+H_2O \leftrightarrow CO+H_2 \quad +131\text{kJ/mol} \tag{5.2}$$

$$\text{Carbon oxidation: } C+O_2 \rightarrow CO_2 \quad 394\text{kJ/mol} \tag{5.3}$$

$$\text{Carbon partial oxidation: } C+0.5O_2 \rightarrow CO \quad 111\text{lj/mol} \tag{5.4}$$

$$\text{Carbon monoxide oxidation: } CO+0.5O_2 \rightarrow CO_2 \quad 283\text{kJ/mol} \tag{5.5}$$

$$\text{Steam methane reforming: } CH_4+H_2O \leftrightarrow CO+3H_2 \quad +206\text{kJ/mol} \tag{5.6}$$

$$\text{Methane oxidation: } CH_4+2O_2 \leftrightarrow CO_2+2H_2O \quad 803\text{kJ/mol} \tag{5.7}$$

$$\text{Water-gas shift reaction: } CO+H_2O \leftrightarrow CO_2+H_2 \quad 41.2\text{kJ/mol} \tag{5.8}$$

$$\text{Boudouard reaction: } C + CO_2 \leftrightarrow 2CO + 172kJ/mol \quad (5.9)$$

After successful validation, the design is used to study the performance of the fixed bed and fluidized bed gasification. Biomass to lignite ratio(B/L), Temperature(T) and ER effect is observed for Fixed bed gasifier. In the fluidized bed reactor, the parameters SBR (Steam to biomass ratio), ER, T, and B/L were varied to examine their impact on the composition of synthesis gas.

5.2 Process Development

In this study, two different gasifiers (fixed-bed and fluidized bed) were utilized, and the operating parameters and values for each gasifier were determined. The biomass-to-lignite ratio, temperature, steam-to-biomass ratio, and equivalence ratio are the operational parameters of the process are given in Table 5.3. In the fixed-bed design, the steam-to-biomass ratio was not utilized as a parameter because the system does not include steam input; only air is supplied.

Table 5.3 Gasification parameters

Biomass to lignite ratio	Temperature (K)	Steam to biomass ratio	ER
0.3	773	0.1	0.12
0.4	873	0.2	0.17
0.5	973	0.3	0.22
0.6	1073	0.4	0.27
0.7	1173	0.5	0.32

5.3 Calculations

5.3.1 Yield Calculations

During gasification, by using biomass ultimate analyses and proximate analyses (Main biomass properties) values, Yield can be calculated for decomposition unit. Only one biomass sample is explained here. Calculations are applied to all biomass samples.

Assumptions:

1 kg / hour total biomass was fed to the system

$$\text{Biomass} = \text{Biomass}_1 + \text{Biomass}_2 \text{ (Lignite Coal)} \tag{5.10}$$

Biomass / Lignite ratio was changed between 0.3, 0.4, 0.5, 0.6 and 0.7, respectively.

$$\text{Yield} = \text{Biomass Properties (wt.\%)} / 100 \tag{5.11}$$

X_1 kg / hour Biomass_1 + (1-X_1) kg / hour Lignite Coal Yield:

$$(Biomass\ Properties/100) * X_1 + [(Lignite\ Properties/100) * (1 - X_1)] \tag{5.12}$$

Table 5.4 presents the biomass-to-lignite ratios along with their corresponding symbols used in the calculations.

Table 5.4 Biomass to lignite ratio values

Symbol	Biomass/Lignite ratio
X_1	0.3
X_2	0.4
X_3	0.5
X_4	0.6
X_5	0.7

Yield calculations for the decomposition unit in Aspen Plus are presented in Figure 5.3 as a representative illustration.

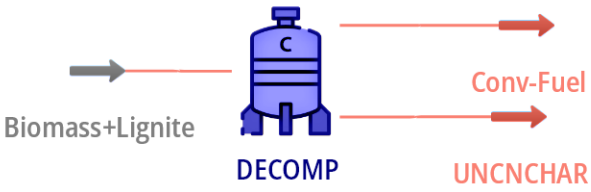


Figure 5.3 Flowsheet of decomposition unit

Yield calculations have been applied to all biomass samples, with hazelnut shell selected as a representative feedstock. The calculations are demonstrated using this feedstock. The yield calculation for a feed mass flow of 0.3 kg/hour of hazelnut shell is provided in Table 5.5.

Table 5.5 Yield calculation of hazelnut shell for 0.3 kg/hour feed mass flow

Biomass properties	Wt.%	%Fraction	$Yield_1$
Ash	0.59	0.0059	0.00177
Moisture	12.08	0.128	0.0384
Carbon	41.07	0.4107	0.12321
Hydrogen	4.83	0.0483	0.01449
Nitrogen	0.09	0.0009	0.00027
Oxygen	39.87	0.3987	0.11961
Sulphur	0.75	0.0075	0.00225
Chlorine	0	0	0
Tar	0	0	0

Since lignite was blended with all biomass types at specific ratios, its yield calculation was also performed separately to determine the mixture's efficiency. The results are presented in Table 5.6.

Table 5.6 Yield calculation of lignite coal for 0.7 kg/hour feed mass flow

Biomass properties	Wt.%	%Fraction	$Yield_2$
Ash	14.04	0.1404	0.09828
Moisture	48	0.48	0.336
Carbon	21.31	0.2131	0.14917
Hydrogen	1.25	0.0125	0.00875
Nitrogen	0.57	0.0057	0.00399
Oxygen	16.12	0.1612	0.11284
Sulphur	0.45	0.0045	0.00315
Chlorine	0	0	0
Tar	0	0	0

Table 5.7 presents the yield calculation results for the mixture with a 0.3 biomass and 0.7 lignite fraction.

Table 5.7 Yield calculation of biomass and lignite coal mixtures for 0.3/0.7 ratio

Biomass properties	$Yield_{1(Biomass)}$	$Yield_{2(Lignite)}$	$Yield_{1,2(Mixed)}$
Ash	0.00177	0.09828	0.10005
Moisture	0.0384	0.336	0.3744
Carbon	0.12321	0.14917	0.27238

Table 5.7 Yield calculation of biomass and lignite coal mixtures for 0.3/0.7 ratio (continued)

Hydrogen	0.01449	0.00875	0.02324
Nitrogen	0.00027	0.00399	0.00426
Oxygen	0.11961	0.11284	0.23245
Sulphur	0.00225	0.00315	0.0054
Chlorine	0	0	0
Tar	0	0	0

5.3.2 Air Mass Flow Calculations

Using ER values, the air mass flow rate can be calculated. The equivalence ratio (ER) can be determined using Equation (5.13).

$$ER = \frac{Actual\ air\ fuel\ ratio}{Stoichiometric\ air\ fuel\ ratio} \tag{5.13}$$

The actual air-fuel ratio is derived based on experimental measurements, whereas the stoichiometric air-fuel ratio is obtained by applying Equation 5.14.

$$CH_aO_b + (O_2 + 3.76N_2) \rightarrow yH_2O + zCO_2 + 3.76xN_2 \tag{5.14}$$

The values of a and b are obtained from the ultimate analysis of the biomass. In this context, y and z denote the stoichiometric coefficients for H_2O and CO_2, respectively, while x represents the stoichiometric coefficient of O_2 and 3.25 times the amount of N_2 [81].

For this study ER values are presented in Table 5.9. This calculation process is applied for all biomass samples with lignite blend.

Air is the oxidizing agent for the fixed-bed design process. Air and steam are the oxidizing agents for the fluidized-bed design process. For 1 kg / hour biomass feed, Y kg / hour air mass flow is requested.

Total moisture and ash content is removed from the total biomass feed mass flow.

$$\text{Moisture} + \text{Ash} = 0.128 + 0.0059 = 0.1339 \quad (5.15)$$

$$\text{Biomass content without moisture and ash} = 1 - 0.1339 = 0.866 \quad (5.16)$$

For 0.8661 kg/h biomass:

$$\text{C content} = 0.4107 * 0.8661 = 0.356 \quad (5.17)$$

$$\text{H content} = 0.0483 * 0.8661 = 0.669 \quad (5.18)$$

$$\text{O content} = 0.3987 * 0.8661 = 1.273 \quad (5.19)$$

Required O_2 for the system under these conditions:

$$C = 0.356 * (32/12) = 0.949 \quad (5.20)$$

$$H = 0.669 * (32/2) = 0.669 \quad (5.21)$$

$$O = (0.949 + 0.669) - 0.399 = 1.273 \quad (5.22)$$

For 1 mol O_2, there is 3.76 mol N_2. Total Oxygen content is 4.76 mol at the air. Therefore, to obtain the air content, determined O_2 is multiplied with 4.76.

$$\text{Air content} = 4.76 * 1.273 = \mathbf{6.057\ kg/h} \quad (5.23)$$

Table 5.8 presents the calculations of elemental composition (C, H, O) within the biomass to determine the required oxygen amount for 1 kg/h of biomass (hazelnut shell). Moisture and ash were excluded from the 1 kg biomass, as they reduce efficiency. It was determined that a feed rate of 0.8661 kg/h is required.

Table 5.8 Air mass flow calculations for hazelnut shell

Biomass$_1$	Dry basis	%	For 0.8661 kg/h	Required O_2
C	41.07	0.411	0.356	0.949
H	4.83	0.048	0.042	0.669

Table 5.8 Air mass flow calculations for hazelnut shell (continued)

O	39.87	0.399	0.345	1.273

For different values of ER, air mass flow is calculated and illustrated below in Table 5.9:

Table 5.9 Air mass flow for different ER

ER	Air mass flow (kg/h)
0.12	0.727
0.17	1.029
0.22	1.333
0.27	1.635
0.32	1.938

This is calculated for 1 kg of biomass content. To find the air feed flow rate for a mixture of X_1 kg of biomass and (1-X_1) kg of lignite coal, the air feed rates at 1 kg feed for both materials are found. The air supply flow rate is then multiplied by the mixing ratios of the biomasses and summed. The results of air mass flow at an equivalence ratio (ER) of 0.12 are presented in Table 5.10.

Table 5.10 Results of air mass flow for ER: 0.12

Biomass/ Lignite	1 kg $Biomass_1$	1 kg Lignite	Total air mass flow (kg/h)
0.3	0.3	0.7	0.310
0.4	0.4	0.6	0.369
0.5	0.5	0.5	0.429

Table 5.10 Results of air mass flow for ER: 0.12 (continued)

0.6	0.6	0.4	0.489
0.7	0.7	0.3	0.548

5.4 Fixed-Bed Process Development

Three distinct Gibbs reactors were utilized to simulate the downdraft gasifier. For its straightforwardness in modeling intricate processes such as gasification, a non-stoichiometric approach based on the minimization of Gibbs free energy was adopted. Additionally, this method does not necessitate the specification of a reaction or conversion rate. From stream properties and sensitivity analysis, the performance parameters of the gasification process—such as syngas composition, yield, heating values, and exergy—can be determined. Following AspenTech's recommendations, the Soave-Redlich-Kwong (SRK) equation of state, coupled with STEAMNBS, was chosen for this analysis.

Characterizing biomass samples is crucial for optimizing gasification efficiency and syngas quality. Biomass properties, including fixed carbon (FC), ash content, volatile matter (VM), moisture content (MC), and elemental composition (C, H, O, N, S), are determined through proximate and elemental analyses. Nine biomass samples and lignite coal mixtures from the literature were selected as feedstocks for the gasification process. The proximate and ultimate analysis results for these samples are presented in Table 4.1.

In the fixed-bed downdraft gasifier model, the following assumptions were considered:

The gasification process was assumed to operate under steady-state, isothermal conditions.

Char was treated as purely carbon.

The syngas composition was assumed to exclude heavy hydrocarbons.

Ash was regarded as an inert substance and excluded from the reactants.

It was assumed that gasification reactions proceed to chemical equilibrium.

H_2S and HCl were formed directly from sulfur and chlorine in the biomass.

Pressure drops within and surrounding the reactors and blocks were neglected. Under these conditions, the exergy of the syngas and its compositional characteristics are investigated. The block units and their description for fixed-bed model are given in Table 5.11.

Table 5.11 Block units, identity and functions of fixed-bed gasifier in Aspen Plus®

Aspen Plus block name	Block ID	Process conditions	Description
DECOMP	RYIELD	T = 273.15 K, P = 1 atm	The biomass sample was initially in a non-conventional form and was subsequently converted into a conventional form.
ZONE1	RGIBBS	T = 673.15 K, P = 1 atm	Gasification reactions take place in this reactor at relatively low Temp.
ZONE2	RGIBBS	T = 1073.15 K, P = 1 atm	Gasification reactions were carried out in this section.
ZONE 3	RGIBBS	T = 1073.15 K, P = 1 atm	Combustion reactions were carried out in this section.
SEP1	SEP	T = 273.15 K, P = 1 atm	Separates the solid material in its nonconventional form.
STM-SPL	FSPLIT	T = 600 K, P = 1 atm	The steam is divided into three separate streams.
SEP2,SEP3	FSPLIT	T = 1073.15 K, T = 673.15 K	The blocks restrict the components from accessing the Gibbs reactors.
MIX	MIXER	T = 1240.77 K, P = 1 atm	The gaseous products are combined within the mixer block.

Table 5.11 Block units, identity and functions of fixed-bed gasifier in Aspen Plus® (continued)

SEP4	SEP	T = 1240.77 K, P = 1 atm	It separates the undesired products and water from the product gas.

5.5 Fluidized-Bed Process Development

The gasification process in a fluidized bed gasifier is outlined as follows: biomass samples react with a gasification agent (air and steam) to produce syngas (H_2, CO, CO_2, and CH_4), tar, and ash. The proximate and ultimate analyses of the biomass samples are presented in Table 4.1. Nine distinct biomass samples, blended with lignite, are utilized in this study. The process parameters, including SBR, T, ER, and BLR, are examined. Under these conditions, the exergy of the syngas and its compositional characteristics are investigated. Assumptions for the gasification process by using a fluidized-bed gasifier are given in 5.1.2. The block units and their description for fluidized-bed model are given in Table 5.12.

Table 5.12 Block units, identity and functions of fluidized-bed gasifier in Aspen Plus®

Aspen Plus block name	Block ID	Process conditions	Description
RYIELD	RYIELD	T = 273.15 K, P = 1 atm	The biomass sample was initially in a non-conventional form and was subsequently converted into a conventional form.
SEP	SEP2	T = 273.15 K, P = 1 atm	Volatile matter is separated from solids.
RGIBBS	RGIBBS	T = 673.15 K, P = 1 atm	Gasification reactions were carried out in this section.
MIXER	MIXER	P = 1 atm	The solids from SEP2, along with water, the air gasifying agent, met.

Table 5.12 Block units, identity and functions of fluidized-bed gasifier in Aspen Plus® (continued)

SEP	B1	T = 810 K, P = 1 atm	It is used to balance the outlet fraction of the gases exiting the RGibbs unit.
CSTR	CSTR	T = 800 K, P = 1 atm	The mixtures exiting the mixer are fed to facilitate the gasification reactions.
SEPII	SEP	T = 800 K, P = 1 atm	It is used to separate unconverted carbon from the synthesis gas mixture.
RGIBBS-II	RGIBBS	T = 820 K, P = 1 atm	It is the final stage where the remaining unconverted materials are transformed into products.
SEP	SEP3	T = 820 K, P = 1 atm	The separation of ash from the synthesis gas is ensured.

5.6 Machine Learning

The exergy value of the synthetic gas will be determined in different parameters. In the second stage of the study, modeling will be done using some machine learning methods. These machine learning methods, such as Gaussian Process Regression, Support Vector Regression, Decision tree, Random Forest Regression will be applied. Support Vector Regression (SVR) has emerged as a successful method in recent years. This approach is grounded in statistical learning theory and addresses learning challenges with a limited number of examples. Additionally, Support Vector Regression (SVR), through the construction of hyperplanes, effectively separates data from different classes. This non-parametric method, enhanced by the use of kernel functions, is one of the most prevalent algorithms within machine learning applications. Similarly, decision trees serve as a widely recognized technique for building predictive models rooted in fundamental logical expressions. The directional basic decision tree is comprised of a root node, internal nodes, and

terminal nodes, progressively segmenting the data into smaller, more homogeneous chunks. In doing so, the model aims to minimize prediction errors within each partition. Thus, the continuous output variable is estimated through the application of a logical rule. Random Forest Regression, an advanced learning technique, is characterized by the integration of numerous decision trees. Within the ensemble learning framework, two dominant approaches prevail: bagging and boosting. In the bagging method, the training data is partitioned through the bootstrap resampling technique, and a regression tree is constructed for each resampled dataset. Conversely, in boosting, all data is introduced into every tree, with misclassified data receiving increased weight in each successive tree. While bagging effectively mitigates overfitting, the boosting approach tends to yield superior results, particularly when dealing with large datasets. The data required for machine learning were collected using Aspen Plus, with various parameters such as ER, T, SBR and BLR and value ranges [82], [83].

6
RESULTS AND DISCUSSION

6.1 Fixed-Bed Sensitivity Analysis

6.1.1 Validation Results for Fixed-Bed Gasifier

Rubberwood and Redwood Waste pellets were used for biomass gasification in a downdraft fixed-bed gasifier. Syngas compositions for the used biomasses and RMSE values are given in Table 6.1. Root Mean Square Error (RMSE) represents the standard deviation of the residuals, indicating the average magnitude of the differences between the predicted values and the actual observed values generated by a statistical model. For rubberwood, the RMSE value derived from the literature is 1.84, whereas the RMSE value obtained in this study is 0.80.

Table 6.1 Comparison of syngas composition among the model and experimental works

Biomass sample	Syngas composition (%v/v.dry)			
Rubberwood	H_2	CO	CO_2	CH_4
Experimental [78]	15.5	19.1	11.4	1.1
Aspen Plus® Model from literature [2]	18.3	19.2	11.4	3.5
Our study of Aspen Plus® model	16.21	19.2	10.28	1.992
RMSE of literature results	1.845			
RMSE of our results	0.801			

Table 6.1 Comparison of syngas composition among the model and experimental works (continued)

Redwood waste pellets				
Experimental [79]	13	19	10	2
Aspen Plus® model from literature [2]	14.4	19.8	11.7	0
Our study of Aspen Plus® model	12.6	15.78	13.1	1.94
RMSE of literature results		1.540		
RMSE of our results		2.244		

Figure 6.1 compares the syngas compositions obtained from rubberwood between this study and literature data.

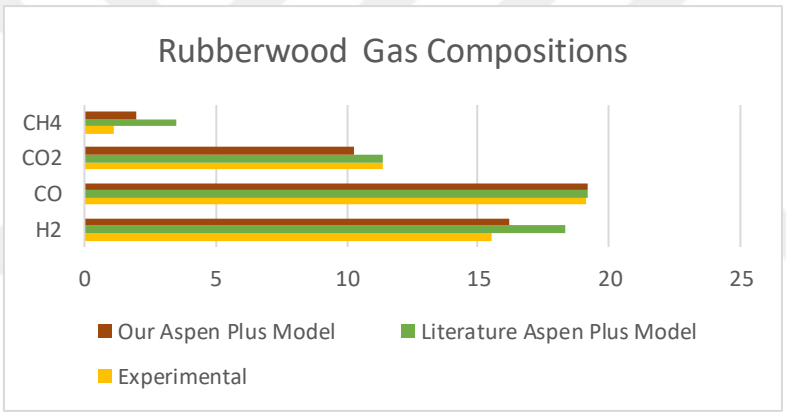


Figure 6.1 Comparison of gas compositions

Figure 6.2 provides a similar comparison for syngas compositions produced from redwood waste pellets.

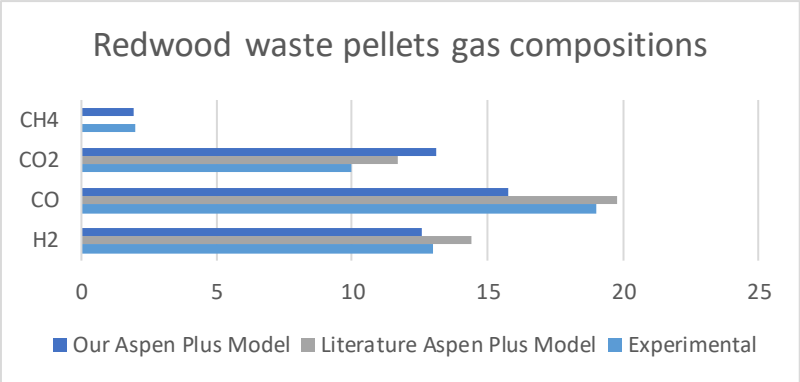


Figure 6.2 Comparison of gas compositions

6.1.2 Model Results for Fixed-Bed Gasifier

In this study, studied biomass samples are given in Table 4.1, section 4. Biomass-to-lignite ratio, Temperature and Equivalence ratio are the input parameters.

For Hazelnut Shell and Lignite mixtures (Table 6.2), parameters and their effects are mentioned.

Table 6.2 Results of ultimate and proximate analyses for hazelnut shell and lignite coal (wt%, dry basis)

		Ultimate analysis					Proximate analysis				
	Sample	C	H	O	N	S	MC	Ash	VM	FC	Ref.
1	Hazelnut Shell	41.07	4.83	39.87	0.09	0.75	12.80	0.59	63.74	22.86	[78]
2	Lignite	21.32	1.25	16.12	0.57	0.45	48	14.04	23.4	14.56	[78]

In the study, 9 different biomass-lignite mixtures were used, and the effects of the variations in all these parameters were analyzed for each mixture. All the results have been recorded in Excel. The effects on a representative biomass are presented.

The data collected from all the biomass samples were later used in the machine learning phase, which is detailed in that section. To observe the effect of each parameter, the parameters other than the one whose effect is to be observed are kept constant, while the parameter of interest is varied.

6.1.2.1 Effect of Biomass to Lignite Ratio on Syngas Gas Compositions and Exergy

The effect of the biomass-to-lignite ratio on the gas composition and exergy of the gas derived from the mixture of hazelnut shell and Lignite coal under the conditions of ER: 0.12 and a temperature of 499.85 °C is presented in Table 6.3.

Table 6.3 Results of sensitivity analysis for biomass-to-lignite ratio variables

Biomass to lignite ratio	CO	CO_2	CH_4	H_2	T (ºC)	ER	Exergy kw
0.3	0.291	0.151	0.063	0.285	499.85	0.12	0.193
0.4	0.305	0.133	0.058	0.277	499.85	0.12	0.210
0.5	0.319	0.117	0.053	0.270	499.85	0.12	0.227
0.6	0.331	0.103	0.049	0.263	499.85	0.12	0.244
0.7	0.343	0.089	0.046	0.257	499.85	0.12	0.260

Effect of the Biomass-to-lignite ratio on syngas compositions is given in Figure 6.3. As the ratio of biomass to lignite increases, an increase in the CO gas composition is observed, while decreases occur in the compositions of CO_2, CH_4, and H_2 gases.

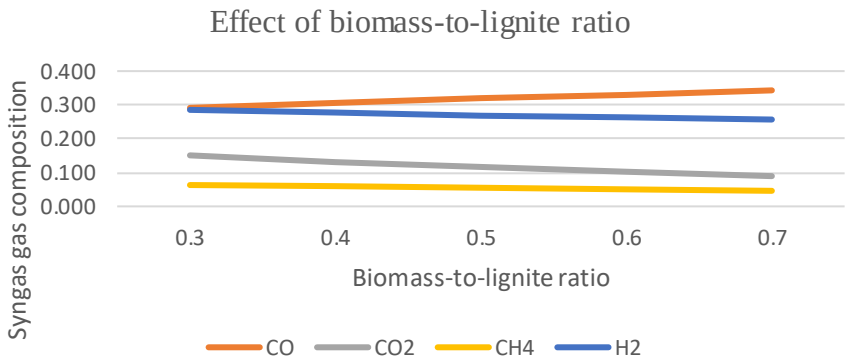


Figure 6.3 Effect of biomass-to-lignite ratio on gas compositions

The effect of the biomass-to-lignite ratio on exergy is presented in Figure 6.4. An increase in the biomass-to-lignite ratio results in a positive rise in exergy.

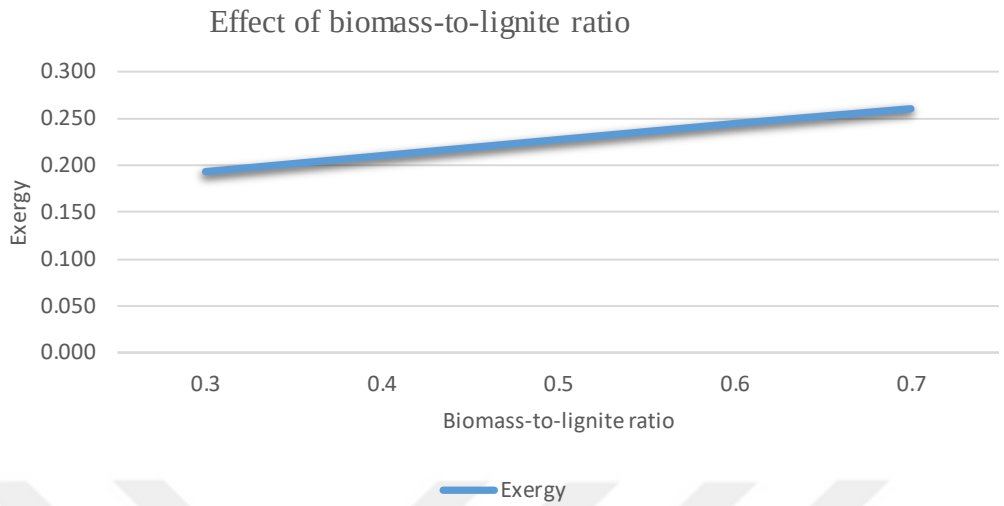


Figure 6.4 Effect of biomass-to-lignite ratio on on exergy of syngas gas compositions

6.1.2.2 Effect of Temperature on Syngas Gas Compositions and Exergy

The effect of temperature on the gas composition and exergy of the gas derived from the mixture of hazelnut shell and lignite coal under the conditions of ER: 0.12 and a biomass to lignite ratio of 0.3 is presented in Table 6.4.

Table 6.4 Results of sensitivity analysis for temperature variables

Biomass to lignite ratio	CO	CO_2	CH_4	H_2	T (ºC)	Exergy kw
0.3	0.291	0.151	0.063	0.285	499.85	0.193
0.3	0.293	0.146	0.050	0.309	599.85	0.207
0.3	0.309	0.129	0.033	0.333	699.85	0.214
0.3	0.315	0.125	0.031	0.334	799.85	0.216
0.3	0.318	0.123	0.031	0.333	899.85	0.219

The effect of temperature is given in Figure 6.5. An increase in temperature led to a rise in H_2 and CO compositions, while causing a decrease in CH_4 and CO_2 gas compositions.

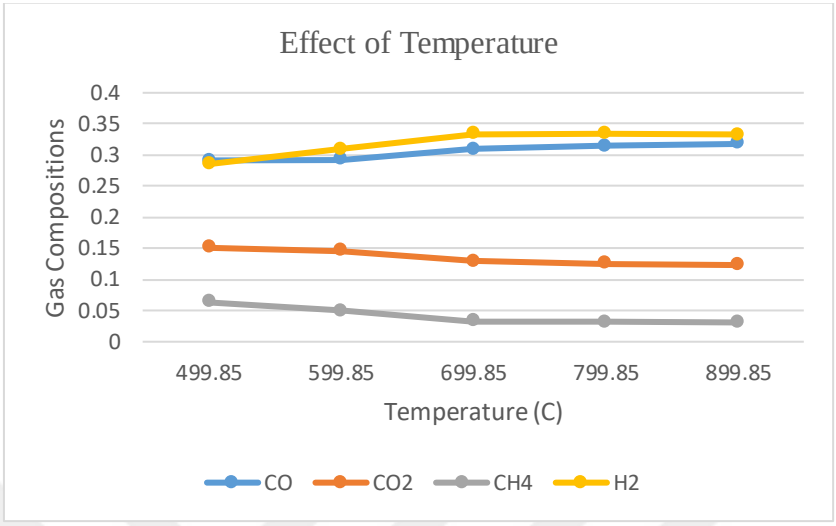


Figure 6.5 Effect of temperature on gas compositions

The effect of temperature is shown in Figure 6.6. The temperature increase resulted in an improvement in exergy.

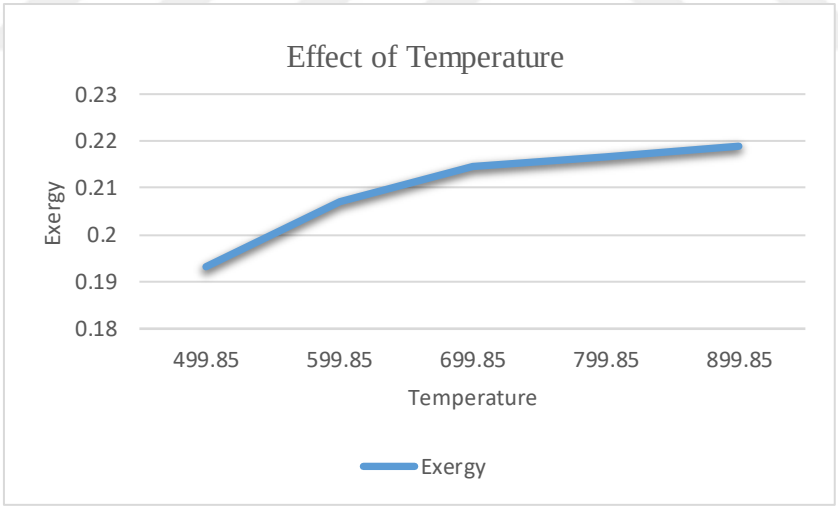


Figure 6.6 Effect of temperature on exergy of syngas gas compositions

6.1.2.3 Effect of equivalence ratio on syngas gas compositions and exergy

The effect of equivalence ratio (ER) on the gas composition and exergy of the gas derived from the mixture of hazelnut shell and lignite coal under the conditions of

temperature: 499.85 °C and a biomass to lignite ratio of 0.3 is presented in Table 6.5.

Table 6.5 Results of sensitivity analysis for ER variables

Biomass to lignite ratio	CO	CO_2	CH_4	H_2	T (ºC)	ER	Exergy kw
0.3	0.291	0.151	0.063	0.285	499.85	0.12	0.193
0.3	0.255	0.162	0.059	0.247	499.85	0.17	0.208
0.3	0.221	0.173	0.056	0.213	499.85	0.22	0.224
0.3	0.191	0.183	0.053	0.183	499.85	0.27	0.239
0.3	0.163	0.192	0.051	0.156	499.85	0.32	0.255

Finally, the effect of the equivalence ratio on synthetic gas composition is presented in Figure 6.7. An increase in the ER ratio resulted in a decrease in the molar fractions of hydrogen and carbon monoxide, while leading to an increase in the amounts of carbon dioxide and methane.

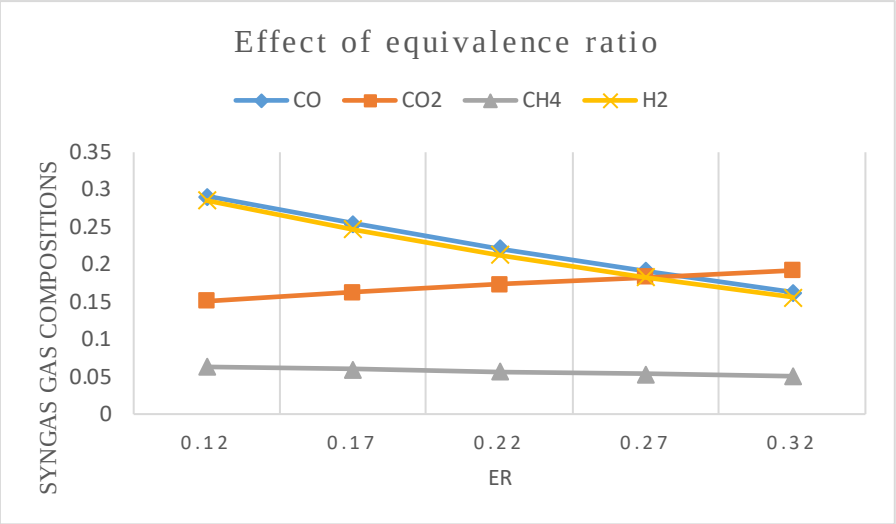


Figure 6.7 Effect of ER on gas compositions

The effect of the equivalence ratio on exergy is highlighted in Figure 6.8.An increase in the ER ratio also led to a rise in the exergy value of the syngas. Therefore, increasing the ER ratio enhances the efficiency of the system.

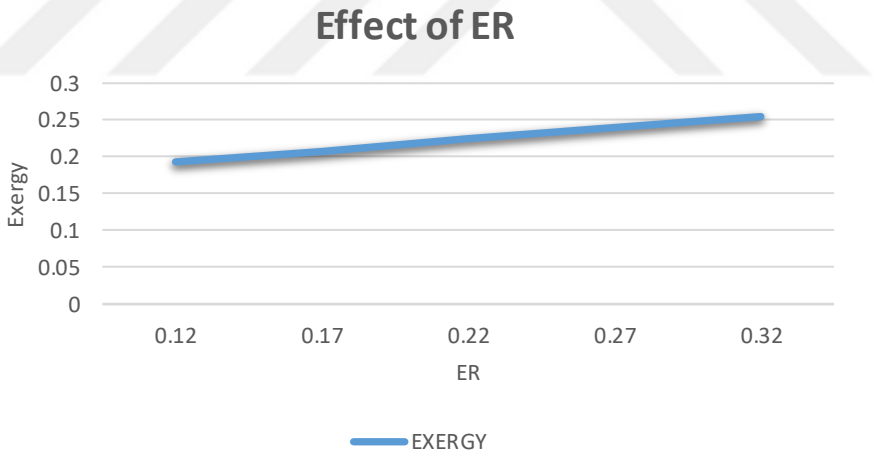


Figure 6.8 Effect of ER on exergy of syngas gas compositions

6.1.2.4 The effect of ER and T on H_2 for Fixed-Bed Model

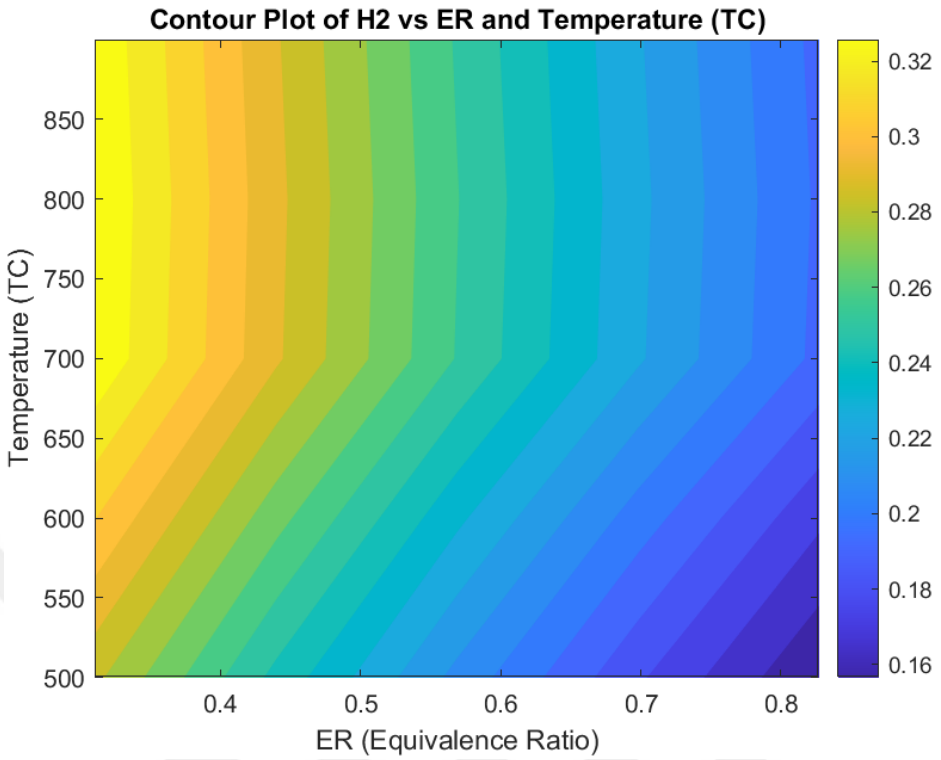


Figure 6.9 T and ER effect on hydrogen, when SBR:0

Figure 6.9 represents temperature and equivalence ratio on hydrogen composition, when steam to biomass ratio is 0.

6.2 Fluidized-Bed Sensitivity Analysis

6.2.1 Validation Results of Fluidized-Bed Gasifer

Prior to modeling the fluidized bed gasifier in Aspen Plus, validation is required. For validation, the study conducted by Li, W., Wang, C., & Song, Y. (2024) was used as a reference. The biomass utilized in this study is waste tires. Certain assumptions must be made prior to validation. These assumptions have also been adopted from the same reference studies. The assumptions are provided in Section 5.1.2. The effect of varying ER operating conditions between 0.15 and 0.4 on syngas compositions was analyzed. The gas composition values at an ER of 0.163 are shown in Figure 18. The R^2 value was found to be 0.96. The success criterion of $R^2 > 0.9$ was also met for the fluidized bed gasifier model. Validation results are given in Table 6.6.

Table 6.6 Validation results of fluidized-bed model

Syngas	H2	CO	CO2	CH4
Literature	0.22	0.051	0.076	0.150
Model	0.23	0.043	0.082	0.13
ER		1.63		
R^2		0.96		
RMSE		1.189		

Figure 6.10 presents a comparison between the gas compositions obtained from the literature and those modeled by Aspen Plus.

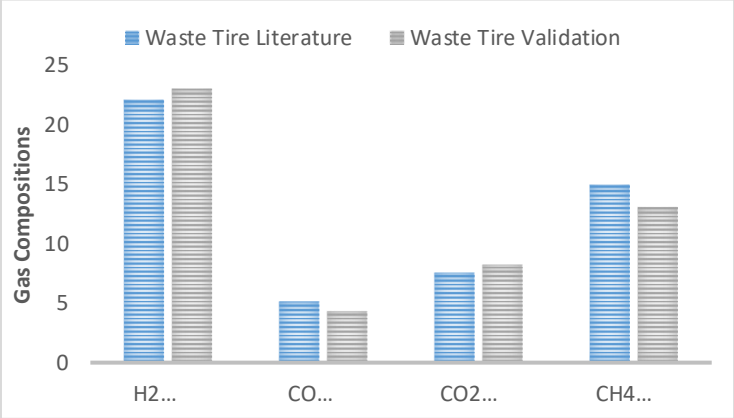


Figure 6.10 Comparison of gas compositions at ER: 0.163

6.2.2 Model Results of Fluidized-Bed Gasifier

In this study, studied biomass samples are given in Table 4.1, section 4. Biomass-to-lignite ratio (BLR), Temperature (T, °C), Equivalence ratio (ER) and Steam to Biomass Ratio (SBR) are the variable parameters. The parameters and their impacts for Hazelnut Shell and Lignite mixtures are detailed in Table 6.7.

Table 6.7 Results of ultimate and proximate analyses for hazelnut shell and lignite coal (wt%, dry basis)

		Ultimate analysis					Proximate analysis				
	Sample	C	H	O	N	S	MC	Ash	VM	FC	Ref.
1	Hazelnut Shell	41.07	4.83	39.87	0.09	0.75	12.80	0.59	63.74	22.86	[78]
2	Lignite	21.32	1.25	16.12	0.57	0.45	48	14.04	23.4	14.56	[78]

In this study, nine distinct biomass-lignite mixtures were utilized, and the impacts of variations in all parameters were analyzed for each mixture. The findings were systematically recorded in Excel, with the results for a representative biomass highlighted and presented. The data gathered from all biomass samples were subsequently utilized in the machine learning phase, as outlined in the corresponding section. To examine the impact of each parameter, all other parameters were held constant while the parameter of interest was systematically varied.

6.2.2.1 Effect of Biomass to Lignite Ratio on syngas gas compositions and exergy

The effect of the biomass-to-lignite ratio on the composition and exergy of the gas obtained from the mixture of hazelnut shells and lignite coal is presented in the figures below under the conditions of SBR: 0.1, ER: 0.12, and a temperature of 499.85°C. Results are also highlighted in Table 6.8.

Table 6.8 Results of sensitivity analysis

Biomass to lignite ratio	H_2	CO	CO_2	CH_4	Exergy kw
0.3	0.367	0.072	0.204	0.144	0.070
0.4	0.335	0.086	0.180	0.174	0.080

Table 6.8 Results of sensitivity analysis (continued)

0.5	0.319	0.085	0.176	0.170	0.082
0.6	0.303	0.083	0.172	0.167	0.085
0.7	0.289	0.082	0.169	0.164	0.088

Figure 6.11 illustrates the effect of the biomass-to-lignite ratio on syngas composition. As the biomass-to-lignite ratio increases, a decrease is observed in the molar fractions of H_2 and CO_2, while the opposite effect is observed for CO and CH_4.

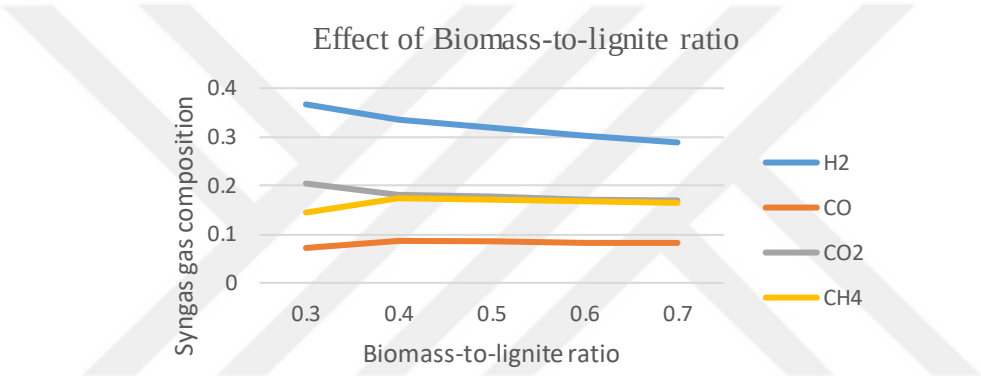


Figure 6.11 Effect of biomass-to-lignite ratio on gas compositions

Figure 6.12 demonstrates its impact on exergy. As the biomass-to-lignite ratio increases, an increase in the system exergy is also observed.

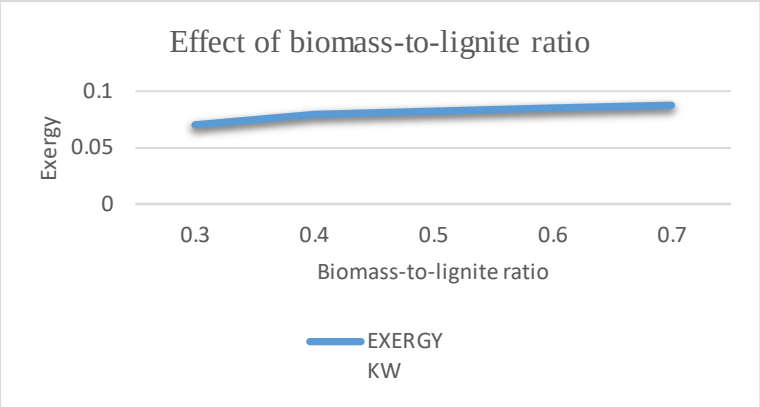


Figure 6.12 Effect of biomass-to-lignite ratio on on exergy of syngas gas compositions

6.2.2.2 Effect of Temperature on syngas gas compositions and exergy

To investigate the effect of temperature on the syngas composition and exergy, the values of ER: 0.12, SBR: 0.2, and BLR: 0.3 have been kept constant. The analysis results are shown in Table 6.9.

Table 6.9 The sensitivity analysis results based on temperature

CSTR Temp (ºC)	H_2	CO	CO_2	CH_4	Exergy kw
499.85	0.367	0.072	0.204	0.144	0.086
599.85	0.357	0.086	0.177	0.181	0.085
699.85	0.357	0.086	0.176	0.181	0.085
799.85	0.358	0.086	0.176	0.182	0.085
899.85	0.358	0.086	0.175	0.182	0.085

The effect of temperature is depicted in Figure 6.13. As the temperature increases, an increase in the molar fractions of CO and CH_4 has been observed, while the opposite effect was seen for the molar fractions of H_2 and CO_2.

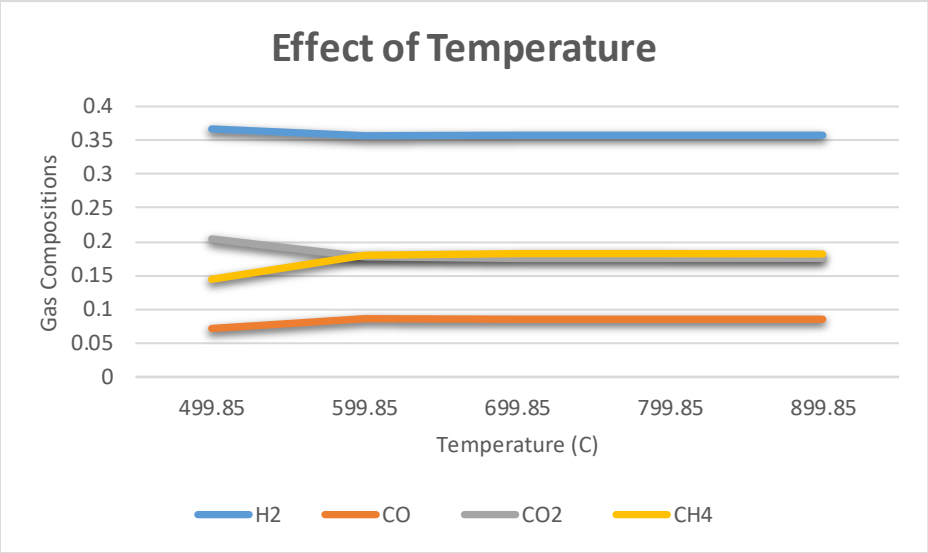


Figure 6.13 Effect of temperature on gas compositions

Figure 6.14 demonstrates its impact on exergy. An increase in temperature has led to a decrease in the system exergy.

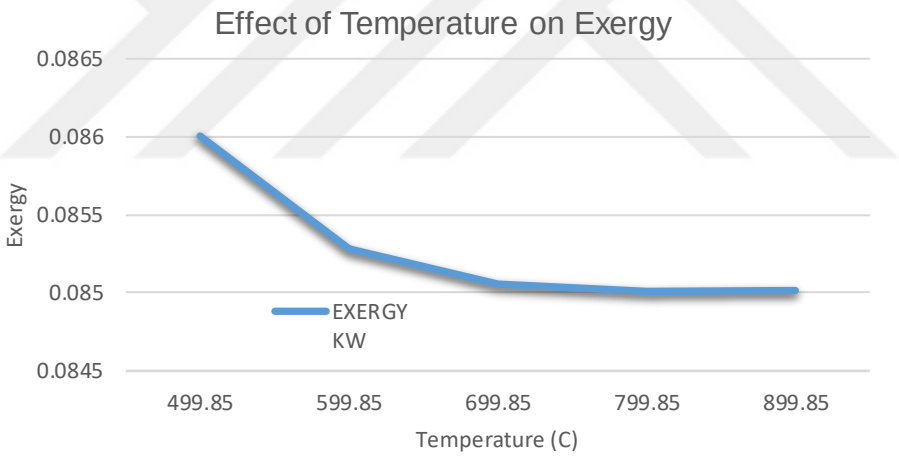


Figure 6.14 Effect of temperature on exergy of syngas gas compositions

6.2.2.3 Effect of Equivalence Ratio on syngas gas compositions and exergy

The effect of the equivalence ratio on the composition and exergy of the gas obtained from the mixture of hazelnut shells and lignite coal is presented in the figures below under the conditions of SBR: 0.1, biomass-to-lignite ratio: 0.3, and a temperature of 499.85°C. The sensitivity analysis results based on ER are shown in Table 6.10.

Table 6.10 The sensitivity analysis results based on ER

ER	H_2	CO	CO_2	CH_4	Exergy kw
0.12	0.367	0.072	0.204	0.144	0.070
0.17	0.326	0.085	0.177	0.158	0.084
0.22	0.304	0.083	0.171	0.142	0.090
0.27	0.284	0.082	0.166	0.129	0.097
0.32	0.267	0.080	0.162	0.118	0.103

Figure 6.15 gives the influence of equivalence ratio on syngas compositions. As the equivalence ratio increases, a decrease in the molar fractions of hydrogen, carbon dioxide, and methane is observed, while an increase in the carbon monoxide gas fraction is noted.

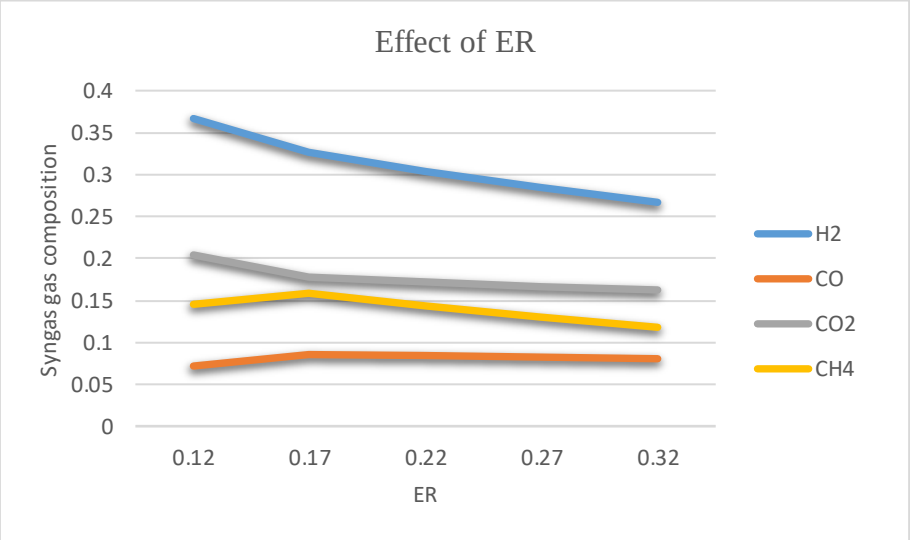


Figure 6.15 Effect of ER on gas compositions

Additionally, Figure 6.16 shows the effect of ER on exergy. As the equivalence ratio increases, an increase in the exergy of the syngas is also observed.

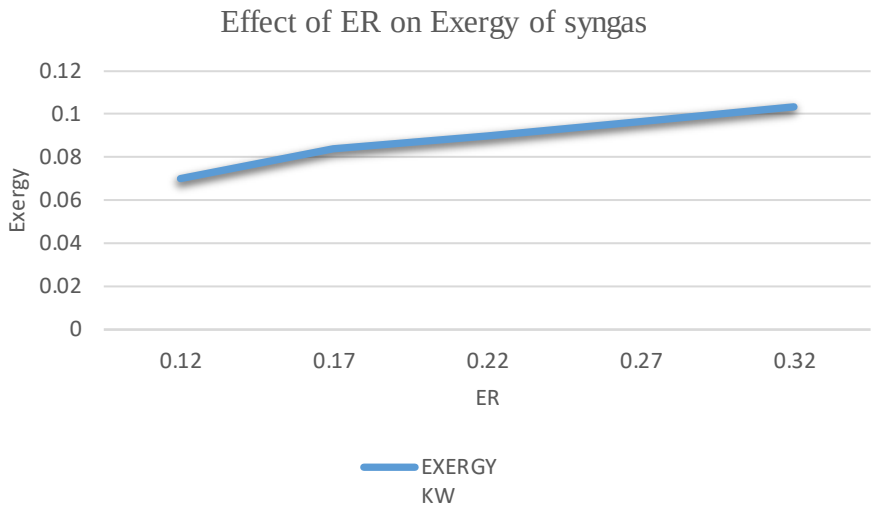


Figure 6.16 Effect of ER on exergy of syngas gas compositions

6.2.2.4 Effect of Steam to Biomass Ratio on syngas gas compositions and exergy

The effect of the steam-to-biomass ratio on the composition and exergy of the gas obtained from the mixture of hazelnut shells and lignite coal is presented in the figures below under the conditions of ER: 0.12, biomass-to-lignite ratio: 0.3, and a temperature of 499.85°C. Table 6.11 presents the results of the sensitivity analysis conducted based on SBR.

Table 6.11 The sensitivity analysis results based on SBR

SBR	H_2	CO	CO_2	CH_4	Exergy kw
0.1	0.367	0.072	0.204	0.144	0.070
0.2	0.372	0.089	0.185	0.177	0.086
0.3	0.388	0.090	0.186	0.176	0.095
0.4	0.401	0.091	0.187	0.175	0.104
0.5	0.411	0.091	0.188	0.174	0.113

Steam-to biomass ratio influence on syngas composition is presented in Figure 6.17. As the equivalence ratio increases, an increase in the fractions of H_2, CO, and CH_4 is observed, while a decrease is noted in the CO_2 fraction.

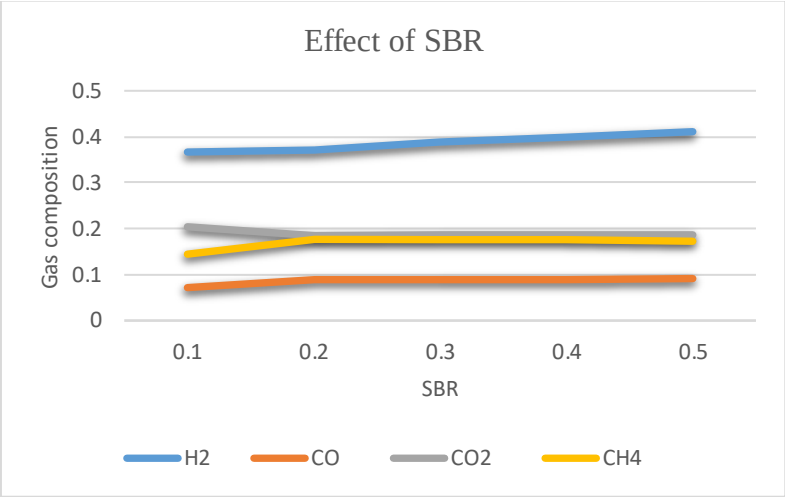


Figure 6.17 Effect of SBR on gas compositions

Furthermore, Figure 6.18 illustrates the effect of steam-to-biomass ratio on exergy. An increase in the steam-to-biomass ratio has been observed to enhance the exergy of the syngas.

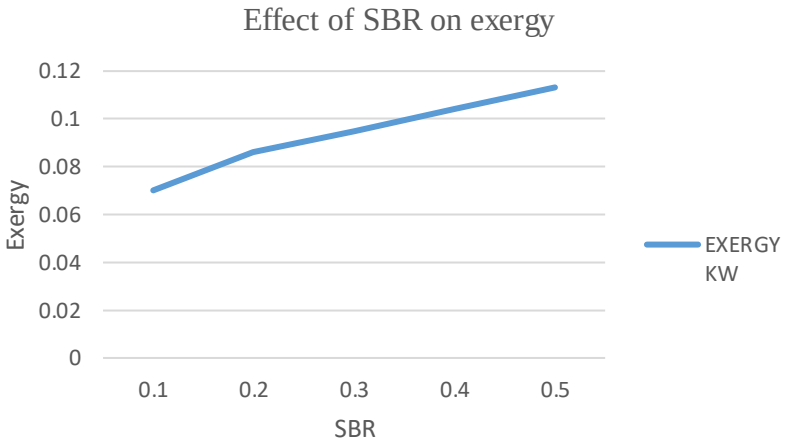


Figure 6.18 Effect of SBR on exergy of syngas gas compositions

6.2.2.5 The effect of ER and T on H_2 for Fluidized-Bed Model

The variation of ER and T on H_2 in fixed SBRs is presented below with contour figures. Figure 6.19 gives the effect on Hydrogen when SBR is 0.1.

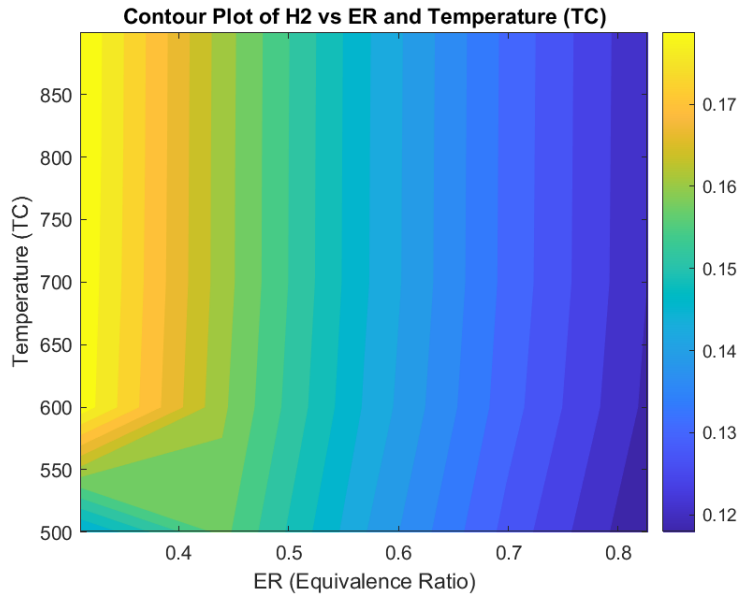


Figure 6.19 Effect of T and ER on hydrogen with 0.1 SBR

Figure 6.20 illustrates the effect of temperature (T) and equivalence ratio (ER) on hydrogen (H_2) composition when SBR is 0.2.

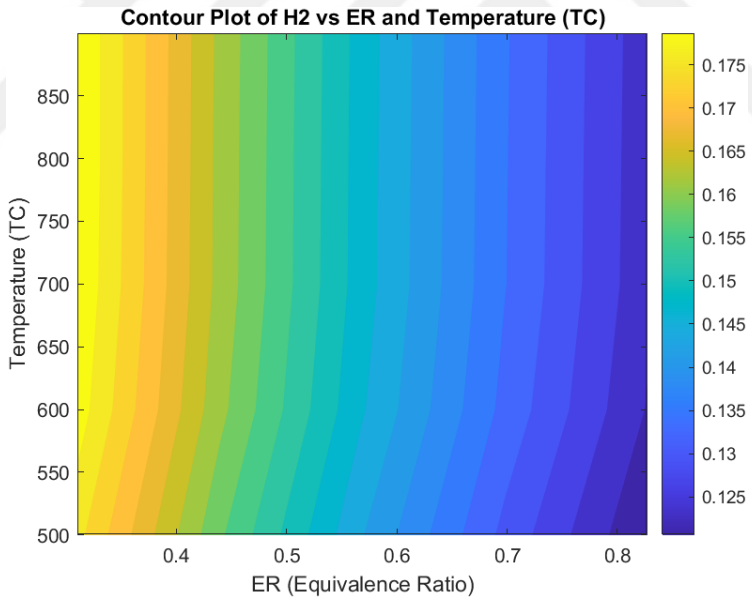


Figure 6.20 Effect of T and ER on hydrogen with 0.2 SBR

Figure 6.21 depicts the influence of temperature (T) and equivalence ratio (ER) on hydrogen (H_2) composition at an SBR of 0.3.

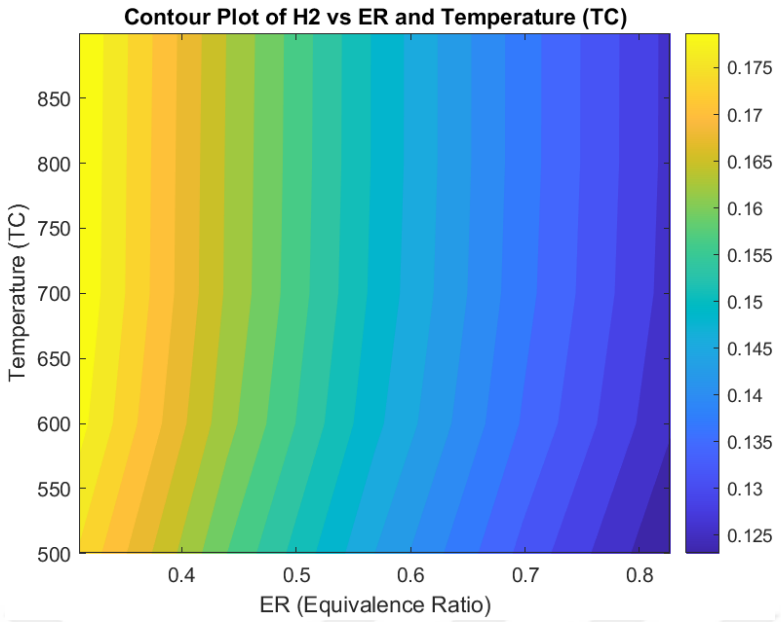


Figure 6.21 Effect of T and ER on hydrogen with 0.3 SBR

Figure 6.22 presents the variation in hydrogen (H_2) composition with temperature (T) and equivalence ratio (ER) at an SBR of 0.4.

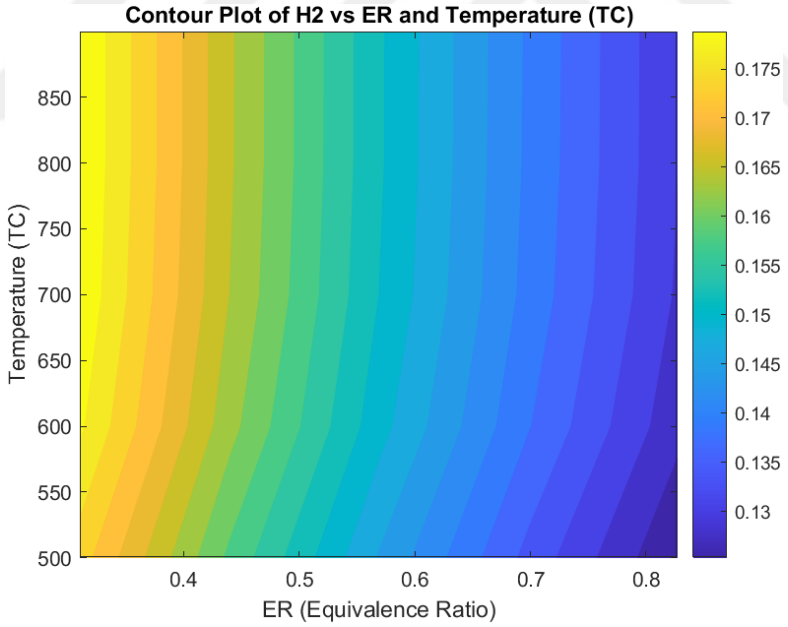


Figure 6.22 Effect of T and ER on hydrogen with 0.4 SBR

How hydrogen (H_2) composition changes with temperature (T) and equivalence ratio (ER) at an SBR of 0.5 is shown in Figure 6.23.

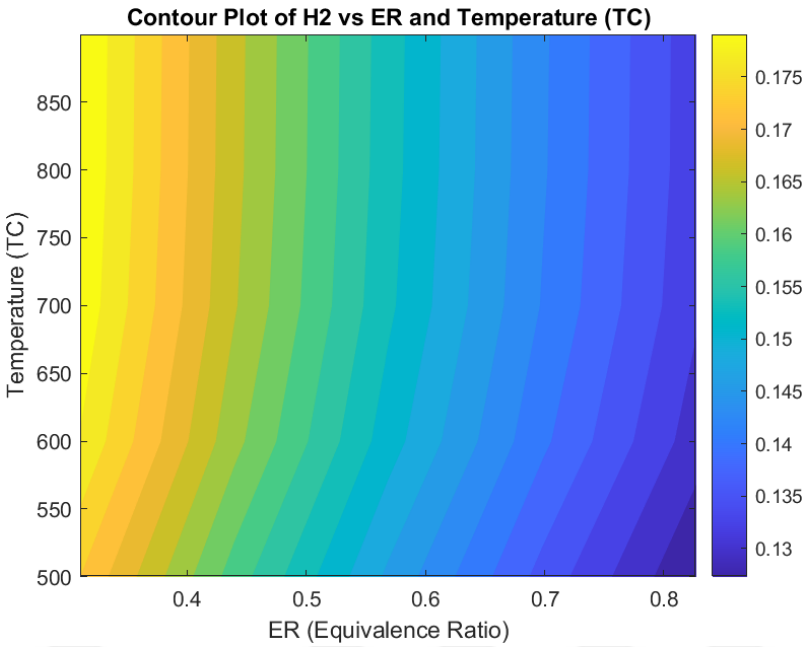


Figure 6.23 Effect of T and ER on hydrogen with 0.4 SBR

6.3 Results of Machine Learning Applications

A robust database comprising 6,750 simulation outcomes was developed for all biomass-lignite mixtures across two distinct models. For the fluidized bed configuration, 5,625 data points were generated (9 × 625), while the downdraft fixed-bed model yielded 1,125 data points (9 × 125). The study aims to model the exergy characterization of syngas derived from selected biomass types through the application of advanced machine learning algorithms. At this stage, a range of sophisticated machine learning techniques was implemented, including Decision Tree, Support Vector Regression (SVR), Gaussian Process Regression (GPR), and Random Forest Regression (RFR). To evaluate machine learning models and measure the accuracy of their predictions, the cross-validation technique is employed. This approach involves running the models on datasets they have not been trained on and assessing the outcomes. In this study, cross-validation was utilized. To elaborate, the dataset is divided into training and testing subsets, with the training data used to develop the model. Predictions are then tested against the testing dataset. However, unforeseen issues can arise during the train/test split. If the dataset division is not performed randomly, a problem known as overfitting may

occur. Overfitting refers to a model's tendency to memorize data instead of learning from it. Cross-validation provides an effective solution to mitigate this issue.

The performance of each model is evaluated using the metrics R^2, adjusted R^2, RMSE, and N-RMSE. The correlation coefficient (R^2) defines the strength and direction of the relationship between variables. Adjusted R^2 indicates how well the terms fit a regression line while accounting for the number of terms in the model. Root Mean Square Error (RMSE) is a widely used metric for assessing the accuracy of a proposed system. Normalized Root Mean Square Error (N-RMSE) serves as a standardized statistical measure to evaluate model performance. The results of these performance metrics are presented below.

6.3.1 Model Results of CO

In the first phase, the data is split into training and testing sets. The model is developed using training data. The model's learning occurs solely with the training data, during which it attempts to identify patterns in the data. After training, the model is evaluated on the test data to determine how accurately it makes predictions. The test data consists of data that the model has never seen during the training process. This is critical for assessing the model's ability to generalize, meaning how well the model can adapt to data it has not encountered before, rather than just fitting the training data.

In the second phase, evaluation is performed solely on the test data, allowing us to determine whether the model has truly learned from the data or merely memorized it as a result of the operations performed in the first phase. Table 6.12 gives R^2 values due to the size of the training data for CO.

Table 6.12 A comparison of the models' R^2 values based on the size of the training data for CO

Train size	DT	SVM	GPR	RFR	DT Test	SVM Test	GPR Test	RFR Test
15	0.918	0.816	0.959	0.948	0.908	0.791	0.956	0.939
25	0.944	0.909	0.961	0.979	0.931	0.885	0.958	0.974

Table 6.12 A comparison of the models' R^2 values based on the size of the training data for CO (continued)

50	0.984	0.968	0.972	0.988	0.978	0.949	0.969	0.982
75	0.992	0.983	0.964	0.991	0.99	0.966	0.969	0.981
85	0.992	0.986	0.974	0.993	0.990	0.976	0.974	0.992

Figure 6.24 gives R^2 values for CO when overall data used.

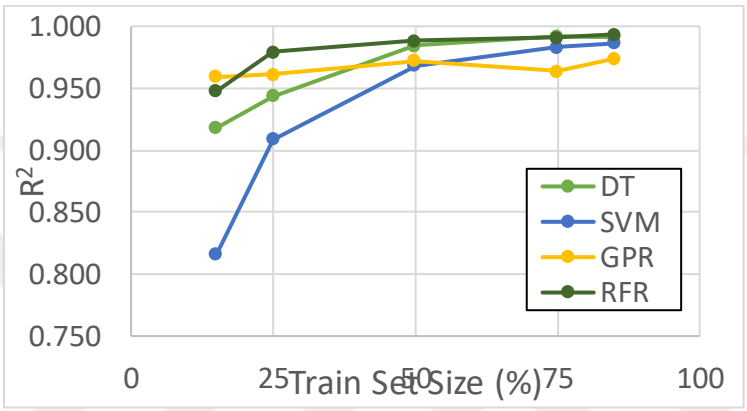


Figure 6.24 The R^2 results of the models using overall data for CO

Figure 6.25 highlights R^2 results of the CO when model learned using only the test data.

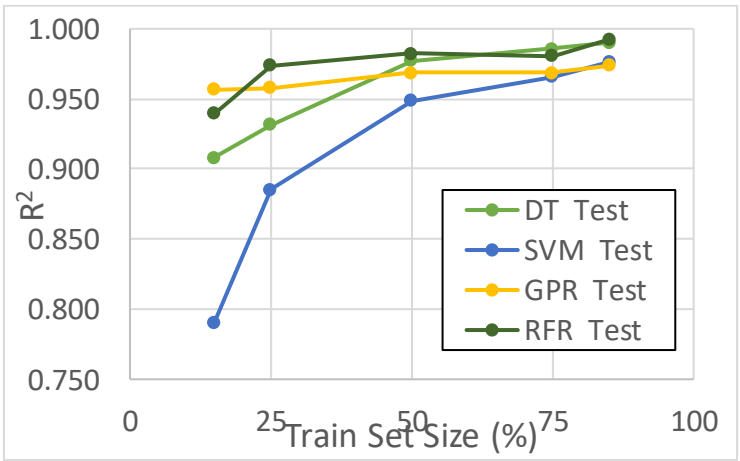


Figure 6.25 The R^2 results of the models learned using only the test data for CO

Upon examining the figures containing the results of the models created for CO gas, it is observed that both figures are nearly identical. Figure 6.24 shows the results obtained by testing the model created using the training data. Figure 6.25, on the other hand, presents the results of the model created using only the test data. The near identical nature of both figures indicates that the model did not memorize the data but rather acquired general knowledge during the learning process. The learning success of the figures is expressed by the R^2 value, and the results in this graph were also obtained based on R^2.

6.3.2 Model Results of CO_2

Table 6.13 illustrates model results based on data points for CO_2.

Table 6.13 A comparison of the models' R^2 values based on the size of the training data for CO_2

Train size	DT	SVM	GPR	RFR	DT Test	SVM Test	GPR Test	RFR Test
15	0.862	0.428	0.431	0.916	0.846	0.400	0.427	0.903
25	0.916	0.651	0.948	0.944	0.900	0.616	0.941	0.927
50	0.963	0.890	0.943	0.976	0.945	0.863	0.889	0.960
75	0.974	0.941	0.979	0.981	0.947	0.916	0.944	0.956
85	0.978	0.949	0.954	0.985	0.958	0.927	0.951	0.973

Figure 6.26 gives R^2 values for CO_2 when overall data is used.

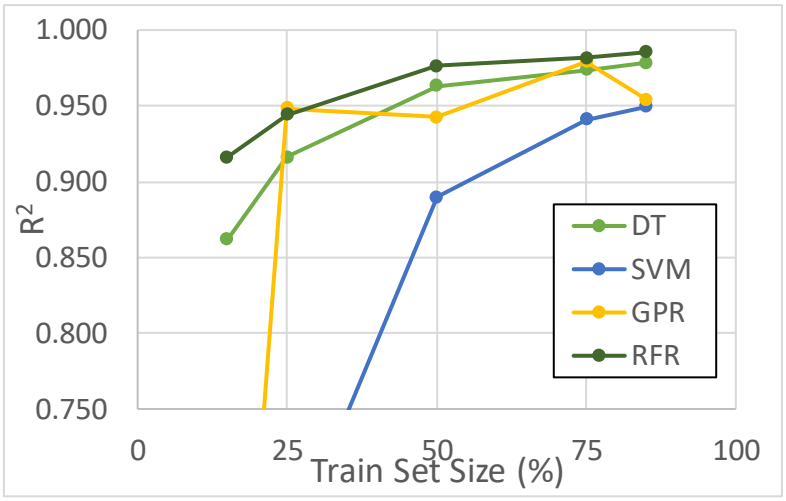


Figure 6.26 The R^2 results of the models using overall data for CO_2

Figure 6.27 gives R^2 results of the CO_2 when model learned using only the test data.

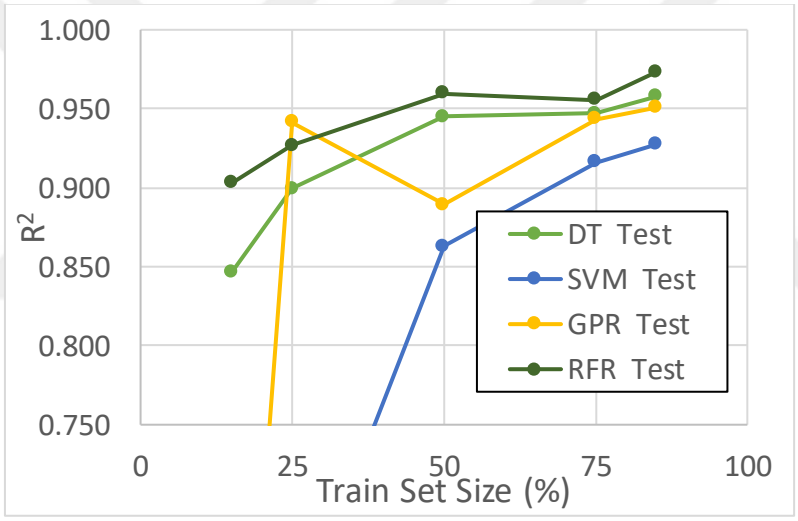


Figure 6.27 The R^2 results of the models learned using only the test data for CO_2

6.3.3 Model Results of CH_4

The R^2 results of the models for CH_4 are presented in Table 6.14.

Table 6.14 A comparison of the models' R^2 values based on the size of the training data for CH_4

Train size	DT	SVM	GPR	RFR	DT Test	SVM Test	GPR Test	RFR Test
15	0.988	0.835	0.992	0.991	0.987	0.814	0.992	0.990

Table 6.14 A comparison of the models' R^2 values based on the size of the training data for CH_4 (continued)

25	0.992	0.938	0.994	0.994	0.990	0.922	0.993	0.992
50	0.995	0.982	0.995	0.997	0.99	0.970	0.995	0.995
75	0.997	0.992	0.996	0.998	0.994	0.981	0.996	0.996
85	0.997	0.994	0.996	0.998	0.995	0.986	0.996	0.996

Figure 6.28 gives R^2 values for CH_4 when overall data is used.

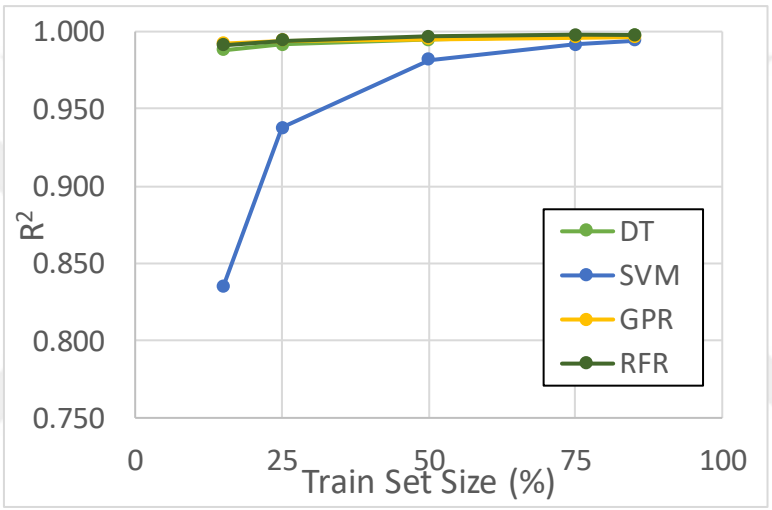


Figure 6.28 The R^2 results of the models using overall data for CH_4

Figure 6.29 gives R^2 results of the CH_4 when model learned using only the test data.

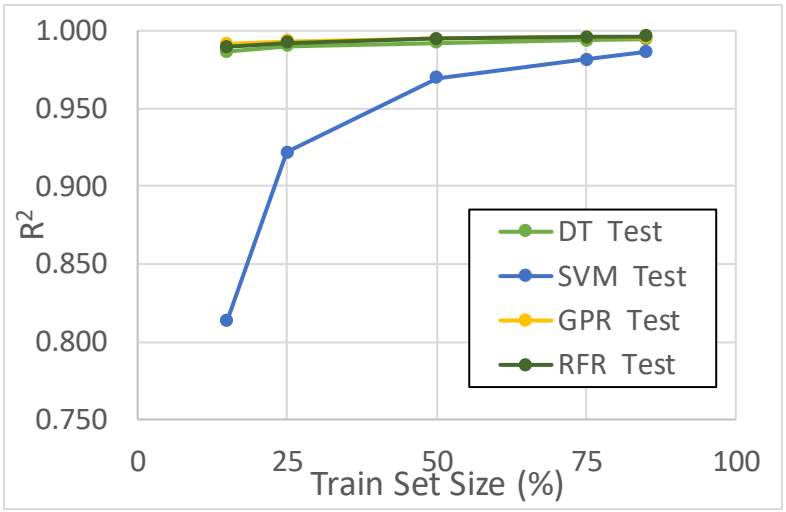


Figure 6.29 The R^2 results of the models learned using only the test data for CH_4

6.3.4 Model Results of H_2

The model results (DT,SVM,GPR and RF) are given in Table 6.15 for hydrogen.

Table 6.15 A comparison of the models' R^2 values based on the size of the training data for H_2

Train size	DT	SVM	GPR	RFR	DT Test	SVM Test	GPR Test	RFR Test
15	0.901	0.565	0.064	0.920	0.888	0.535	0.058	0.907
25	0.902	0.772	0.916	0.944	0.874	0.745	0.910	0.925
50	0.952	0.908	0.921	0.968	0.922	0.886	0.918	0.944
75	0.973	0.949	0.924	0.986	0.958	0.928	0.924	0.978
85	0.975	0.956	0.923	0.985	0.961	0.944	0.916	0.982

Figure 6.30 presents R^2 values for H_2 when overall data used.

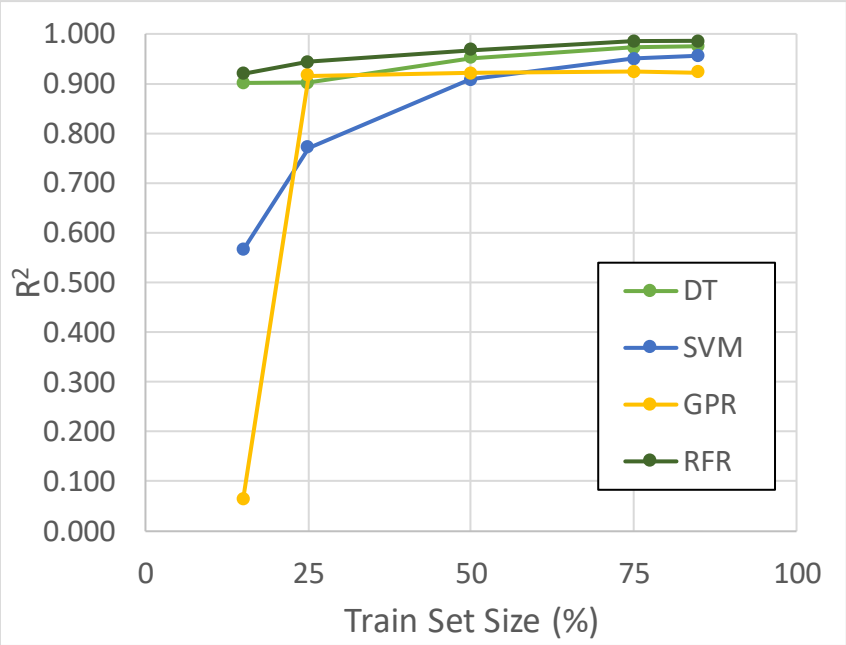


Figure 6.30 The R^2 results of the models using overall data for H_2

Figure 6.31 gives R^2 results of the H_2 when model learned using only the test data.

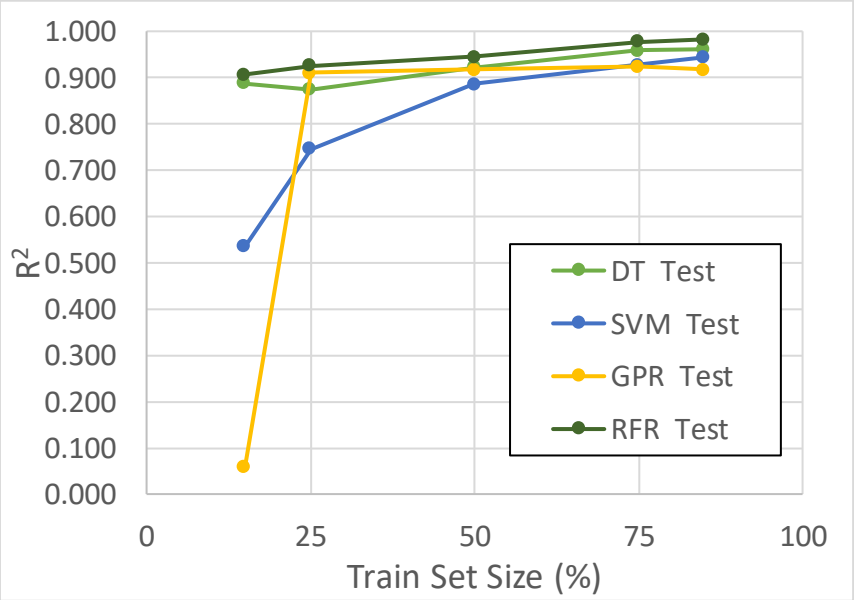


Figure 6.31 The R^2 results of the models learned using only the test data for H_2

6.3.5 Model Results for the Exergy of Syngas

Results of four models used during the analysis on predicting exergy are presented in Table 6.16.

Table 6.16 A comparison of the models' R^2 values based on the size of the training data for exergy

Train size	DT	SVM	GPR	RFR	DT Test	SVM Test	GPR Test	RFR Test
15	0.494	0.178	0.038	0.783	0.436	0.158	0.030	0.758
25	0.537	0.260	0.399	0.867	0.468	0.228	0.373	0.838
50	0.925	0.372	0.938	0.945	0.885	0.348	0.899	0.895
75	0.958	0.424	0.951	0.992	0.893	0.386	0.904	0.980
85	0.941	0.437	0.953	0.990	0.863	0.348	0.885	0.965

Figure 6.32 presents model performances for exergy of syngas, when overall data used.

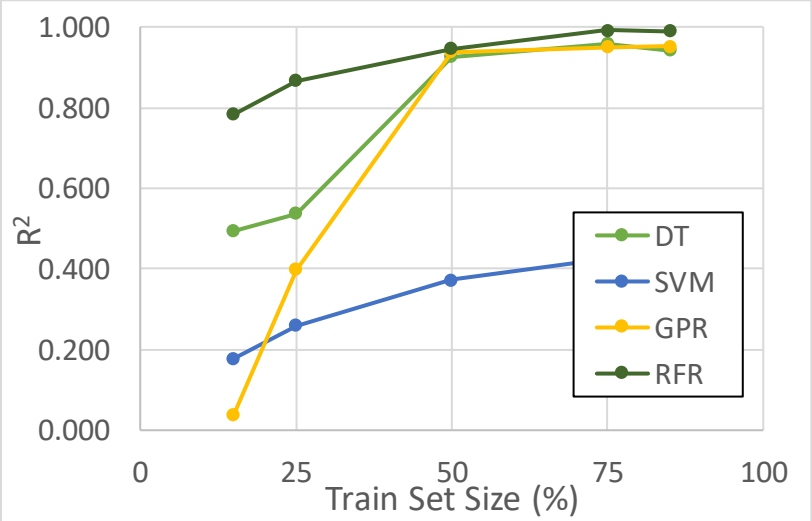


Figure 6.32 The R^2 results of the models using overall data for exergy

Model performances are presented in Figure 6.33 for predicting exergy of syngas when models only used test data.

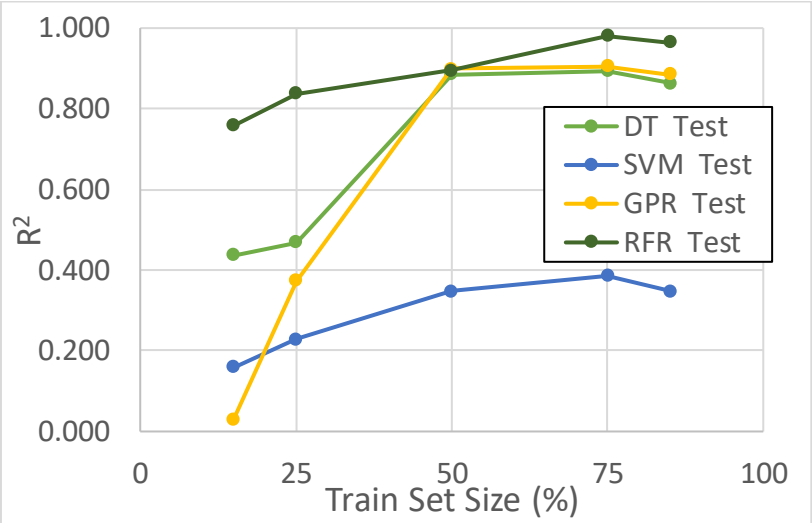


Figure 6.33 The R^2 results of the models learned using only the test data for exergy

In the figures of the results obtained for the exergy of CO_2, CH_4, H_2, and syngas, similar relationships to those observed for CO gas are evident. This allows us to make a similar interpretation regarding the models used and the methods applied. In the first phase, the dataset was split into training and testing data. In the second phase, the model's learning was performed solely on the test data. The near identical nature of the graphs obtained from both phases indicates that the model did not memorize the data and learned correctly. This result confirms that the model underwent a general learning process and did not simply recall the data.

6.4 Cross Validation

The model performing well on only a single test data set may indicate overfitting. K-fold cross-validation tests the model's generalization capability by splitting the data in different ways. Underfitting, or an overly simplistic model, typically performs poorly on all data. The K-fold method can also detect this issue.

6.4.1 10-Fold Cross Validation for Exergy

To perform cross validation for predicting the exergy of syngas, 10 fold is used.

Independent variables (Predictors): Biomass-to-lignite ratio, equivalence ratio, temperature, steam-to-biomass ratio

Dependent variable (Response): Exergy

Validation: 10-fold cross-validation

Results are represented in Table 6.17.

Table 6.17 10-Fold cross-validation results for exergy

Model	Model type	RMSE (Validation)	MSE (Validation)	RSquared (Validation)	MAE (Validation)
Fine Tree	Tree	0.047	0.002	0.913	0.005
Medium Tree	Tree	0.044	0.002	0.921	0.006
Coarse Tree	Tree	0.093	0.009	0.651	0.014
Linear	SVM	0.126	0.016	0.357	0.020
Quadratic	SVM	0.124	0.015	0.379	0.011
Cubic	SVM	0.124	0.015	0.381	0.010
Fine Gaussian	SVM	0.120	0.015	0.415	0.016
Medium Gaussian	SVM	0.124	0.015	0.380	0.010
Coarse Gaussian	SVM	0.125	0.016	0.373	0.015
Rational Quadratic	GPR	0.066	0.004	0.824	0.005
Squared Exponential	GPR	0.048	0.002	0.906	0.005
Matern 5/2	GPR	0.071	0.005	0.797	0.006
Exponential	GPR	0.054	0.003	0.884	0.005
Boosted Trees	Ensemble	0.044	0.002	0.923	0.010
Bagged Trees	Ensemble	0.042	0.002	0.930	0.004

As a result of the applied 10-fold cross-validation, the best performance was demonstrated by Random Forest Bagged Trees, with an R^2 value of 0.93.

6.4.2 10-Fold Cross Validation for Hydrogen

Another important aspect of the study is investigating hydrogen composition. Therefore, cross-validation is also applied to predict hydrogen compositions.

Independent variables (Predictors): Biomass-to-lignite ratio, equivalence ratio, temperature, steam-to-biomass ratio, Exergy

Dependent variable (Response): Hydrogen fraction

Validation: 10-fold cross-validation

Results of 10-fold cross validation for hydrogen are represented in Table 6.18.

Table 6.18 10- Fold cross validation results for H_2

Model	Model type	Status	RMSE Validation	MSE Validation	RSquared Validation	MAE Validation
Fine Tree	Tree	Trained	0.0077	0.0001	0.9845	0.0033
Medium Tree	Tree	Trained	0.0102	0.0001	0.9729	0.0047
Coarse Tree	Tree	Trained	0.0139	0.0002	0.9498	0.0074
Linear	SVM	Trained	0.0219	0.0005	0.8746	0.0106
Quadratic	SVM	Trained	0.0056	0.0000	0.9918	0.0023
Qubic	SVM	Trained	0.0027	0.0000	0.9981	0.0019
Fine Gaussian	SVM	Trained	0.0161	0.0003	0.9324	0.0065
Medium Gaussian	SVM	Trained	0.0051	0.0000	0.9931	0.0023
Coarse Gaussian	SVM	Trained	0.0127	0.0002	0.9581	0.0060
Rational Quadratic	GPR	Trained	0.0021	0.0000	0.9989	0.0003
Squared Exponential	GPR	Trained	0.0022	0.0000	0.9987	0.0003
Matern 5/2	GPR	Trained	0.0022	0.0000	0.9988	0.0003
Exponential	GPR	Trained	0.0031	0.0000	0.9975	0.0006

Table 6.18 10- Fold cross validation results for H_2 (continued)

Boosted Trees	Ensemble	Trained	0.0142	0.0002	0.9472	0.0100
Bagged Trees	Ensemble	Trained	0.0066	0.0000	0.9885	0.0028

Through the implementation of 10-fold cross-validation to determine H_2, the Rational Quadratic Gaussian Process Regression model exhibited the highest performance, achieving an R^2 value of 0.999.

7
CONCLUSION

This project serves multiple purposes. To enumerate these objectives: the aim is to utilize the abundant lignite coal in Turkey in a sustainable manner that causes less harm to the environment, by blending it with various biomasses. The purpose here is to evaluate Turkey's resources and reduce dependency on imports. Biomasses such as Hazelnut Shell, Cattle Manure, Electronic Scrap, Sewage Sludge, Agricultural waste, Microalgae, Macroalgae, Treated Wood, and Plastic (PVC) have been mixed with lignite in specific ratios. The reason for using different biomasses is to observe their effects on the biomass gasification process. Two different designs have been used for biomass gasification in Aspen Plus: one employing a fixed-bed gasifier, and the other using a fluidized-bed gasifier. The aim is to measure the efficiency of synthetic gas products and assess the performance of these gasifiers. In the model with the fixed-bed gasifier, parameters such as Equivalence Ratio, biomass-to-lignite ratio, and temperature were varied within specific ranges, and their effects on the system's exergy and the composition of the exit gas were examined. Similarly, in the design using the fluidized-bed gasifier, the steam-to-biomass ratio was additionally studied to determine its impact on the system's exergy and the composition of the synthetic gas. This distinction arises because the fixed-bed uses only air as the agent, while the fluidized-bed uses both steam and air as gasifying agents.

During the validation of these designs conducted in the Aspen Plus simulation program, the following studies were utilized as references. For the validation of the fixed-bed gasifier, the works of S. Sezer, et al., U. Kumar, et al. and T. Maneerung, et al. were referenced. For the fluidized-bed gasifier design, the study by W. Li, et al. 2024 was used as a reference. The validation results for the fixed-bed design are

presented in Table 15. Among the referenced studies, the RMSE value of the gas compositions reported by U. Kumar, et al. was 1.845, while the RMSE value of the exit gas compositions from our design was found to be 0.80 [78]. Similarly, the RMSE value of the synthetic gas compositions obtained in the study by T. Maneerung, et al. was 1.54, whereas the RMSE value for our design was 2.24 [79]. Based on these results, it can be concluded that the validation for the fixed-bed gasifier was nearly a one-to-one match. In the validation of the fluidized-bed gasifier design, the molar compositions of the synthetic gas components reported by W. Li, et al. were 0.22123936, 0.050748992, 0.076076024, and 0.14985585 for H_2, CO, CO_2, and CH_4, respectively. In our design, the corresponding molar compositions were found to be 0.23, 0.043, 0.082, and 0.13 for H_2, CO, CO_2, and CH_4, respectively. At an equivalence ratio (ER) of 0.163, the RMSE value was determined to be 1.19. Based on these results, it can be concluded that the validation was successfully achieved for the fluidized-bed gasifier.

In transitioning to the fixed-bed design, the composition and exergy of the syngas obtained from the mixture of biomass and lignite coal were analyzed. Analyses were conducted for all types of biomass; however, while presenting the Aspen Plus analysis results, data from one biomass type (hazelnut shell and lignite coal mixture) were provided. Data obtained from nine different biomass and lignite coal mixtures were compiled in Excel and used as input for machine learning. According to the results of the fixed-bed Aspen Plus analysis, it was observed that the system exergy increased with higher biomass-to-lignite ratios and rising temperatures. Both temperature and the increase in the equivalence ratio had a positive effect on the system exergy. While an increase in the equivalence ratio led to an increase in the CO_2 composition, reductions were observed in the molar fractions of H_2, CO, and CH_4. An increase in temperature led to an increase in the H_2 and CO gas compositions, while causing a decrease in the CH_4 and CO_2 gas compositions. On the other hand, an increase in the biomass-to-lignite ratio resulted in an increase in the CO composition, while decreases were observed in the H_2, CH_4, and CO_2 compositions. In the fluidized bed gasifier design, gasification conducted with a mixture of hazelnut shell and lignite coal showed that an increase in the biomass-to-lignite ratio negatively affected the H_2 and CO_2 gas compositions, while leading

to a favorable increase in CO and CH_4 outputs. Temperature resulted in an increase in CO and CH_4 compositions and a decrease in H_2 and CO_2 compositions. The equivalence ratio (ER) led to a positive increase only in the CO composition, while causing a decrease in the compositions of the other gases. An increase in the steam-to-biomass ratio resulted in a decrease in CO_2 and an increase in the compositions of the other gases. When examining the effects of ER, temperature, SBR, and the biomass-to-lignite ratio on system exergy, it was observed that an increase in all parameters led to an increase in system exergy. In the reference study conducted by H. Yaka, et al. an R^2 value greater than 0.9 was observed. Similarly, in another study by S. Sezer, et al. using the ANN method, an R^2 greater than 0.9 was also found. Therefore, for this study to be considered successful, the results of each design are expected to be consistent with the reference papers, and an R^2 greater than 0.9 should be achieved. An R^2 of 0.98 was found for the fixed-bed reactor, and 0.96 for the fluidized-bed reactor. The data obtained from the validation studies confirm that this level of success has been achieved.

As a result of the simulations conducted, a total of 6750 data points were obtained, and this dataset was used for training and testing machine learning algorithms. In the study, Decision Tree, Support Vector Regression (SVR), Gaussian Process Regression (GPR), and Random Forest algorithms were applied, and the performance of the models was compared. The Random Forest algorithm demonstrated superior performance, achieving the highest R^2 value. The R^2 value was calculated as 0.93, indicating that this model performed the most successful learning compared to the other algorithms.

To test the model's learning success and generalization ability, a 10-fold cross-validation method was applied. As a result, similar performance values were obtained, and it was determined that the model did not memorize the data but instead learned it effectively.

In this study, the potential applications of machine learning methods in the energy field and their comparisons with each other were analyzed in detail. The findings demonstrate that the Random Forest algorithm provides superior performance in such energy-focused applications and that machine learning approaches can be a powerful tool in process optimization.

7.1 Recommendation

Within the scope of this project, the biomass gasification process was modeled using the Aspen Plus simulation program under specific parameters. Various biomass types mixed with lignite in certain proportions were used. Two different models, namely the fixed-bed and fluidized-bed gasifiers, were employed. In Work Packages 1 and 2, R^2 values greater than 0.9 were obtained for both models, and the simulations ran without errors.

The simulation outputs obtained were used as datasets for training and testing machine learning algorithms. Decision Tree, Support Vector Regression, Gaussian Process Regression, and Random Forest algorithms were applied, and the performance of the models was compared.

As a result of the analyses, the Random Forest algorithm achieved the best results compared to the other models. This algorithm effectively learned the complex relationships in the dataset and demonstrated better performance in terms of prediction accuracy. This finding demonstrates that Random Forest is an effective method for understanding multiple parameter effects and handling noisy data. Furthermore, the R^2 performance metric was observed to be greater than 0.9, indicating that Work Package 3 was successfully completed.

Since K-Fold trains and tests the model K times, the computational cost is higher than the standard training/test split method. However, because it tests on different data splits, the performance evaluation becomes more reliable. By applying 10-fold cross-validation, it was observed that the R^2 value exceeded 0.9. Therefore, it can be concluded that Work Package 4 was also successfully achieved. This method prevents the model from overfitting or underfitting and reflects the model's learning performance.

The gasification of lignite coal and biomass mixtures is of strategic importance for increasing Turkey's energy security and reducing dependence on foreign energy sources. Machine learning-based process optimization supports the efficient use of domestic resources by improving syngas yield and exergy values in this process. The widespread adoption of gasification technologies can contribute to local economies, balance migration flows, and increase employment. The clean and

efficient use of the produced syngas will contribute to reducing carbon emissions and aligning with national and international climate policies.

Strengthening legal regulations and increasing incentives could facilitate the realization of large-scale projects by encouraging private sector investments. Furthermore, international collaborations and technology transfers would support Turkey's position as a regional hub for energy technologies. Collecting performance data from different regions in a centralized database would provide a valuable guide for decision-makers. In this context, integrating machine learning-supported gasification approaches into long-term energy strategies will be a critical step toward achieving energy independence and sustainable development goals.

In future studies based on this project, expanding the parameter ranges used in the simulation could allow for the testing of model performance under different conditions. Additionally, by considering different and numerous biomass types in the simulation study, the generalizability of the results could be increased. A dataset for machine learning could be created using the rich data obtained from the simulations, and the performance of models could be compared with other modern algorithms, enhancing the diversity and accuracy of the results. The applicability of the developed models to industrial-scale gasification processes could be evaluated, marking a significant step in terms of practical use and economic contribution.

This study presents an effective method for optimizing and predicting biomass gasification processes, and it may serve as a reference for future research in this field.

REFERENCES

[1] D. Jeong, S. Hwang, J. Kim, H. Yu, and E. Park, "Public perspective on renewable and other energy resources: Evidence from social media big data and sentiment analysis," Energy Strategy Reviews, vol. 50, Nov. 2023, doi: 10.1016/j.esr.2023.101243.

[2] S. Sezer, F. Kartal, and U. Özveren, "Prediction of chemical exergy of syngas from downdraft gasifier by means of machine learning," Thermal Science and Engineering Progress, vol. 26, Dec. 2021, doi: 10.1016/j.tsep.2021.101031.

[3] C. Koroneos, A. Dompros, and G. Roumbas, "Hydrogen production via biomass gasification-A life cycle assessment approach," Chemical Engineering and Processing: Process Intensification, vol. 47, no. 8, pp. 1261–1268, 2008, doi: 10.1016/j.cep.2007.04.003.

[4] M. M. Aba, I. L. Sauer, and N. B. Amado, "Comparative review of hydrogen and electricity as energy carriers for the energy transition," Feb. 29, 2024, Elsevier Ltd. doi: 10.1016/j.ijhydene.2024.01.034.

[5] M. Younas, S. Shafique, A. Hafeez, F. Javed, and F. Rehman, "An Overview of Hydrogen Production: Current Status, Potential, and Challenges," May 15, 2022, Elsevier Ltd. doi: 10.1016/j.fuel.2022.123317.

[6] C. Fetting, "The European green deal, https://www.esdn.eu/fileadmin/ESDN_Reports/ESDN_Report_2_2020.pdf, 01.05.2024.

[7] I. Energy Agency, "World energy outlook 2019." [Online]. Available: www.iea.org/weo

[8] “Maden Tetkik ve Arama Genel Müdürlüğü.” Accessed: Oct. 12, 2024. [Online]. Available: https://www.mta.gov.tr/v3.0/hizmetler/maden-yataklari

[9] I. Renewable Energy Agency, renewable energy statistics 2022 statistiques d’énergie renouvelable 2022 estadísticas de energía renovable 2022 About IRENA. 2022. [Online]. Available: www.irena.org

[10] United Nations Framework Convention on Climate Change,https://unfccc.int/files/essential_background/background_publications_htmlpdf/application/pdf/conveng.pdf, 10.07.2024.

[11] The Sustainable Development Goals Report, https://unstats.un.org/sdgs/report/2024/The-Sustainable-Development-Goals-Report-2024.pdf, 10.07.2024.

[12] “The Paris agreement,” 2016. [Online]. Available: https://treaties.un.org/Pages/ViewDetails.aspx?src=TREATY&mtdsg_no=XXVII-7-

[13] “Paris Anlaşması.” Accessed: Sep. 10, 2023. [Online]. Available: https://www.mfa.gov.tr/paris-anlasmasi.tr.mfa

[14] “Seventh national communication of turkey under the unfccc.” [Online]. Available: www.csb.gov.tr

[15] New Energy and new technology, https://ticaret.gov.tr/data/65dc9d3113b8762768385d66/ETKB%20SKDM%20Sunum-Yenilenebilir%20Enerji_23022024.pdf, 05.07.2024.

[16] “Turkey Hydrogen Technologies Strategy and Roadmap”, Accessed: Sep. 12, 2024. [Online]. Available: https://enerji.gov.tr/Media/Dizin/SGB/tr/Kurumsal_Politikalar/HSP/ETKB_Hidro jen_Stratejik_Plan2023.pdf

[17] Global Hydrogen Review 2023, [Online]. Available: www.iea.org, 10.10.2023.

[18] G. Yilmaz et al., “Hydrogen energy development in Turkey: Challenges and opportunities,” Int J Hydrogen Energy, vol. 52, pp. 1304–1311, Jan. 2024, doi: 10.1016/j.ijhydene.2023.11.230.

[19] S. H. Chang and M. F. Rajuli, “An overview of pure hydrogen production via electrolysis and hydrolysis,” Sep. 26, 2024, Elsevier Ltd. doi: 10.1016/j.ijhydene.2024.08.245.

[20] Z. Dong, M. Chen, D. Qin, and S. Han, “Recent advances and perspective of modified TiO2-based photoanodes toward photoelectrochemical water splitting,” Oct. 01, 2024, Elsevier Ltd. doi: 10.1016/j.fuel.2024.132366.

[21] S. Chen, T. Takata, and K. Domen, “Particulate photocatalysts for overall water splitting,” Nat Rev Mater, vol. 2, Aug. 2017, doi: 10.1038/natrevmats.2017.50.

[22] H. Kawaguchi, C. Ogino, and A. Kondo, “Microbial conversion of biomass into bio-based polymers,” Dec. 01, 2017, Elsevier Ltd. doi: 10.1016/j.biortech.2017.06.135.

[23] J. B. McKinlay and C. S. Harwood, “Photobiological production of hydrogen gas as a biofuel,” Jun. 2010. doi: 10.1016/j.copbio.2010.02.012.

[24] M. Ostadi, L. Bromberg, G. Zang, D. R. Cohn, and E. Gençer, “Flexible and synergistic methanol production via biomass gasification and natural gas reforming,” Cleaner Chemical Engineering, p. 100120, Dec. 2024, doi: 10.1016/j.clce.2024.100120.

[25] Hydrogen strategy enabling a low-carbon economy, https://www.energy.gov/sites/prod/files/2020/07/f76/USDOE_FE_Hydrogen_Strategy_July2020.pdf, 12.06.2024.

[26] M. Martino, C. Ruocco, E. Meloni, P. Pullumbi, and V. Palma, “Main hydrogen production processes: An overview,” May 01, 2021, MDPI. doi: 10.3390/catal11050547.

[27] “Monthly Energy Review,” 2025. [Online]. Available: www.eia.gov/mer

[28] A. Molino, S. Chianese, and D. Musmarra, “Biomass gasification technology: The state of the art overview,” Journal of Energy Chemistry, vol. 25, no. 1, pp. 10–25, Jan. 2016, doi: 10.1016/j.jechem.2015.11.005.

[29] S. Safarian, R. Unnþórsson, and C. Richter, “A review of biomass gasification modelling,” Aug. 01, 2019, Elsevier Ltd. doi: 10.1016/j.rser.2019.05.003.

[30] D. Baruah and D. C. Baruah, “Modeling of biomass gasification: A review,” 2014, Elsevier Ltd. doi: 10.1016/j.rser.2014.07.129.

[31] M. M. Sahu and P. A. Sahoo, “Simulation of process parameters and bed-hydrodynamic studies for fluidized bed biomass gasification using aspen plus Bachelor of Technology (Chemical Engineering) Under the guidance of,” 2011.

[32] A. K. Rajvanshi, “Biomass gasification,” Alternative Energyin Agriculture, Vol. II, CRC Press, Boca Raton, pp. 83-102, 1986.

[33] A. Tursi, “A review on biomass: Importance, chemistry, classification, and conversion,” 2019, Green Wave Publishing of Canada. doi: 10.18331/BRJ2019.6.2.3.

[34] A. Demirbas, “Importance of biomass energy sources for Turkey,” Energy Policy, vol. 36, no. 2, pp. 834–842, Feb. 2008, doi: 10.1016/j.enpol.2007.11.005.

[35] O. Oney, “The significance of using lignite as a fuel in electricity generation in Turkey and its application facilities in clean coal technologies,” Jan. 02, 2020, Taylor and Francis Inc. doi: 10.1080/15567036.2019.1587051.

[36] “TUIK”, Accessed: Nov. 27, 2024. [Online]. Available: https://data.tuik.gov.tr/Search/Search?text=linyit

[37] D. Vamvuka and S. Sfakiotakis, “Combustion behaviour of biomass fuels and their blends with lignite,” Thermochim Acta, vol. 526, no. 1–2, pp. 192–199, Nov. 2011, doi: 10.1016/j.tca.2011.09.021.

[38] I. Dincer and M. A. Rosen, “Energy, environment and sustainable development.” [Online]. Available: www.elsevier.com/locate/apenergy

[39] D. Hou, S. Shao, Y. Zhang, S. L. Liu, Y. Chen, and S. S. Zhang, “Exergy analysis of a thermal power plant using a modeling approach,” Clean

Technol Environ Policy, vol. 14, no. 5, pp. 805–813, 2012, doi: 10.1007/s10098-011-0447-0.

[40] T. D. Gray and J. Schlup, "An introduction to exergy and its evaluation using Aspen Plus," 2019.

[41] E. Querol, B. Gonzalez-Regueral, A. Ramos, and J. L. Perez-Benedito, "Novel application for exergy and thermoeconomic analysis of processes simulated with Aspen Plus®," Energy, vol. 36, no. 2, pp. 964–974, 2011, doi: 10.1016/j.energy.2010.12.013.

[42] E. E. Ozbas, D. Aksu, A. Ongen, M. A. Aydin, and H. K. Ozcan, "Hydrogen production via biomass gasification, and modeling by supervised machine learning algorithms," Int J Hydrogen Energy, vol. 44, no. 32, pp. 17260–17268, Jun. 2019, doi: 10.1016/j.ijhydene.2019.02.108.

[43] G. C. Umenweke, I. C. Afolabi, E. I. Epelle, and J. A. Okolie, "Machine learning methods for modeling conventional and hydrothermal gasification of waste biomass: A review," Feb. 01, 2022, Elsevier Ltd. doi: 10.1016/j.biteb.2022.100976.

[44] F. Elmaz, Ö. Yücel, and A. Y. Mutlu, "Predictive modeling of biomass gasification with machine learning-based regression methods," Energy, vol. 191, Jan. 2020, doi: 10.1016/j.energy.2019.116541.

[45] S. Ascher, I. Watson, and S. You, "Machine learning methods for modelling the gasification and pyrolysis of biomass and waste," Mar. 01, 2022, Elsevier Ltd. doi: 10.1016/j.rser.2021.111902.

[46] B. V. Ayodele, S. I. Mustapa, R. Kanthasamy, N. Mohammad, A. AlTurki, and T. S. Babu, "Performance analysis of support vector machine, Gaussian Process Regression, sequential quadratic programming algorithms in modeling hydrogen-rich syngas production from catalyzed co-gasification of biomass wastes from oil palm," Int J Hydrogen Energy, vol. 47, no. 98, pp. 41432–41443, Dec. 2022, doi: 10.1016/j.ijhydene.2022.05.066.

[47] H. Yaka, M. A. Insel, O. Yucel, and H. Sadikoglu, "A comparison of machine learning algorithms for estimation of higher heating values of

biomass and fossil fuels from ultimate analysis," Fuel, vol. 320, Jul. 2022, doi: 10.1016/j.fuel.2022.123971.

[48] A. I. M. Abdelrahim and Ö. Yücel, "A machine learning based regression methods to predicting syngas composition for plasma gasification system," Fuel, vol. 381, Feb. 2025, doi: 10.1016/j.fuel.2024.133575.

[49] Z. Ceylan and S. Ceylan, "Application of machine learning algorithms to predict the performance of coal gasification process," Applications of Artificial Intelligence in Process Systems Engineering, pp. 165–186, Jan. 2021, doi: 10.1016/B978-0-12-821092-5.00003-6.

[50] J. Y. Kim, D. Kim, Z. J. Li, C. Dariva, Y. Cao, and N. Ellis, "Predicting and optimizing syngas production from fluidized bed biomass gasifiers: A machine learning approach," Energy, vol. 263, p. 125900, Jan. 2023, doi: 10.1016/J.ENERGY.2022.125900.

[51] M. A. Insel, O. Yucel, and H. Sadikoglu, "Higher heating value estimation of wastes and fuels from ultimate and proximate analysis by using artificial neural networks," Waste Management, vol. 185, pp. 33–42, Jul. 2024, doi: 10.1016/J.WASMAN.2024.05.044.

[52] G. C. Umenweke, I. C. Afolabi, E. I. Epelle, and J. A. Okolie, "Machine learning methods for modeling conventional and hydrothermal gasification of waste biomass: A review," Bioresour Technol Rep, vol. 17, p. 100976, Feb. 2022, doi: 10.1016/J.BITEB.2022.100976.

[53] J. Y. Kim, D. Kim, Z. J. Li, C. Dariva, Y. Cao, and N. Ellis, "Predicting and optimizing syngas production from fluidized bed biomass gasifiers: A machine learning approach," Energy, vol. 263, p. 125900, Jan. 2023, doi: 10.1016/J.ENERGY.2022.125900.

[54] E. E. Ozbas, D. Aksu, A. Ongen, M. A. Aydin, and H. K. Ozcan, "Hydrogen production via biomass gasification, and modeling by supervised machine learning algorithms," Int J Hydrogen Energy, vol. 44, no. 32, pp. 17260–17268, Jun. 2019, doi: 10.1016/J.IJHYDENE.2019.02.108.

[55] F. Kartal and U. Özveren, “Investigation of the chemical exergy of torrefied biomass from raw biomass by means of machine learning,” Biomass Bioenergy, vol. 159, p. 106383, Apr. 2022, doi: 10.1016/J.BIOMBIOE.2022.106383.

[56] S. Sezer and U. Özveren, “Investigation of syngas exergy value and hydrogen concentration in syngas from biomass gasification in a bubbling fluidized bed gasifier by using machine learning,” Int J Hydrogen Energy, vol. 46, no. 39, pp. 20377–20396, Jun. 2021, doi: 10.1016/J.IJHYDENE.2021.03.184.

[57] S. Ascher, I. Watson, and S. You, “Machine learning methods for modelling the gasification and pyrolysis of biomass and waste,” Renewable and Sustainable Energy Reviews, vol. 155, p. 111902, Mar. 2022, doi: 10.1016/J.RSER.2021.111902.

[58] S. Ascher, X. Wang, I. Watson, W. Sloan, and S. You, “Interpretable machine learning to model biomass and waste gasification,” Bioresour Technol, vol. 364, p. 128062, Nov. 2022, doi: 10.1016/J.BIORTECH.2022.128062.

[59] Y. Yang et al., “Predicting municipal solid waste gasification using machine learning: A step toward sustainable regional planning,” Energy, vol. 278, p. 127881, Sep. 2023, doi: 10.1016/J.ENERGY.2023.127881.

[60] K. D. Olca and Ö. Yücel, “Unveiling the potential of operating time in improving machine learning models’ performance for waste biomass gasification systems,” Renew Energy, vol. 237, p. 121621, Dec. 2024, doi: 10.1016/J.RENENE.2024.121621.

[61] N. Kardani, A. Zhou, M. Nazem, and X. Lin, “Modelling of municipal solid waste gasification using an optimised ensemble soft computing model,” Fuel, vol. 289, p. 119903, Apr. 2021, doi: 10.1016/J.FUEL.2020.119903.

[62] Y. Ayub, Y. Hu, and J. Ren, “Estimation of syngas yield in hydrothermal gasification process by application of artificial intelligence models,” Renew

Energy, vol. 215, p. 118953, Oct. 2023, doi: 10.1016/J.RENENE.2023.118953.

[63] J. Pan et al., “Machine learning optimization for enhanced biomass-coal co-gasification,” Renew Energy, vol. 229, p. 120772, Aug. 2024, doi: 10.1016/J.RENENE.2024.120772.

[64] G. C. Umenweke, I. C. Afolabi, E. I. Epelle, and J. A. Okolie, “Machine learning methods for modeling conventional and hydrothermal gasification of waste biomass: A review,” Bioresour Technol Rep, vol. 17, p. 100976, Feb. 2022, doi: 10.1016/J.BITEB.2022.100976.

[65] Z. Lian et al., “Hydrogen Production by Fluidized Bed Reactors: A Quantitative Perspective Using the Supervised Machine Learning Approach,” J (Basel), vol. 4, no. 3, pp. 266–287, Jul. 2021, doi: 10.3390/j4030022.

[66] D. K. Singh and S. Kumar, “Techno-economics of high ash coal gasification: A machine learning approach using CatBoost model,” J Clean Prod, vol. 481, p. 144160, Nov. 2024, doi: 10.1016/J.JCLEPRO.2024.144160.

[67] M. Rahimi and S. A. Salaudeen, “Optimizing hydrogen-rich gas production by steam gasification with integrated CaO-based adsorbent materials for CO2 capture: Machine learning approach,” Int J Hydrogen Energy, vol. 95, pp. 695–709, Dec. 2024, doi: 10.1016/J.IJHYDENE.2024.11.179.

[68] A. Sakheta, T. Raj, R. Nayak, I. O’Hara, and J. Ramirez, “Improved prediction of biomass gasification models through machine learning,” Comput Chem Eng, vol. 191, p. 108834, Dec. 2024, doi: 10.1016/J.COMPCHEMENG.2024.108834.

[69] J. S. Santhappan, M. Boddu, A. S. Gopinath, and T. Mathimani, “Analysis of 27 supervised machine learning models for the co-gasification assessment of peanut shell and spent tea residue in an open-core downdraft gasifier,” Renew Energy, vol. 235, p. 121318, Nov. 2024, doi: 10.1016/J.RENENE.2024.121318.

[70] S. Azadvar and O. Tavakoli, “Data-driven interpretation, comparison and optimization of hydrogen production from supercritical water gasification of biomass and polymer waste: Applying ensemble and differential evolution in machine learning algorithms,” Int J Hydrogen Energy, vol. 85, pp. 511–525, Oct. 2024, doi: 10.1016/J.IJHYDENE.2024.08.081.

[71] K. Kundu, A. Kumar, H. Kodamana, and K. K. Pant, “Obtaining high H2-rich syngas yield and carbon conversion efficiency from biomass gasification: From characterization to process optimization using machine learning with experimental validation,” Fuel, vol. 378, p. 132931, Dec. 2024, doi: 10.1016/J.FUEL.2024.132931.

[72] J. Bai et al., “Production of high calorific value hydrogen-rich combustible gas by supercritical water gasification of straw assisted by machine learning,” Bioresour Technol, vol. 410, p. 131275, Oct. 2024, doi: 10.1016/J.BIORTECH.2024.131275.

[73] N. Mahinpey, A. Abdalla, and A. Farooqui, “Biomass gasification for hydrogen production: a pathway to cleaner energy transition,” Biomass to Bioenergy: Modern Technological Strategies for Biorefineries, pp. 205–235, Jan. 2024, doi: 10.1016/B978-0-443-15377-8.00009-6.

[74] D. Baruah and D. C. Baruah, “Modeling of biomass gasification: A review,” Renewable and Sustainable Energy Reviews, vol. 39, pp. 806–815, Nov. 2014, doi: 10.1016/J.RSER.2014.07.129.

[75] E. D. Kasembe, G. R. John, and C. F. Mhilu, “EXERGY ANALYSIS OF HIGH TEMPERATURE BIOMASS GASIFICATION”.

[76] V. S. Sikarwar et al., “An overview of advances in biomass gasification,” Oct. 01, 2016, Royal Society of Chemistry. doi: 10.1039/c6ee00935b.

[77] P. Parthasarathy and K. S. Narayanan, “Hydrogen production from steam gasification of biomass: Influence of process parameters on hydrogen yield – A review,” Renew Energy, vol. 66, pp. 570–579, Jun. 2014, doi: 10.1016/J.RENENE.2013.12.025.

[78] Phyllis2. (2023). Database for (treated) biomass, algae, feedstocks for biogas production and biochar. In TNO Biobased and Circular Technologies. https://phyllis.nl/

[79] U. Kumar and M. C. Paul, "CFD modelling of biomass gasification with a volatile break-up approach," Chem Eng Sci, vol. 195, pp. 413–422, Feb. 2019, doi: 10.1016/J.CES.2018.09.038.

[80] W. Li, C. Wang, and Y. Song, "Simulation of waste tire gasification in bubbling fluidized bed by Aspen: Contribution ratio analysis," Renew Energy, vol. 222, p. 119995, Feb. 2024, doi: 10.1016/J.RENENE.2024.119995.

[81] R. Jayathilake and S. Rudra, "Numerical and experimental investigation of equivalence ratio (ER) and feedstock particle size on birchwood gasification," Energies (Basel), vol. 10, no. 8, Aug. 2017, doi: 10.3390/en10081232.

[82] X. Wang et al., "Tar inhibition for hydrogen production from biomass gasification assisted by machine learning," Int J Hydrogen Energy, vol. 102, pp. 790–799, Feb. 2025, doi: 10.1016/J.IJHYDENE.2025.01.034.

[83] K. Kundu, A. Kumar, H. Kodamana, and K. K. Pant, "Obtaining high H2-rich syngas yield and carbon conversion efficiency from biomass gasification: From characterization to process optimization using machine learning with experimental validation," Fuel, vol. 378, p. 132931, Dec. 2024, doi: 10.1016/J.FUEL.2024.132931.

PUBLICATIONS FROM THE THESIS

Conference Papers

1. M. Cakar, M.A. Insel, O. Yucel, H. Sadikoglu, "Simulation of Fixed and Fluidized Bed Gasifiers for Gasification of Lignite Coal and Biomass Mixtures," in Proceedings of the 7th International Conference on Advances in Mechanical Engineering, Istanbul 2024. pp. 942.

Projects

1. TUBITAK 1002 (scholarship holder),

M. Cakar, M.A. Insel, O. Yucel, H. Sadikoglu, "Prediction of Syngas and Exergy Data from Gasification of Lignite Coal and Biomass Blends Using Machine Learning Algorithms," 2024.